UNIVERSIDAD AUTÓNOMA DEL ESTADO DE MORELOS

FACULTAD DE CIENCIAS BIOLOGICAS

DETECCIÓN Y DELIMITACIÓN DE ESPECIES CRÍPTICAS EN VECTORES DE LA ENFERMEDAD DE CHAGAS (HEMIPTERA: REDUVIIDAE: TRIATOMINAE) BAJO MÚLTIPLES LÍNEAS DE EVIDENCIA

T E S I S

QUE PARA OBTENER EL GRADO DE

DOCTOR EN CIENCIAS NATURALES

PRESENTA:

M. EN C. DARYL DAVID CRUZ FLORES

ASESOR: DRA. ELIZABETH ARELLANO ARENAS

CUERNAVACA, MORELOS **MARZO 2022**

AGRADECIMIENTOS

No son pocas las personas que, de una manera u otra, me han apoyado en la elaboración de este documento. A todos les doy mi más sincero agradecimiento. No puedo dejar de mencionar, sin embargo, a aquellos que han sido participes directos de esta travesía desde su comienzo.

A mi directora de tesis, la Dra. Elizabeth Arellano Arenas, por aceptarme como su estudiante de doctorado y brindarme este proyecto que no careció desde el inicio de desafíos importantes pero que, afortunadamente pudimos superar. Le agradezco, además, que no solo hayamos desarrollado una gran relación profesional, sino que esa relación trascendió en una gran amistad y eso es algo más importante que cualquier logro académico alcanzado. Muchas gracias.

Le agradezco a su familia, el Dr. Francisco, JuanPa y Lore, que desde el inicio nos recibieron con los brazos abiertos y nos hicieron sentir en familia.

A la Dra. Elizabeth Nava, muchas gracias por todas sus enseñanzas, por dedicarme tanto tiempo a entrenarme en el laboratorio y por siempre atender mis dudas. Le agradezco mucho su amistad.

A los miembros de mi comité, el Dr. Raúl E. Alcalá, la Dra. Elizabeth Nava, la Dra. Sandra Milena Ospina y el Dr. Carlos Ibarra Cerdeña, les agradezco todo el intercambio que siempre hubo en cada seminario, cada revisión de los capítulos que conforman este documento de tesis, las discusiones metodológicas, etc. He aprendido muchísimo de ustedes y sin duda alguna son parte fundamental de esta tesis y de mi formación profesional. En especial, le agradezco al Dr. Carlos Ibarra Cerdeña por transmitirme sus conocimientos sobre triatominos, por apoyarme cada vez que tuve dudas acerca del grupo y la estrecha colaboración que hemos tenido en este tiempo. Muchas gracias, además, a la Dra. Ana Erika Gutiérrez y la Dra. María Ventura por aceptar ser parte del comité revisor del documento de tesis.

Le agradezco al Programa del Doctorado en Ciencias Naturales por estar siempre al pendiente de nuestras dudas y por mantener un constante seguimiento de nuestra trayectoria. Gracias al Consejo de Ciencia y Tecnología (CONACyT) por el apoyo económico y al gobierno de México por brindarnos la oportunidad a extranjeros de cursar estudios de postgrado en este país y apoyarnos en todo momento. Gracias al Centro de Investigación en Biodiversidad y Conservación (CIByC) y su comunidad por hacernos sentir a gusto y parte del centro.

A mi familia, le agradezco todo el apoyo brindado durante este tiempo a pesar de la distancia. Agradezco a mis amigos, los de siempre y los nuevos. Todos han constituido un gran apoyo de una u otra manera.

A mi esposa Daily, no puedo expresar todo mi agradecimiento y orgullo hacia ti. Gracias por aceptar recorrer junto a mi esta aventura. Cada uno de los buenos momentos que han devenido durante este tiempo han sido mejores porque los hemos compartido juntos y porque han sido de los dos. Los desafíos presentados han sido más fáciles de superar gracias a ti.

Gracias también a mis hermosos Marcos y Daniel. A cada uno les debo demasiado y solo espero poder estar a la altura de lo que se merecen.

Una vez más, gracias a todos.

Resumen

La delimitación de especies crípticas tiene implicaciones importantes en estudios sobre biodiversidad, conservación, enfermedades transmitidas por vectores, entre otros. Actualmente, el empleo de la taxonomía integradora es la vía más certera para delimitar especies. Dos de las especies más importantes de triatominos en México son *Triatoma pallidipennis* y *Triatoma dimidiata*. El estatus específico de *T. pallidipennis* ha sido cuestionado en trabajos previos a partir de datos moleculares. Para *T. dimidiata*, estudios filogenéticos propusieron tres haplogrupos para México y parte de Centroamérica. Diferentes investigaciones han intentado reconocer estos haplogrupos con técnicas de modelado de nicho ecológico y morfométricas, alcanzando porcentajes altos de discriminación, pero aun insuficientes para su correcto reconocimiento. En esta tesis analizamos secuencias de ADN con métodos probabilísticos para esclarecer el estatus taxonómico de *T. pallidipennis*, empleamos el modelado de nicho ecológico para apoyar el posible reconocimiento de entidades crípticas en esta especie y empleamos la morfometría geométrica y el patrón de manchas para diferenciar haplogrupos de *T. pallidipennis* y *T. dimidiata*. Analizamos las relaciones filogenéticas de *T. pallidipennis* con matrices mitonucleares, estimamos tiempos de divergencia y delimitamos posibles nuevos taxones con tres métodos de delimitación de especies. Se obtuvieron distancias genéticas y posibles rutas de conectividad basadas en haplotipos compartidos entre poblaciones de *T. pallidipennis*. La variación en forma entre haplogrupos de *T. pallidipennis* fue evaluada con un protocolo morfométrico, empleando imágenes de la cabeza y el pronoto. Se generó una configuración de puntos anatómicos de referencia y semimarcas para obtener variables de forma. Con estas, se realizaron análisis estadísticos para ver su valor en la discriminación de haplogrupos. Finalmente, se estimó la segregación ecológica entre haplogrupos a partir de modelos de nicho ecológico con Maxent y NicheA. La discriminación de haplogrupos de *T. dimidiata* fue analizada con la descripción del contorno del cuerpo con Descriptores Elípticos de Fourier y el patrón de manchas del conexivo. Para ambos casos, una combinación de pruebas estadísticas se realizó para evaluar la capacidad de discriminación de las variables empleadas. Se encontraron cinco haplogrupos para *T. pallidipennis*, basados en métodos de delimitación y distancias genéticas. La divergencia de estos comenzó en el Pleistoceno. Ninguno de los haplogrupos mostró rutas potenciales de conectividad entre ellos, lo que evidencia la falta de flujo de genes y sugieren la existencia de un nuevo complejo de especies crípticas en lo que actualmente se reconoce como *T. pallidipennis*. Las variables de forma mostraron diferencias significativas entre algunos de los haplogrupos analizados, demostrando que, al menos parcialmente, hay divergencias morfométricas que pueden asociarse a los procesos de especiación recientes detectados. A su vez, se encontraron diferencias ecológicas entre los haplogrupos, lo que sugiere que la segregación ecológica puede estar jugando un papel importante en la especiación de estos. Tanto el contorno del cuerpo entero, así como el patrón de manchas del conexivo presentan alto valor para la discriminación de haplogrupos en *T. dimidiata*, aumentando considerablemente los porcentajes de discriminación con respecto a lo encontrado en trabajos previos. Se concluye que la combinación de métodos constituye la vía más certera para detectar y delimitar especies crípticas en el género *Triatoma*.

Palabras claves: triatominos, especies crípticas, taxonomía integradora, haplogrupos

Abstract

The delimitation of cryptic species has important implications in studies on biodiversity, conservation, vector-borne diseases, among others. Currently, the use of integrative taxonomy is the most accurate way to delimit species. Two of the most important species of triatomines in Mexico are Triatoma pallidipennis *and* Triatoma dimidiata. *The specific status of* T. pallidipennis *has been questioned in previous works based on molecular data. For* T. dimidiata*, phylogenetic studies have proposed three haplogroups for Mexico and part of Central America. Different investigations have tried to recognize these haplogroups with morphometric and ecological niche modeling techniques, reaching high percentages of discrimination, but still insufficient for their correct recognition. In this thesis we analyze DNA sequences with probabilistic methods to clarify the taxonomic status of* T. pallidipennis*, we use ecological niche modeling to support the possible recognition of cryptic entities in this species, and we use geometric morphometry and spot patterning to differentiate haplogroups. of* T. pallidipennis *and* T. dimidiata. *We analyze the phylogenetic relationships of* T. pallidipennis *with mitonuclear data, estimate divergence times, and delimit possible new taxa with three species delimitation methods. Genetic distances and possible connectivity routes based on shared haplotypes between* T. pallidipennis *populations were obtained. The variation in shape between haplogroups of* T. pallidipennis *was evaluated with a morphometric protocol, using images of the head and pronotum. A configuration of anatomical reference points and semi-marks was generated to obtain shape variables. With these, statistical analyzes were performed to see their value in haplogroup discrimination. Finally, the ecological segregation between haplogroups was estimated from ecological niche models with Maxent and NicheA. The discrimination of haplogroups of* T. dimidiata *was analyzed with the description of the body contour with Elliptic Fourier Descriptors and the spot pattern of the conexivum. For both cases, a combination of statistical tests was performed to assess the discrimination capacity of the variables used. Five haplogroups were found for* T. pallidipennis*, based on delimitation methods and genetic distances. The divergence of these began in the Pleistocene. None of the haplogroups showed potential landscape connectivity between them, indicating a lack of gene flow and suggesting the existence of a new complex of cryptic species in what is currently recognized as* T. pallidipennis. *The shape variables showed significant differences between some of the analyzed haplogroups, showing that, at least partially, there are morphometric differences that can be associated with the recent speciation processes detected. In turn, ecological differences were found between the haplogroups, suggesting that ecological segregation may be playing an important role in their speciation. Both the contour of the entire body, as well as the spot pattern on the conexivum, present a high value for the discrimination of haplogroups in* T. dimidiata*, considerably increasing the percentages of discrimination with respect to what was found in previous works. It is concluded that the combination of methods (integrative taxonomy) constitutes the most accurate way to detect and delimit cryptic species in the genus* Triatoma.

Keywords: triatomines, cryptic species, integrative taxonomy, haplogroups

ÍNDICE

1. INTRODUCCIÓN GENERAL

La correcta delimitación de las especies crípticas tiene implicaciones importantes en estudios sobre biodiversidad, conservación, tratamiento de enfermedades transmitidas por vectores, entre otros (Bickford *et al.* 2006). Con gran frecuencia la delimitación de estas especies crípticas se logra mediante el empleo de múltiples herramientas como las moleculares, el uso de datos ecológicos, de comportamiento y mediante análisis morfométricos (Dayrat, 2005). Esta combinación de métodos, conocida como taxonomía integradora (Jörger y Schrödl, 2013), es considerada la manera más segura y precisa de determinar los límites de especies en la actualidad (Smith *et al.,* 2008).

Las especies crípticas constituyen un gran reto para los biólogos sistemáticos, debido a que la especiación no siempre está acompañada por características morfológicas distintivas y distribuciones alopátricas que permitan el reconocimiento de las diferentes entidades (Rivera *et al.* 2018). Esto es cierto particularmente para entidades taxonómicas con amplia distribución. Como consecuencia, el número real de especies es posible que sea mayor al que se encuentra actualmente reportado. En el caso de organismos con importancia médica, el correcto reconocimiento de sus especies es de gran importancia para comprender la estructura de sus poblaciones, ciclos de vida, historias evolutivas, entre otros aspectos (Martínez *et al.,* 2006). Esto permite inferir tendencias y hacer predicciones sobre la dinámica de los vectores y en consecuencia de los patógenos que transmiten (p.ej. Piccinali *et al.*, 2009).

La subfamilia Triatominae incluye alrededor de 157 especies de insectos que se alimentan de la sangre de vertebrados (Monteiro *et al.*, 2018; Alevi *et al.*, 2021). En este grupo se encuentran los vectores más importantes del protozoo *Tripanosoma cruzi*, agente causal de la enfermedad de Chagas (EC), de los cuales destacan las especies pertenecientes al género

Triatoma (Martínez *et al.,* 2006). Para este último hay descritas aproximadamente 70 especies y es el género de mayor distribución dentro de la subfamilia (Panzera *et al.,* 1997).

En México se han reportado 31 especies autóctonas de Triatominae, la mayoría agrupadas en el género *Triatoma* (Ramsey *et al.,* 2015). Las especies de este género pertenecen a dos subgrupos: *protracta* y *rubrofasciata* (Lent y Wygodzinsky, 1979). El primero está compuesto por los complejos de especies *protracta* y *lecticularia* (Galvão *et al.,* 2003, Kjos *et al.,* 2009). El subgrupo *rubrofasciata* contiene los complejos de especies *rubida*, *dimidiata* y *phyllosoma*, este último distribuido solamente en México. La presencia de tantos complejos de especies ha conllevado a que diversos estudios subrayen la necesidad de revisar la taxonomía de este género, ya que, estudios filogenéticos han demostrado diferencias con la taxonomía actual propuesta para el grupo (Ibarra-Cerdeña *et al.,* 2014; Justi *et al.,* 2014).

El complejo *phyllosoma* es considerado el más importante en México (Martínez *et al.,* 2006). Esto se debe, principalmente, al hecho de que todas las especies incluidas en él son transmisoras de la EC con diferentes porcentajes de infección (Ramsey *et al.,* 2000; Vidal-Acosta *et al.,* 2000; Martínez-Ibarra *et al.,* 2001). Además, en su conjunto presentan la mayor distribución en el país, donde destaca la región central (Martínez *et al.,* 2006, Ramsey *et al.,* 2015). Para este grupo se han reportado múltiples cuestionamientos taxonómicos inter e intraespecíficos, lo que se ha evidenciado con la inclusión y exclusión de especies en este complejo a lo largo del estudio de su sistemática y taxonomía (Lent y Wygodzinsky, 1979; Flores *et al.,* 2001; Bustamante *et al.,* 2004; Rengifo-Correa *et al.,* 2021). Incluso se ha propuesto la transferencia de las especies de este complejo al género *Meccus* (Carcavallo *et al.,* 2000; Galvão *et al.,* 2003). Esto, unido a la posible presencia de especies crípticas en lo que actualmente se considera una sola entidad taxonómica, resalta la importancia de abordar la sistemática de sus miembros.

Dos de las especies más importantes de triatominos en México son *Triatoma pallidipennis* Stål, 1872, endémica del país y con gran relevancia vectorial (Lent y Wygodzinsky, 1979; Ramsey *et al.*, 2015) y *Triatoma dimidiata* (Latreille, 1811) (formalmente aceptada como complejo *dimidiata*, aunque recientemente Rengifo-Correa *et al.*, 2021 lo fusiona con el complejo *phyllosoma*). El estatus específico de *T. pallidipennis* ha sido cuestionado en trabajos previos a partir de datos moleculares (Harris, 2003; Mayares, 2014). Sin embargo, la baja representatividad geográfica de las poblaciones empleadas en los estudios anteriores no permitió arribar a conclusiones robustas acerca del estatus taxonómico de la especie. Harris (2003) sugiere reevaluar las relaciones filogenéticas de las poblaciones de *T. pallidipennis*, debido a la sospecha de que constituye un complejo de especies crípticas.

Para *T. dimidiata*, estudios filogenéticos propusieron tres haplogrupos para México y parte de Centroamérica (Bargues *et al.,* 2008; Gómez-Palacio *et al.,* 2015), recientemente reafirmados por Pech-May *et al.* (2019). De estos, dos han sido descritos como nuevas especies recientemente (Dorn *et al.,* 2018; Lima-Cordón *et al.,* 2019). Varias investigaciones han intentado reconocer estos haplogrupos basándose en técnicas de modelado de nicho ecológico (Gómez-Palacio *et al.,* 2015) y morfométricas, con puntos anatómicos de referencia (Gurgel-Concalves *et al.,* 2011). Si bien, en estas investigaciones se alcanzaron porcentajes relativamente altos de discriminación, la necesidad de explorar otras técnicas que garanticen mayores porcentajes es necesario.

Aun cuando el análisis genético permite revelar la presencia de especies crípticas, además de comprender la variación genética que han sufrido las poblaciones a lo largo del tiempo, la caracterización morfológica y ecológica usualmente ayudan a confirman el estatus específico (Rivera *et al.,* 2018). El uso de la morfometría geométrica, en contraste con la clásica, ha abierto nuevas perspectivas para la evaluación de caracteres morfológicos en el contexto

taxonómico, complementa la utilización de otros métodos de discriminación (Francoy *et al.*, 2009) y ha sido utilizada para el reconocimiento de especies crípticas, incluso en el género *Triatoma* (Gurgel-Goncalves *et al.*, 2011; Nouvellet *et al.*, 2011).

A su vez, como herramientas alternativas e innovadoras, las técnicas de modelado de nicho ecológico (MNE) han permitido reconocer especies crípticas a partir del análisis de la segregación del nicho e índices y métricas de similitud y equivalencia de nichos (Warren *et al.*, 2008; Martínez-Gordillo *et al.*, 2010; Gurgel-Goncalves *et al.*, 2011). La integración de información filogenética y de nicho ecológico también ha sido útil en el esclarecimiento de complejos de especies en diferentes grupos (Palhano *et al.*, 2018; Rivera *et al.*, 2018) y permiten, de conjunto con el uso de los Sistemas de Información Geográfica, fusionar datos genéticos y espaciales con el propósito de construir y poner a prueba hipótesis filogeográficas (Kidd y Ritchie, 2006; Kozak *et al.*, 2008; Chan *et al.*, 2011). En este sentido, dicha fusión de datos permite explorar patrones de conectividad genética entre poblaciones para estimar la direccionalidad del flujo de genes entre poblaciones a través del paisaje.

Esta aproximación es particularmente interesante, ya que identifica aquellas regiones que son cruciales para mantener el flujo de genes y aquellas que pueden constituir barreras a este flujo (Chan *et al.*, 2011). Esto es importante, ya que analizar los patrones genéticos sin tener en cuenta la complejidad espacial puede subestimar el efecto de la historia ambiental en la dispersión de los organismos a través del tiempo (Kozak *et al.*, 2008) y, por ende, en sus posibles procesos de especiación. Específicamente para *T. pallidipennis*, su variación morfométrica no se ha descrito y los estudios de distribución mediante técnicas de MNE solo han analizado su distribución potencial actual y futura (Ramsey *et al.*, 2015; Carmona-Castro *et al.*, 2019), sin poner a prueba hipótesis sobre la posible presencia de linajes crípticos y las posibles diferencias entre los nichos ecológicos de estos linajes.

Teniendo en cuenta lo anterior, el esclarecimiento del estatus taxonómico de *T. pallidipennis* y el correcto reconocimiento de los posibles nuevos linajes que se detecten a partir de un análisis filogenético con alta representación geográfica, así como la evaluación de métodos que permitan mejorar la discriminación de los haplogrupos ya propuestos para *T. dimidiata*, son aspectos de gran importancia desde el punto de vista evolutivo, taxonómico y de control vectorial. Abordar estas cuestiones bajo un enfoque de taxonomía integradora y evaluada bajo una perspectiva filogenética, tomando como modelos de estudio estas dos especies, podría aportar información relevante para éstas y extenderse esta práctica a otras especies de este grupo para su correcto reconocimiento. Por lo tanto, nuestra hipótesis es que **el empleo de múltiples líneas de evidencia permite la detección y la correcta delimitación de especies crípticas en el género *Triatoma***.

Para probar nuestra hipótesis nos proponemos a) analizar datos de secuencias de ADN con métodos probabilísticos para esclarecer el estatus taxonómico de *T. pallidipennis*, b) utilizar técnicas de morfometría geométrica empleando puntos anatómicos de referencia para diferenciar haplogrupos de *T. pallidipennis* y análisis de contornos y el patrón de coloración para discriminar los haplogrupos de *T. dimidiata* y c) emplear el modelado de nicho ecológico para apoyar el posible reconocimiento de entidades crípticas en *T. pallidipennis*.

LITERATURA CITADA

1. Alevi, K. C. C., de Oliveira, J., da Silva Rocha, D., & Galvão, C. (2021). Trends in Taxonomy of Chagas Disease Vectors (Hemiptera, Reduviidae, Triatominae): From Linnaean to Integrative Taxonomy. Pathogens, 10(12), 1627.
2. Bargues, M. D., Klisiowicz, D. R., Gonzalez-Candelas, F., Ramsey, J. M., Monroy, C., Ponce, C., ... & Mas-Coma, S. (2008). Phylogeography and genetic variation of *Triatoma dimidiata*, the main Chagas disease vector in Central America, and its position within the genus *Triatoma*. PLoS neglected tropical diseases, 2(5), e233.
3. Bickford, D., Lohman, D. J., Sodhi, N. S., Ng, P. K., Meier, R., Winker, K., ... & Das, I. (2007). Cryptic species as a window on diversity and conservation. Trends in ecology & evolution, 22(3), 148-155.
4. Bustamante, D. M., Monroy, C., Menes, M., Rodas, A., Salazar-Schettino, P. M., Rojas, G., ... & Dujardin, J. P. (2004). Metric variation among geographic populations of the Chagas vector *Triatoma dimidiata* (Hemiptera: Reduviidae: Triatominae) and related species. Journal of Medical Entomology, 41(3), 296-301.
5. Carcavallo, R. U., Jurberg, J., Lent, H., Noireau, F., & Galvão, C. (2000). Phylogeny of the Triatominae (Hemiptera: Reduviidae). Proposals for taxonomic arrangements. Entomología y Vectores, 7(Suplemento 1).
6. Carmona-Castro, O., Moo-Llanes, D. A., & Ramsey, J. M. (2018). Impact of climate change on vector transmission of *Trypanosoma cruzi* (C hagas, 1909) in N orth A merica. Medical and veterinary entomology, 32(1), 84-101.
7. Chan, L. M., Brown, J. L., & Yoder, A. D. (2011). Integrating statistical genetic and geospatial methods brings new power to phylogeography. Molecular phylogenetics and evolution, 59(2), 523-537.
8. Dayrat, B. (2005). Towards integrative taxonomy. Biological journal of the Linnean society, 85(3), 407-417.
9. Dorn, P. L., Justi, S. A., Dale, C., Stevens, L., Galvão, C., Lima-Cordón, R., & Monroy, C. (2018). Description of *Triatoma mopan sp. n.* from a cave in Belize (Hemiptera, Reduviidae, Triatominae). ZooKeys, (775), 69.
10. Flores, A., Gastélum, E. M., Bosseno, M. F., Ordoñez, R., Kasten, F. L., Espinoza, B., ... & Brenière, S. F. (2001). Isoenzyme variability of five principal triatomine vector species of Chagas disease in Mexico. Infection, Genetics and Evolution, 1(1), 21-28.
11. Francoy, T. M., Silva, R. A. O., Nunes-Silva, P., Menezes, C., & Imperatriz-Fonseca, V. L. (2009). Gender identification of five genera of stingless bees (Apidae, Meliponini) based on wing morphology. Genetics and molecular research, 8(1), 207-214.
12. Galvão, C., Carcavallo, R., Rocha, D. D. S., & Jurberg, J. (2003). A checklist of the current valid species of the subfamily Triatominae Jeannel, 1919 (Hemiptera, Reduviidae) and their geographical distribution, with nomenclatural and taxonomic notes. Zootaxa, 202(1), 1-36.

13. Gómez-Palacio, A., Arboleda, S., Dumonteil, E., & Peterson, A. T. (2015). Ecological niche and geographic distribution of the Chagas disease vector, *Triatoma dimidiata* (Reduviidae: Triatominae): Evidence for niche differentiation among cryptic species. Infection, genetics and evolution, 36, 15-22.
14. Gurgel-Gonçalves, R., Ferreira, J. B. C., Rosa, A. F., Bar, M. E., & Galvão, C. (2011). Geometric morphometrics and ecological niche modelling for delimitation of near-sibling triatomine species. Medical and Veterinary Entomology, 25(1), 84-93.
15. Harris, K. (2003). Taxonomy and Phylogeny of North American Triatominae: Public Health Implications. Moorehouse School of Medicine, Atlanta, GA. Doctoral Thesis.
16. Ibarra-Cerdeña, C. N., Zaldívar-Riverón, A., Peterson, A. T., Sánchez-Cordero, V., & Ramsey, J. M. (2014). Phylogeny and niche conservatism in North and Central American triatomine bugs (Hemiptera: Reduviidae: Triatominae), vectors of Chagas' disease. PLoS neglected tropical diseases, 8(10), e3266.
17. Jörger, K. M., & Schrödl, M. (2013). How to describe a cryptic species? Practical challenges of molecular taxonomy. Frontiers in zoology, 10(1), 1-27.
18. Justi, S. A., Russo, C. A., Mallet, J. R. D. S., Obara, M. T., & Galvão, C. (2014). Molecular phylogeny of Triatomini (Hemiptera: Reduviidae: Triatominae). Parasites & vectors, 7(1), 1-12.
19. Kidd, D. M., & Ritchie, M. G. (2006). Phylogeographic information systems: putting the geography into phylogeography. Journal of Biogeography, 33(11), 1851-1865.
20. Kjos, S. A., Snowden, K. F., & Olson, J. K. (2009). Biogeography and *Trypanosoma cruzi* infection prevalence of Chagas disease vectors in Texas, USA. Vector-Borne and Zoonotic Diseases, 9(1), 41-50.
21. Kozak, K. H., Graham, C. H., & Wiens, J. J. (2008). Integrating GIS-based environmental data into evolutionary biology. Trends in ecology & evolution, 23(3), 141-148.
22. Lent, H., & Wygodzinsky, P. (1979). Revision of the Triatominae (Hemiptera, Reduviidae), and their significance as vectors of Chagas' disease. Bulletin of the American museum of Natural History, 163(3), 123-520.
23. Lima-Cordón, R. A., Monroy, M. C., Stevens, L., Rodas, A., Rodas, G. A., Dorn, P. L., & Justi, S. A. (2019). Description of *Triatoma huehuetenanguensis sp. n.*, a potential Chagas disease vector (Hemiptera, Reduviidae, Triatominae). ZooKeys, (820), 51.
24. Martínez, F. H., Villalobos, G. C., Cevallos, A. M., De la Torre, P., Laclette, J. P., Alejandre-Aguilar, R., & Espinoza, B. (2006). Taxonomic study of the *Phyllosoma* complex and other triatomine (Insecta: Hemiptera: Reduviidae) species of epidemiological importance in the transmission of Chagas disease: using ITS-2 and mtCytB sequences. Molecular Phylogenetics and Evolution, 41(2), 279-287.
25. Martínez-Gordillo, D., Rojas-Soto, O., & Espinosa De Los Monteros, A. (2010). Ecological niche modelling as an exploratory tool for identifying species limits: an example based on Mexican muroid rodents. Journal of Evolutionary Biology, 23(2), 259-270.

26. Martínez-Ibarra, J. A., Bárcenas-Ortega, N. M., Nogueda-Torres, B., Alejandre-Aguilar, R., Lino Rodríguez, M., Magallón-Gastélum, E., ... & Romero-Nápoles, J. (2001). Role of two *Triatoma* (Hemiptera: Reduviidae: Triatominae) species in the transmission of *Trypanosoma cruzi* (Kinetoplastida: *Trypanosoma*tidae) to man in the west coast of Mexico. Memórias do Instituto Oswaldo Cruz, 96, 141-144.
27. Mayares, D.I. (2014). Phylogeography of *Triatoma pallidipennis* (Hemíptera: Reduviidae) in the State of Morelos. UAEM, Mexico. Master's thesis.
28. Monteiro, F. A., Weirauch, C., Felix, M., Lazoski, C., & Abad-Franch, F. (2018). Evolution, systematics, and biogeography of the Triatominae, vectors of Chagas disease. Advances in parasitology, 99, 265-344.
29. Nouvellet, P., Ramirez-Sierra, M. J., Dumonteil, E., & Gourbière, S. (2011). Effects of genetic factors and infection status on wing morphology of *Triatoma dimidiata* species complex in the Yucatan peninsula, Mexico. Infection, Genetics and Evolution, 11(6), 1243-1249.
30. Palhano, S., Raposo, M. A., Cordeiro, P. H., & Weksler, M. (2018). Genealogical and niche modeling analyses reveal recent expansion and limited genetic divergence in the *Formicivora serrana* complex (Passeriformes: Thamnophilidae). Journal of ornithology, 159(1), 79-92.
31. Panzera, F., Hornos, S., Pereira, J., Cestau, R., Canale, D., Diotaiuti, L., ... & Perez, R. (1997). Genetic variability and geographic differentiation among three species of Triatomine bugs (Hemiptera-Reduviidae). The American journal of tropical medicine and hygiene, 57(6), 732-739.
32. Pech-May, A., Mazariegos-Hidalgo, C. J., Izeta-Alberdi, A., López-Cancino, S. A., Tun-Ku, E., De la Cruz-Felix, K., ... & Ramsey, J. M. (2019). Genetic variation and phylogeography of the *Triatoma dimidiata* complex evidence a potential center of origin and recent divergence of haplogroups having differential *Trypanosoma cruzi* and DTU infections. PLoS neglected tropical diseases, 13(1), e0007044.
33. Piccinali, R. V., Marcet, P. L., Noireau, F., Kitron, U., Gürtler, R. E., & Dotson, E. (2009). Molecular population genetics and phylogeography of the Chagas disease vector *Triatoma infestans* in South America. Journal of Medical Entomology, 46(4), 796-809.
34. Ramsey, J. M., Ordoñez, R., Cruz-Celis, A., Alvear, A. L., Chavez, V., Lopez, R., ... & Carrillo, S. (2000). Distribution of domestic Triatominae and stratification of Chagas disease transmission in Oaxaca, Mexico. Medical and Veterinary Entomology, 14(1), 19-30.
35. Ramsey, J. M., Peterson, A. T., Carmona-Castro, O., Moo-Llanes, D. A., Nakazawa, Y., Butrick, M., ... & Ibarra-Cerdeña, C. N. (2015). Atlas of Mexican Triatominae (Reduviidae: Hemiptera) and vector transmission of Chagas disease. Memórias do Instituto Oswaldo Cruz, 110, 339-352.
36. Rengifo-Correa, L., Esteban, L., Huerta, H., & Morrone, J. J. (2021). The *Triatoma* phyllosoma species group (Hemiptera: Reduviidae: Triatominae), vectors of Chagas disease: diagnoses and a key to the species. Zootaxa, 5023(3), 335-365.

37. Rivera, P. C., González-Ittig, R. E., Robainas Barcia, A., Trimarchi, L. I., Levis, S., Calderón, G. E., & Gardenal, C. N. (2018). Molecular phylogenetics and environmental niche modeling reveal a cryptic species in the Oligoryzomys flavescens complex (Rodentia, Cricetidae). Journal of Mammalogy, 99(2), 363-376.
38. Smith, M. A., Rodriguez, J. J., Whitfield, J. B., Deans, A. R., Janzen, D. H., Hallwachs, W., & Hebert, P. D. (2008). Extreme diversity of tropical parasitoid wasps exposed by iterative integration of natural history, DNA barcoding, morphology, and collections. Proceedings of the National Academy of Sciences, 105(34), 12359-12364.
39. Vidal-Acosta, V., Ibáñez-Bernal, S., & Martínez-Campos, C. (2000). Natural *Trypanosoma cruzi* infection of Triatominae bugs associated with human habitations in Mexico. Salud Publica de Mexico, 42(6), 496-503.
40. Warren, D. L., Glor, R. E., & Turelli, M. (2008). Environmental niche equivalency versus conservatism: quantitative approaches to niche evolution. Evolution: International Journal of Organic Evolution, 62(11), 2868-2883.

Capítulo I.

An improved and low-cost protocol for high-quality DNA isolation for the Chagas disease vectors

Infection, Genetics and Evolution 80 (2020) 104201

Contents lists available at ScienceDirect

Infection, Genetics and Evolution

journal homepage: www.elsevier.com/locate/meegid

An improved and low-cost protocol for high-quality DNA isolation for the Chagas disease vectors

ARTICLE INFO

Keywords:
DNA isolation
Genomic DNA
True bugs
Chagas disease

ABSTRACT

An improved protocol for DNA extraction for the Chagas disease vectors is proposed based on modification to a low cost method described twenty years ago. Quality DNA and high molecular weight were obtained from all samples. NADH-4 gene was successfully amplified by PCR using the isolated DNA. The extraction protocol presented in this technical note is a fast, low-cost, and non-aggressive method to human health for obtaining genetic data from this group of epidemiological importance and potentially other insects.

1. Introduction

Chagas disease affects about 8 million people worldwide, being Triatominae subfamily insects considered to be the main form of transmission (Pereira et al., 2011) of this neglected disease (WHO, 2019). In order to address questions related to their epidemiological control, the molecular study of these species is essential to understand aspects related to phylogenetic relationships, population dynamics and evolutionary trends (Dos Santos et al., 2007). Phylogenetic analyses in this group have employed molecular data obtained via methods for DNA isolation based on corrosive and toxic chemicals (phenol-chloroform, ethidium bromide, among others; García and Powell, 1998; Dujardin et al., 2015) or the use of extraction kits (Justi et al., 2017; López-Vivas et al., 2018). These have, among other drawbacks, the possible risk to human health, in the case of the first one, and the high costs for the second one. Therefore, the optimization of a low cost, a non-aggressive protocol to human health, and efficient for the DNA isolation from these insects of epidemiological relevance (and other potential arthropod groups) is of great importance.

DNA extraction from *Triatoma* Laporte, 1832 species with traditional methods frequently results in bad quality and low concentrations (Mayares, 2014). Fetzner Jr (1999) optimized a method of DNA extraction from reptile skin samples in zoological collections, by using a modification of the Puregene DNA extraction kit. This method has been successfully applied in other groups as fishes (Nguyen et al., 2006), reptiles (Pellegrino et al., 2005; Goicoechea et al., 2016) and rodents (Vargas et al., 2012; Vallejo and González-Cózatl, 2012; Almendra et al., 2014), obtaining high-quality DNA, but it has never been used in insects. Due to its potential efficiency for this group, in this communication, we suggest an improved protocol for DNA extraction, based on Fetzner Jr (1999) method, and validate it with *Triatoma pallidipennis* (Stål, 1872) legs.

2. Material and methods

Triatoma pallidipennis specimens from the states of Jalisco, Colima, Estado de Mexico and Puebla, Mexico, were used to test the method proposed here. Species identification was carried out using the identification keys available (Lent and Wygodzinsky, 1979). All sued specimens were previously preserved in 95% alcohol until they were processed. DNA isolation followed three steps: cell lysis, protein precipitation, and DNA hydration; main improvements of the protocol consist on the way samples are manipulated and timings for each step, as follow:

2.1. Cell lysis

Two or three legs (depending on the available material) of each individual were used, which were removed with entomological forceps. These were carefully cut into very small pieces to expose the tissue out of the chitin cover, in all cases without maceration, since in previous trials the maceration greatly fragmented the DNA. All pieces were deposited into independent 1.5 ml tubes for each specimen, to which 900 µl of lysis solution (10 mM Tris-base, 10 mM EDTA, 2% sodium dodecyl sulfate [SDS], pH 8.0) was added followed by 9 µl of proteinase K. A vortex was used for 15 s to ensure correct homogenization of the solution and then placed in a stove previously heated to 55 °C. The tubes were kept for 48 h on top of a shaker in the stove with occasional vortexed during the lysis time, to assure the degradation in this step.

After 48 h, samples were cooled to room temperature and 1.8 µl of RNAse was applied to each one, vortexed to mix well and then incubated at 37 °C for one hour. Then, samples were quick centrifuged, to precipitate non-degradable chitin residues. Next, the supernatant was extracted to new 1.5 ml tubes.

2.2. Protein precipitation

Once separated in new tubes, the supernatant was cooled down to room temperature and 300 µl of protein precipitation solution was added; then vortexed to mix correctly and placed in a freezer for 25 min. After that time, samples were left at room temperature for 5 min and subsequently centrifuged at 15,000 rpm for three minutes. This procedure ensured the formation of a visible compact layer of polysaccharides at the bottom of the tubes. If polysaccharides layer is

https://doi.org/10.1016/j.meegid.2020.104201
Received 4 November 2019; Received in revised form 14 January 2020; Accepted 19 January 2020
Available online 21 January 2020

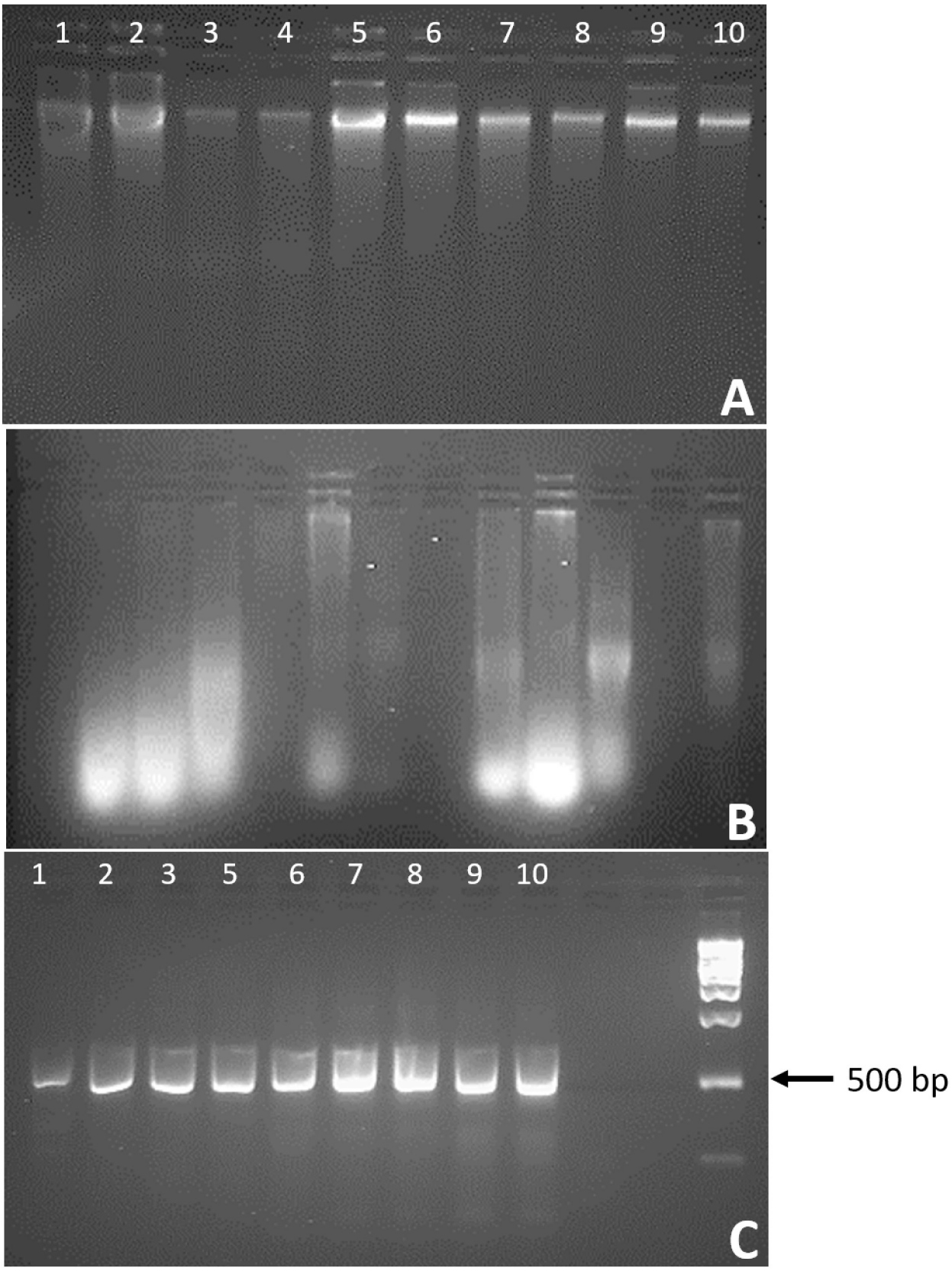

Fig. 1. Electrophoresis showing the quality of extractions of genomic DNA obtained using our method (A), DNA obtained in a previous study (B; Mayares, 2014), and PCR amplification of the NADH4 gene (C).

not enough compacted, this last step can be repeated.

2.3. Precipitation and hydration of DNA

The supernatant containing the DNA was separated into new 1.5 ml tubes, avoiding touching the polysaccharides layer at the bottom of the tubes. Each sample was divided in two, so there were two 1.5 ml tubes with 600 µl of supernatant per sample. Subsequently, 450 µl of Isopropanol was added to each tube and these were slowly inverted 50 times. At this time, it is possible to observe a DNA button, size might vary for each sample, depending on the concentration, but in most cases, DNA it's not visible, so be careful not to lose it.

Next, to precipitate the DNA at the bottom of the tubes, samples were centrifuged at 15,000 rpm for 1 min. Supernatant was carefully removed, remember that DNA is precipitated at the bottom of the tube, and tubes allowed to dry briefly on absorbent paper towells. Subsequently, 1 ml of 70% alcohol was added and then tubes were inverted several times to wash DNA. After that, samples were centrifuged again at 15,000 rpm for 1 min. The alcohol was subsequently removed, taking care of the DNA button (if visible) did not detach from the wall of the tube. Frequently it is not possible to see DNA, so the alcohol elimination must be extremely careful. Tubes were dried on absorbent paper for 15 min and then placed in a vacuum centrifuge at 35 ˚C at least for 15 min to dry out completely.

Finally, samples were hydrated with hydration solution (10 mM Tris base, 0.1 MM EDTA, pH 8.0). Those with a defined DNA button were hydrated with 75–100 µl. Samples without a visible or very small DNA button were hydrated with 50 µl of hydration solution. Quality of isolated DNA was verified through a visualization gel and then performing a PCR to amplify the mitochondrial gene of the subunit 4 of the NADH dehydrogenase (ND4-A).

For the amplification of the ND4-A gene, the following primers were used: 5 ′TCA ACA TGA GCC CTT GGA AG-3′ (F) and 5 ′TAA TTC GTT GTC ATG GTA ATG-3′ (R) (Dotson and Beard, 2001). The PCR reaction for the fragment consisted of a period of initial denaturation at 94 ˚C for 5 min, followed by 40 cycles: denaturation (94 ˚C, 30s), alignment (48 ˚C, 30s), and extension (72 ˚C, 2 min), and a final extension step at 72 ˚C, for 7 min. The amplified products were visualized, with a molecular weight marker of 1 kb to confirm the size of the amplified fragments.

3. Results and discussion

The results of both, extraction and PCR visualizations in 1% agarose gel, are shown in Fig. 1. The DNA obtained by this protocol was of high quality in most cases (Fig. 1A). Samples 1–10 (except the samples 3–4) presented the highest quality, with high DNA molecular weight (Fig. 1A.). Comparing our results with those obtained by Mayares (2014), who extracted *T. pallidipennis* DNA from legs with a different extraction protocol (Fig. 1B), the quality of the DNA obtained with our protocol was considerably better. This author used the DNAzol protocol, one of the most commonly used chemicals in many investigations with the *Triatoma* genus (Ramsey et al., 2012; Perez et al., 2013; Bustamante et al., 2014; Pech-May et al., 2019). As shown in Fig. 1B, DNA obtained by Mayares (2014) is in low concentration and highly fragmented.

Regardless of the quality of DNA obtained from extraction, the NADH4 gene was successfully amplified for all samples (Fig. 1C), even for samples 1, 3 and 4, who were those with minor DNA quality extraction.

Reliability, feasibility, and reproducibility of molecular genetics studies are often limited by the preliminary step of DNA isolation (Pereira et al., 2011). The isolation of large amounts of high-quality DNA from small quantities of tissue (as the present using insect legs) is often a laborious task. Good DNA isolation is a crucial and determinant step to obtain high-quality PCR products, and therefore real estimations in terms of molecular and evolutionary analysis. The protocol presented here offers a quick, simple and really cost-effective approach to DNA extraction in triatomines. The extracted DNA is of high quality and suitable for gene amplification using the PCR technique. Although in this communication we only presented results from *T. pallidipennis*, its extension to other species of the genus or even to other arthropods is very likely. This protocol of genomic DNA isolation can be applied in different molecular studies, especially for population genetics that require a large number of high-quality DNA extractions, sometimes with low quantity of tissue, and in a short time.

Declaration of Competing Interest

None.

Acknowledgements

Authors want to thank MSc. Daily Martínez Borrego and Dr. Dennis Denis Ávila, who provided comments on the manuscript. We also want to thank the anonymous reviewers for their comments and suggestions. To Dr. María Magdalena Ramírez Martínez for providing samples. This study was supported by the CONACYT scholarship program 2018-000012-01NACF-11846.

References

Almendra, A.L., Rogers, D.S., González-Cózatl, F.X., 2014. Molecular phylogenetics of the *Handleyomys chapmani* complex in Mesoamerica. J. Mammal. 95, 26–40.

Bustamante, D.M., De Urioste-Stone, S.M., Juárez, J.G., Pennington, P.M., 2014. Ecological, social and biological risk factors for continued *Trypanosoma cruzi* transmission by Triatoma dimidiata in Guatemala. PLoS One 9, e104599.

Dos Santos, S.M., López, C.M., Dujardin, J.P., Panzera, F., Pérez, R., de la Fuente, A.C., Pacheco, R., Noireau, F., 2007. Evolutionary relationships based on genetic and phenetic characters between *Triatoma maculata*, *Triatoma pseudomaculata* and morphologically related species (Reduviidae: Triatominae). Infect. Genet. Evol. 7, 469–475.

Dotson, E., Beard, C.B., 2001. Sequence and Organization of the Mitochondrial genome of the Chagas disease vector, *Triatoma dimidiata*. Insect Mol. Biol. 10, 205–215.

Dujardin, J.P., Thi, K.P., Xuan, L.T., Panzera, F., Pita, S., Schofield, C.J., 2015. Epidemiological status of kissing-bugs in South East Asia: a preliminary assessment. Acta Trop. 151, 142–149.

Fetzner Jr., J.W., 1999. Extracting high-quality DNA from shed reptile skins: a simplified method. Biotechniques 26, 1052–1054.

García, B.A., Powell, J.R., 1998. Phylogeny of species of *Triatoma* (Hemiptera: Reduviidae) based on mitochondrial DNA sequences. J. Med. Entomol. 35, 232–238.

Goicoechea, N., Frost, D.R., De la Riva, I., Pellegrino, K.C., Sites Jr., J., Rodrigues, M.T., Padial, J.M., 2016. Molecular systematics of teioid lizards (Teioidea/Gymnophthalmoidea: Squamata) based on the analysis of 48 loci under tree-alignment and similarity-alignment. Cladistics 32, 624–671.

Justi, S.A., Cahan, S., Stevens, L., Monroy, C., Lima, R., Dorn, P.L., 2017. Vectors of diversity: genome wide diversity across the geographic range of the Chagas disease vector *Triatoma dimidiata* sensu lato (Hemiptera: Reduviidae). Mol. Phylogenet. Evol. https://doi.org/10.1016/j.ympev.2017.12.016.

Lent, H., Wygodzinsky, P., 1979. Revision of Triatominae (Hemiptera: Reduviidae) and their significance as vector of Chagas' disease. Bull. Am. Museum Nat. His. 163, 123–520.

López-Vivas, F.I., Vázquez-Chagoyán, J.C., Acosta-Dibarrat, J.P., Medina-Torres, I., Diaz-Albiter, H.M., Fernández-Rosas, P., de Oca-Jiménez, R.M., 2018. Molecular characterization of *Trypanosoma cruzi* in infected *Meccus pallidipennis* in the southern region of the state of Mexico, Mexico. Vector-Borne Zoo. Dis. 18, 683–689.

Mayares, D.I., 2014. Filogeografía de Triatoma pallidipennis (Hemíptera: Reduviidae) en el Estado de Morelos. Tesis de Maestría, UAEM, México.

Nguyen, T.T., Ingram, B., Sungan, S., Gooley, G., Sim, S.Y., Tinggi, D., De Silva, S.S., 2006. Mitochondrial DNA diversity of broodstock of two indigenous mahseer species, *Tor tambroides* and *T. douronensis* (Cyprinidae) cultured in Sarawak, Malaysia. Aquaculture 253 (1–4), 259–269.

Pech-May, A., Mazariegos-Hidalgo, C.J., Izeta-Alberdi, A., López-Cancino, S.A., Tun-Ku, E., De la Cruz-Félix, K., Ibarra-Cerdeña, C.N., González Ittig, R.E., Ramsey, J.M., 2019. Genetic variation and phylogeography of the *Triatoma dimidiata* complex evidence a potential center of origin and recent divergence of haplogroups having differential *Trypanosoma cruzi* and DTU infections. PLoS Negl. Trop. Dis. 13, e0007044.

Pellegrino, K.C., Rodrigues, M.T., Waite, A.N., Morando, M., Yassuda, Y.Y., Sites Jr., J.W., 2005. Phylogeography and species limits in the *Gymnodactylus darwinii* complex (Gekkonidae, Squamata): genetic structure coincides with river systems in the Brazilian Atlantic Forest. Biol. J. Linn. Soc. 85 (1), 13–26.

Pereira, J.C., Chaves, R., Bastos, E., Leitão, A., Guedes-Pinto, H., 2011. An Efficient Method for Genomic DNA Extraction fromDifferent Molluscs Species. Int. J. Mol. Sci. 12, 8086–8095. https://doi.org/10.3390/ijms12118086.

Perez, E., Monje, M., Chang, B., Buitrago, R., Parrado, R., Barnabé, C., Noireau, F., Brenière, S.F., 2013. Predominance of hybrid discrete typing units of *Trypanosoma*

cruzi in domestic *Triatoma infestans* from the Bolivian Gran Chaco region. Infect. Genet. Evol. 13, 116–123.
Ramsey, J.M., Gutiérrez-Cabrera, A.E., Salgado-Ramírez, L., Peterson, A.T., Sánchez-Cordero, V., Ibarra-Cerdeña, C.N., 2012. Ecological connectivity of *Trypanosoma cruzi* reservoirs and *Triatoma pallidipennis* hosts in an anthropogenic landscape with endemic Chagas disease. PLoS One 7, e46013.
Vallejo, R.M., González-Cózatl, F.X., 2012. Phylogenetic affinities and species limits within the genus Megadontomys (Rodentia: Cricetidae) based on mitochondrial sequence data. J. Zool. Syst. Evol. Res. 50 (1), 67–75.
Vargas, V., Valenzuela-Galván, D., Alcalá, R.E., 2012. Is genetic structure of the southern pygmy mouse *Baiomys musculus* (Cricetidae) related to human-induced spatial landscape heterogeneity in a tropical dry forest? Genetica 140 (7–9), 287–295.
WHO (World Health Organization), 2019. Chagas Disease (American Trypanosomiasis). World Health Organization. https://www.who.int/chagas/disease/en/ accessed 20 December 2019.

Daryl David Cruz[a,*], Elizabeth Nava-García[b], Elizabeth Arellano[a]
[a] *Centro de Investigaciones en Biodiversidad y Conservación, Universidad Autónoma del Estado de Morelos, Av. Universidad 1001 Col. Chamilpa, Cuernavaca, Morelos 62209, Mexico*
[b] *Facultad de Biología, Universidad Autónoma del Estado de Morelos, Av. Universidad 1001 Col. Chamilpa, Cuernavaca, Morelos 62209, Mexico*
E-mail addresses: daryl.cruzflo@uaem.edu.mx (D.D. Cruz), elizabeth.nava@uaem.mx (E. Nava-García), elisabet@uaem.mx (E. Arellano).

* Corresponding author.

Capítulo II.

Molecular data confirm *Triatoma pallidipennis* Stål, 1872 (Hemiptera: Reduviidae: Triatominae) as a novel cryptic species complex

Acta Tropica 229 (2022) 106382

Contents lists available at ScienceDirect

Acta Tropica

journal homepage: www.elsevier.com/locate/actatropica

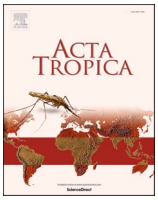

Molecular data confirm *Triatoma pallidipennis* Stål, 1872 (Hemiptera: Reduviidae: Triatominae) as a novel cryptic species complex

Daryl D. Cruz, Elizabeth Arellano *

Centro de Investigación en Biodiversidad y Conservación (CIByC), UAEM, Cuernavaca, Morelos, Mexico

ARTICLE INFO

Keywords:
Triatomines
Cryptic species
ND4
ITS-2
Species delimitation

ABSTRACT

Triatoma pallidipennis constitues one of the most important Chagas disease vector in Mexico. Previous studies based on molecular data suggest *T. pallidipennis* as a complex of cryptic species. For that reason, we analyzed the phylogenetic relationships of *T. pallidipennis* using DNA sequences from the mitochondrial *ND4* gene and the *ITS-2* gene. In addition, the divergence times were estimated, and possible new taxa were delimited with three species delimitation methods. Finally, genetic distances and possible connectivity routes based on shared haplotypes were obtained among the *T. pallidipennis* populations. Five haplogroups (possible cryptic species) were found, based on delimitation methods and genetic distances. Haplogroup divergence began about 3 Ma, in the Pleistocene. Moreover, none of the haplogroups showed potential connectivity routes between them, evidencing lack of gene flow. Our results suggest the existence of a new cryptic species complex within what is currently recognized as a *T. pallidipennis*.

1. Introduction

"Species" constitutes the fundamental unit in biology (Mayr, 1982; De Queiroz, 2007) and its conceptualization and delimitation are central for the development of systematic biology, as well as for biogeographical, ecological, and evolutionary studies (Caldecott et al., 1996; Agapow et al., 2004; Padial et al., 2010). The presence of morphologically unrecognizable (or cryptic) species, even in well-studied taxa, suggests that there are more species than are currently recorded or estimated (Stuart et al., 2006; Stal, 1872).

Cryptic species are one of the great challenges for systematic biologists because they lack the distinctive morphological characters and allopatric distributions that usually help to distinguish species-level entities (Rivera et al., 2018). However, the increasing availability of molecular data has made it possible to detect and differentiate morphologically similar species (based on the phylogenetic species concept) (Chan et al., 2014). Currently, DNA sequences provide many characters that can be compared between entities to assess the evolutionary independence of putative species (Vogler and Monaghan, 2007; Cardoso et al., 2009).

Cryptic species occur frequently in several orders of insects (Jackson and Resh, 1998; Schonrogge et al., 2002). In many cases, the cryptic species was detected using phylogenetic analyses (e.g., Williams et al., 2006). In epidemiology, the correct identification of insect species of medical importance is a key component for the development of vector control and surveillance strategies (Abad-Franch and Monteiro, 2005). This is mainly because different species can vary in terms of their competence as vectors and their epidemiological importance (Gurgel--Goncalves et al., 2011).

Triatomines (Hemiptera: Triatominae), the main vectors of Chagas disease, are highly epidemiologically relevant on the American continent, with more than 100 of the 157 described species having medical relevance (Monteiro et al., 2018; Alevi et al., 2021) and of these three fossils (Alevi et al. 2021; Paiva et al., 2022). 31 species of Triatominae have been reported as native to Mexico, most of them from the genus *Triatoma* Laporte, 1832 (Ramsey et al., 2015). For this group, multiple inter- and intra-species taxonomic questions have been addressed, evidenced by the relatively frequent inclusion and exclusion of species in different complexes (Lent and Wygodzinsky, 1979; Schofield, 1994; Flores et al., 2001; Bustamante et al., 2004; Alevi et al., 2012, 2017a, 2017b; Pita et al., 2016) and, in the case of triatomines from Mexico, by the generic reorganization of *T. phyllosoma* complex species, which were grouped in the genus *Meccus* and are currently considered *Triatoma* (Justi et al., 2014; Cesaretto et al., 2021). This, together with the detection of cryptic species within this genus, highlights the importance of addressing the systematics of its members (Bargues et al., 2008;

* Corresponding author.
E-mail address: elisabet@uaem.mx (E. Arellano).

https://doi.org/10.1016/j.actatropica.2022.106382
Received 12 January 2022; Received in revised form 17 February 2022; Accepted 17 February 2022
Available online 19 February 2022

Gómez-Palacio et al., 2015; Ibarra-Cerdeña et al., 2014; Justi et al., 2014; Pech-May et al., 2019).

Although recently Garcia et al. (2021) highlighted to the necessity for morphological/morphometric studies to correctly apply the cryptic species/speciation terms in triatomines, phylogenetic studies continue to point to possible cryptic species (Bargues et al., 2008; Panzera et al., 2015; Alevi et al., 2018; Pech-May et al., 2019). These phylogenetic studies are important because many species initially suggested as cryptic by molecular data were characterized as new taxa, such as *T. huehuetenanguensis* Lima-Cordón, (Lima-Cordon et al., 2019) and *T. mopan* (Dorn et al., 2018), which were described from triatomines initially considered as *T. dimidiata* (Latreille, 1811) (Dorn et al., 2018; Lima-Cordón et al., 2019) and *T. rosai*(Alevi et al., 2020) which was described from the population of *T. sordida* Chagas, 1912 from Argentina.

One of the most important endemic species in the transmission of CD in Mexico is *T. pallidipennis* Stål, 1872; (Cruz et al., 2020). It is widely distributed in the country (Ramsey et al., 2015), found in 10 states in Mexico (Rengifo-Correa et al., 2021). It also has one of the broadest habitats ranges within the species group and is generally found at high densities. In the state of Morelos, for example, the species is present in more than 80% of 1,078 urban communities (Cruz et al., 2020). In addition, the percentage of infection (88%) reported for this species is one of the highest among Mexican triatomines (Cortés-Jiménez et al., 1996).

Previous phylogenetic analyses using *ND4* and *16S* gene sequences detected high values of genetic divergence (up to 9.7%) between isolated populations (Harris, 2003; Mayares, 2014). This suggests that *T. pallidipennis* may be a species complex composed of two or more cryptic species. However, the low geographical representativeness of the populations used in previous studies did not allow for robust conclusions about the taxonomic status of the species. Thus, Harris (2003) suggested that the phylogenetic relationships among *T. pallidipennis* populations should be reassessed, due to the suspicion that it constituted a cryptic species complex.

The existing molecular evidence available for this species and the high frequency of cryptic speciation in Triatominae lead us to hypothesize that *T. pallidipennis* constitutes an undetected cryptic species complex. Given its importance as a vector of CD in Mexico and because previous research provides relevant, but not decisive, information on the taxonomic status of this species, the aim of this study was to clarify the phylogenetic relationships among populations of *T. pallidipennis* and detect and delimit possible cryptic lineages within *T. pallidipennis* by analyzing the mitochondrial gene *ND4* and the ribosomal gene *ITS-2* of individuals covering the largest geographical representation studied to date.

2. Materials and methods

2.1. Samples

Individuals of *T. pallidipennis* were donated by the Instituto Nacional de Diagnóstico y Referencia Epidemiológico (INDRE), the Ministry of Health of the State of Mexico, the State Laboratory of Medical Entomology (LME) of the State of Mexico, as well as direct collections carried out by LME personnel in the state of Guerrero. The rest of the specimens used were from the triatomine collection of the Centro de Investigación en Biodiversidad y Conservación (CIByC). In addition, we considered sequences available in GenBank for *T. pallidipennis*. In total, 73 samples were analyzed for the *ND4* gene (39 constitute new sequences generated in this study) and 33 for *ITS-2* (30 new sequences), covering the states of Morelos, México, Puebla, Oaxaca, Guerrero, Michoacán, Colima, and Jalisco (Table 1). The *ND4* and *ITS-2* genes were used due to their effectiveness in detecting possible cryptic species in the genus *Triatoma* (e.g., Gómez-Palacio et al., 2015; Pech-May et al., 2019). GenBank accession numbers of the sequences obtained in this study and those available from previous studies are listed in Supplementary Data SD1. Specimens were identified using the keys proposed by Lent and Wygodzinsky (1979).

2.2. Obtaining molecular data

Total genomic DNA was obtained from at least two legs of each individual following a modification of Fetzner (1999) method proposed by Cruz et al. (2020). The *ND4* gene was amplified by Polymerase Chain Reaction (PCR) using the primers proposed by Dotson and Beard (2001) (initiators: 5′ TCA ACA TGA GCC CTT GGA AG-3′ (F) and 5′ TAA TTC GTT GTC ATG GTA ATG-3′ (R)). A segment approximately 620 bp long was amplified. The conditions and parameters for PCR used were the same as Mayares (2014). The primers used for *ITS-2* gene amplification were ITS2-F (5′-CTAAGCGGTGGATCACTCGG-3′) and ITS2-R (5′-GCACTATCAAGCAACACGACTC-3′), proposed by Wong et al. (2016), and PCR conditions used were the same as Richards et al. (2013).

The samples were sequenced at Macrogen USA, Inc. (http://www.macrogenusa.com). The obtained sequences were edited with *CodonCode Aligner* v.8.0.2 (CodonCode Corporation, Dedham, MA) and aligned using the *Muscle* method (Edgar, 2004), using the default parameters in the program UGENE v.1.32.0 program (Okonechnikov et al., 2012).

2.3. Phylogenetic analysis

The best-fitting model of sequence evolution for both genes was selected using the Bayesian informative criterion (BIC) in ModelFinder v2. (Kalyaanamoorthy et al., 2017). ModelFinder determines whether the data needs to be partitioned by codons when using coding genes, as is the case of *ND4*. For *ND4*, the selected model of evolution was HKY+F+I for partitions 1+2 and HKY+F+G4 for partition 3. The best model of evolution selected for the *ITS-2* gene was F81.

Phylogenetic reconstruction was estimated under the Maximum Likelihood (ML) criterion in IQ-TREE v1.6.10 (Nguyen et al., 2015) and Bayesian inference reconstruction in MrBayes 3.2.2 (Ronquist and Huelsenbeck, 2003), considering the *ND4* gene separately and considering a concatenated file with information from both genes (1086 bp). In both cases, we used the sister species as the outgroup (as recommended by Nixon and Carpenter (1993), which in this case were two sequences of *T. phyllosoma* (Burmeister, 1835). Both analyses were performed in CIPRES Science Gateway (Miller et al., 2012).

In ML analysis, branch support was calculated using 10000 replicates of *Ultrafast Boostrap* (UFBoot; Minh et al., 2013). The GENESITE resampling strategy was used for the *ND4* gene alone and for the concatenated (*ND4*+*ITS-2*) dataset, which allows resampling of partitions and sites within the partitions (Gadagkar et al., 2005). UFBoot support values $\geq$ 95% support the hypothesis that a branch constitutes a true clade (Minh et al., 2013).

Bayesian inference for *ND4, ITS-2*, and the concatenated dataset (*ND4*+*ITS-2*) was performed using two independent runs with eight chains. Each run consisted of 10 million Metropolis Coupled Markov Chain Monte Carlo (MCMC) generations. The default parameters of the model were not modified, and trees were sampled every 1000 generations. We discarded the first 25% of the samples as burn-in and the two runs performed converged on very similar posterior estimates, with an average standard deviation of split frequencies of 0.005. The convergence and combination of both runs were visually assessed using Tracer v1.7.1 (Rambaut and Drummond 2007). The posterior probability (pP) was obtained for individual nodes by constructing a majority-rule consensus without discarding trees as *burn-in.* Pp values >= 0.95 were considered strongly supported (Huelsenbeck and Ronquist 2001).

2.4. Estimation of divergence times

We estimated the divergence times among *ND4* clades using Beast v1.7 (Drummond et al., 2012). For each gene partition (unlinked substitution model), we used the same parameters and models of nucleotide substitution as were used for the phylogenetic analyses. Trees were constructed under the assumptions of an uncorrelated lognormal relaxed-clock model to allow rate variation between branches (Arbogast et al., 2002). A nucleotide replacement rate of 0.11 substitutions/site/million years (Myr) was used. The priors for the molecular clock were normally distributed with a mean of 0.11 and standard deviation of 0.011 (Pech-May et al., 2019). Subsequent distributions of parameters were estimated using the Coalescent Exponential Growth option for the Metropolis-coupled Markov chain Monte Carlo (MCMC) analysis. The first 10% of the trees were discarded (burn-in). Posterior distribution of parameters, tree topology, and divergence times were determined using MCMC analysis with two runs of 10 million generations each, sampling trees every 1000 generations. The appropriate composition of the MCMC (convergence of independent runs) search was analyzed using Tracer v.1.7 (Rambaut and Drummond, 2007) by calculating the effective sample sizes (ESS>200) for each parameter. The maximum clade credibility tree was obtained using the TreeAnotator v.1.7 program in the Beast2 package and visualized using FigTree v.1.4 (Rambaut, 2014).

2.5. Cryptic species delimitation

The phylogenetic species concept (Cracraft, 1989; De Queiroz and Donoghue, 1990) was used to determine which lineages could be considered cryptic species. The validation of cryptic species was performed with three species delimitation methods: two distinct single locus methods using the *ND4* phylogenetic reconstructions and a multiple loci method, using the concatenated data. The *single-locus* methods used were the Multi-rate Poisson tree process (MPTP) (Kapli et al., 2017) and the Bayesian General Mixed Yule-Coalescent Model (bGMYC) (Reid and Carstens, 2012), while the multiple loci method was the Species Tree and Classification Estimation, Yarely (STACEY, Jones, 2017). The use of different species delimitation methods has been suggested since, according to Carstens et al. (2013), the correct delimitation must be based on the congruence among methods. These authors propose that if inconsistencies are found among methods, the inferences drawn from these analyses should be conservative, since it is preferable to fail to delimit species than to falsely delimit entities that do not represent real evolutionary lineages.

The mPTP method is based on the phylogenetic species concept (Cracraft, 1989; Queiroz and Donoghue 1990) and the number of nucleotide substitutions (branch lengths), using the Akaike informational criterion (AIC) to decide the number of species resulting from a given phylogenetic tree (Zhang et al., 2013). The analysis was developed using as input data the phylogenetic tree obtained by Bayesian inference. We used the default model specifications and MCMC characteristics from the Exelixis Lab platform (http://www.exelixis-lab.org).

The bGMYC method uses coalescence theory as a search principle and assumes that it is at the branching points of a tree that divergence of species (Yule process) or coalescence of lineages within a species occur (Zhang et al., 2013). The input data used were the 100 ultrametric trees derived from the analysis of divergence times, obtained in the LogCombiner v2.6.3 program of the BEAST2 package. The delimitation analysis was implemented in the bGMYC package (Reid and Carstens 2012) of the R library (R Core Team 2018) with the following input parameters: mcmc=100,000, burnin=90,000, thinning=100, t1=2, t2=8 (based on the upper range of species detected with mPTP considering outgroup), py1=0.5, py2=1.5, pc1=0.1, pc2=0.5, start=c(1.0, 0.1, 11), scale=c(20, 10, 5.00).

Genetic distances (Gd) among lineages suggested by both species' delimitation methods were calculated in MEGA ver 6.0 (Tamura et al., 2013) using the Kimura 2P mutational model. In this work, a Gd value > 3% was considered as the threshold for delimiting species.

The STACEY method uses the Birth-Death-collapsed tree model as prior and is implemented as a package within BEAST2. The SpeciesDelimitationAnalyzer (speciesDA.jar) program was used to calculate the frequency with which each pair of taxa were assigned to the same clade. In this program, the species.tree file generated by STACEY was used as input data (parameters: burnin=1000 collapse height=0.0001, and similarity cutoff=1.0).

2.6. Phylogeographic analyses

2.6.1. Diversity and genetic differentiation

We analyzed genetic diversity for each cryptic lineage detected with at least five sequences, since in previous studies these have been the minimum sequences numbers used for this type of analysis (Martinez-Hernandez et al., 2021) and considering only the information from the *ND4* gene. Lineages containing fewer than five individuals were excluded from the analysis. Several indices were calculated: number of mutations (η), number of segregating sites (S), number of unique sites (Su), mean number of differences by pairs (k), number of haplotypes (h), haplotype diversity (Hd), nucleotide diversity (π), and the nucleotide polymorphism index (Θ). All indices were estimated with DNASP v.6.12 (Rozas et al., 2017). Historical changes in the population size of *T. pallidipennis* were inferred from the estimation of the neutrality tests of Tajima (1989) and Fs (Fu, 1997). In addition, to complement the genetic distances, genetic differentiation (F_{ST}) among lineages was also calculated, with Arlequin v.3.5 (Excoffier and Lischer, 2010). To enable the values of F_{ST} to be interpreted correctly, the overall value of this index for *T. pallidipennis* was also calculated.

2.6.2. Haplotypic networks

To analyze the genealogical relationships among lineages, haplotypic networks were constructed with the *ND4* and *ITS-2* gene information separately. We used the median-joining (MJ) method assuming an epsilon of 0 and with 1000 permutations, in PopART ver.1.7 (Leigh and Bryant, 2015). This type of network makes it possible to recover recent evolutionary relationships and the distribution of genetic variation more explicitly in a geographical context (Cassens et al., 2003). Specifically, the median-joining method estimates the relative abundance of each haplotype and the genealogical relationships between them. In addition, it finds median vectors corresponding to theoretical consensus sequences, possible unsampled sequences, or extinct ancestral sequences using a parsimony criterion.

2.6.3. Population connectivity based on shared haplotypes

Genetic connectivity patterns were explored between the demarcated species within *T. pallidipennis* based on the delimitation methods. We used the method implemented by Chan et al., 2014, which integrates ecological niche models (ENM) and haplotype networks to estimate putative dispersal corridors based on habitat suitability and shared haplotypes. This analysis allows us to infer the existence of gene flow (population connectivity) or identify possible barriers to dispersal (Chan et al., 2014), as well as corroborate hypotheses about speciation processes among populations that display high genetic divergence.

We used the haplotypes obtained previously for both genes. For the ENM, Worldclim 2 bioclimatic layers database (Fick and Hijmans, 2017) with a spatial resolution of ~ 1 km^2 were used as environmental predictors, eliminating highly correlated variables (Pearson's r > 0.8; Supplementary Data S2). The occurrence points were the coordinates of the collection localities of the individuals present in the phylogeny. We complemented these data with coordinates obtained from the free database generated by Ramsey et al. (2015) (available at https://doi.org/10.5061/dryad.rq120). Occurrence data with inconsistent information were not included in the analysis.

We performed spatial thinning of occurrence to avoid

autocorrelation, using a minimum distance of 5 km between localities. The model calibration areas were determined with a minimum convex polygon. The data processing and selection of the best fit parameters for the construction of the final model were performed in the Wallace (Kass et al., 2018; Supplementary Data S2) R package. The final model was obtained in Maxent v3.4.1 (Phillips et al., 2006) with 50 bootstrap replicates and keeping the cloglog maxent output.

A database comprised of *ND4* and *ITS-2* haplotypes and the geographical coordinates of their site(s) of origin was used as input data in the landscape connectivity analysis. A friction layer was generated from the ENM obtained for *T. pallidipennis*, where the areas of little or no probability of presence of the species depicted areas of high cost for dispersal (Chan et al., 2014). Then, least-cost corridors and least-cost paths were calculated among the populations analyzed. For each comparison, the least cost paths were classified into three categories as suggested by Chan et al., 2014, and the least cost corridors with the highest connectivity values were interpreted as probable migration routes. This analysis was performed with the SDMtoolbox extension (Brown et al., 2017) in ArcGIS v10.1 (ESRI 2011).

3. Results

3.1. Phylogenetic analysis with the ND4 gene

The phylogenetic reconstruction under both criteria (ML and BI) converged on similar topologies and recovered, in both cases the monophyly of *Triatoma pallidipennis*. However, the ML tree presented unresolved relationships (polytomies) (FS1), while the BI tree did not. We therefore present only the results from the BI-based phylogeny (Fig. 1). *T. pallidipennis* was correctly separated from the outgroup *(T. phyllosoma)*.

The 73 individuals of *T. pallidipennis* were grouped into four highly supported clades, hereafter considered haplogroups (Pp > 0.95) within the phylogenetic tree (Fig. 1). Haplogroup I contained all specimens from Oaxaca and Puebla and most of the specimens from Morelos. Haplogroup II was the most heterogeneous; it included all specimens from Guerrero, some samples from Morelos (Localities of Puente de Ixtla and Vista Hermosa), and some from Mexico State (Locality of Tlataya). Haplogroup III contained individuals from Mexico State and the three specimens from Michoacán. Finally, haplogroup IV was composed of specimens from Jalisco and Colima (Fig. 1).

3.2. Phylogenetic analysis of the combined data

The topology of the BI-based phylogenetic reconstruction using the concatenated data was very similar to the *ND4*-based tree. The main haplogroups were recovered with high support values (pP >=0.95), despite the large reduction in samples. The main difference in terms of topology was that haplogroup III was more closely related to haplogroups I and II, while in the *ND4*-based phylogeny it was closer to haplogroup IV (Fig. 2).

3.3. Delimitation of cryptic species, genetic distances, and differentiation

When performing the species delimitation analysis using the *Multirate Poisson tree process* (MPTP) method, eight possible cryptic species

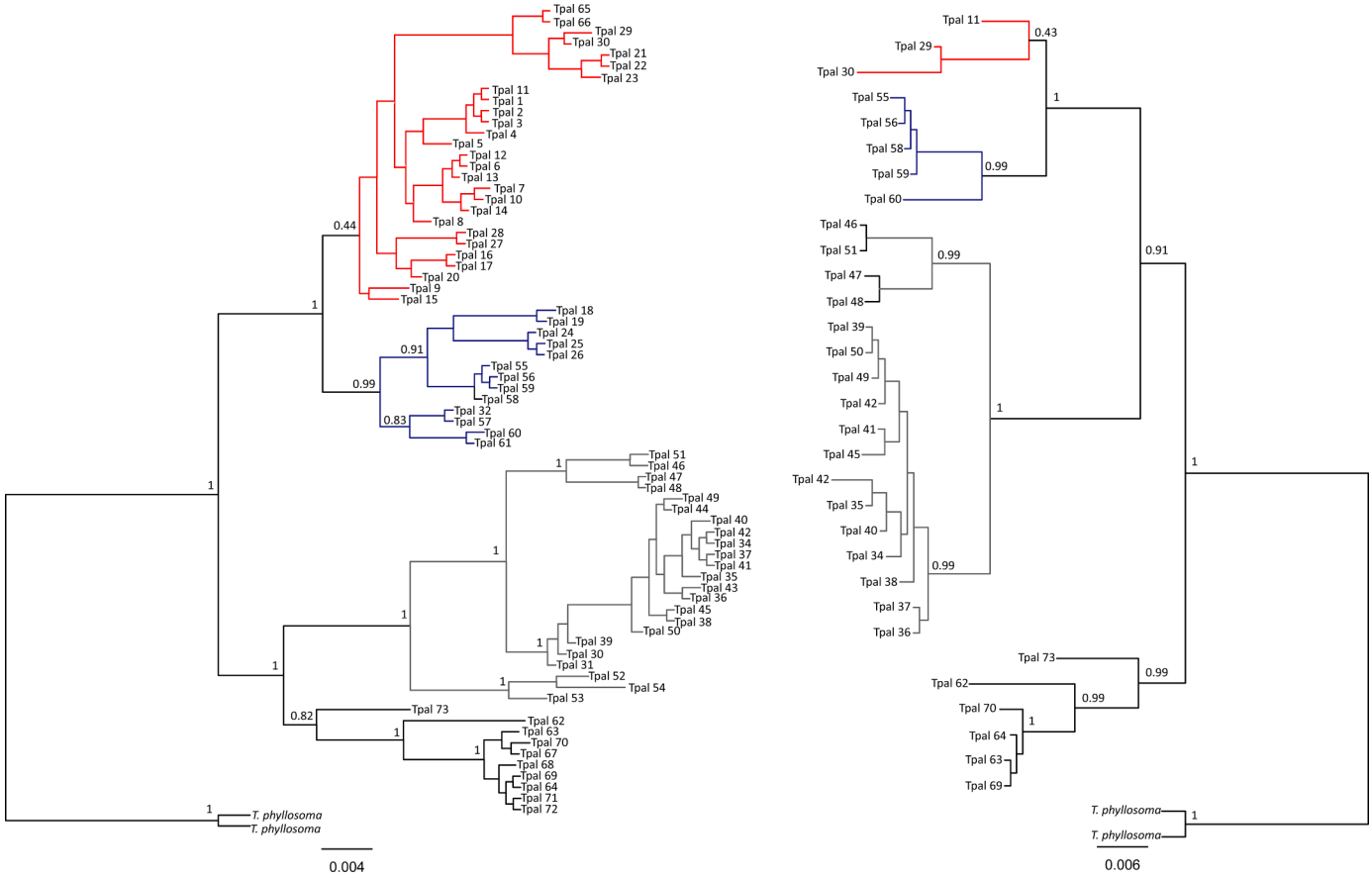

Fig. 1. Phylogenetic reconstruction using the *ND4* gene and the concatenated data matrix (*ND4*+ITS2 gene) for *Triatoma pallidipennis* (Hemiptera: Reduviidae: Triatominae), based on the Bayesian inference method. For *ND4* was implemented the evolutionary model HKY+F+I for partitions 1+2 and HKY+F+G4 for partition 3 and the evolutionary model F81 for *ITS-2*. Support values of subsequent probability are shown on the branches. Haplogroup I (Red), Haplogroup II (blue), Haplogroup III (grey), and Haplogroup IV (black).

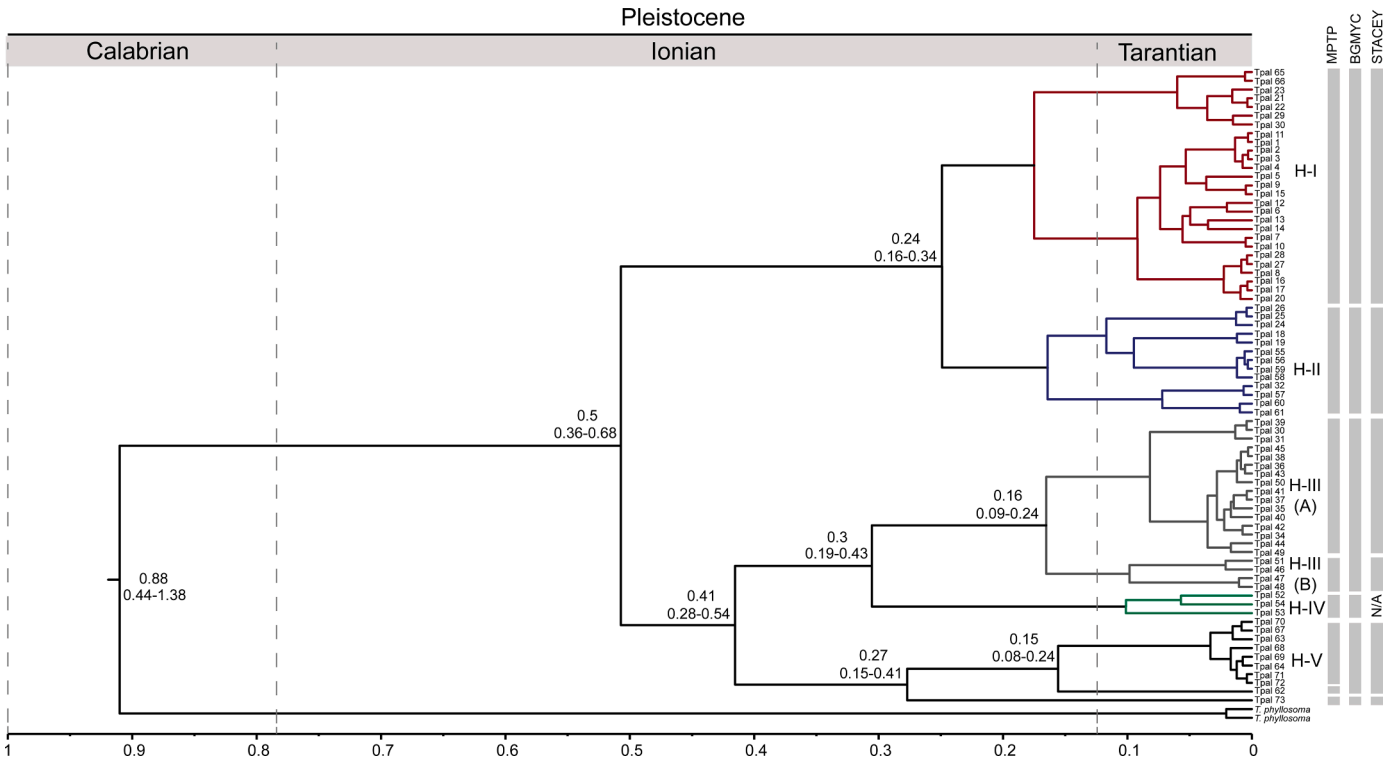

Fig. 2. *ND4* phylogeny estimated divergence times, and species delimitation in *Triatoma pallidipennis* (Hemiptera: Reduviidae: Triatominae) implementing the evolutionary model HKY+F+I for partitions 1+2 and HKY+F+G4 for partition 3. Divergence times (top) are shown above each branch. The bars on the right side of the figure correspond to the species delimitation obtained by the *Multi-rate Poisson Tree Process* (mPTP; leftmost), the *Bayesian General Mixed Yule-Coalescent Model* (bGMYC; middle), and the Species Tree And Classification *Estimation, Yarely* (STACEY; rightmost).

(haplogroups) were obtained, all with high support values (≥0.95) (Fig. 2). When comparing with the groupings defined when analyzing the BI phylogenetic tree, the main differences were that haplogroup III was split into two groups (H-IIIA and H-IIIB) and that the specimens from Michoacán formed a new haplogroup. Also, under this method of delimitation, one specimen from Colima (Tpal 73) and one from Jalisco (Tpal 62) were each proposed as new taxonomic entities.

Under the *Bayesian General Mixed Yule-Coalescent Model* (bGMYC), six possible cryptic species with support ≥0.95 were detected. Four of the haplogroups coincided with those predicted by the mPTP; all specimens from haplogroup III were maintained as a single taxonomic entity, as was the individual from Jalisco (Tpal 62) (Fig. 2).

The STACEY method using the concatenated dataset proposed six cryptic species (Fig. 2), without considering the specimens from Michoacán, since they did not present data for *ITS-2*. This method was consistent with the mPTP proposal in that haplogroup III was split into two lineages, while haplogroup V was proposed with the same delimitation as in the bGMYC.

Genetic distances between haplogroups of *T. pallidipennis* ranged from 3.081 to 7.340%. The lowest Gd values were between haplogroup V and the individual from Jalisco that was proposed as a separate entity (2.820%) and between the two subclades of haplogroup III (H-IIIA and H-IIIB), with a value of 2.946% (Table 2). The Gd values were above 3% for all pairs of clades except between haplogroups I and II and between the two subclades of haplogroup III. Given the low Gd value between the subclades of haplogroup III, we considered haplogroup III to be a single entity in the rest of the analyses. All pairwise comparisons of F_{ST} values were statistically significant.

3.4. Divergence times

The ultrametric tree converged on a topology identical to the BI-based tree for *ND4* gene (Fig. 2). The divergence times estimated for each of the possible cryptic species placed the initial divergence of the haplogroups at about 0.5 Mya (time to the most recent common ancestor). Haplogroups I and II began to diverge about 0.24 Mya (95% HPD=0.16–0.34), while haplogroup V diverged from the most recent ancestor of H-III and H-IV about 0.41 Mya (95% HPD=0.28–0.54). These values place haplogroup V as the most ancestral clade in *T. pallidipennis*.

3.5. Genetic diversity among haplogroups of Triatoma pallidipennis

When comparing genetic diversity among four of the five haplogroups (haplogroup IV was not included because of its low representativeness), differences were found between most estimators. We found 18, 8, 10, and 6 haplotypes for haplogroups I, II, III, and V, respectively. Haplotypic diversity (Hd) was high only for haplogroup I. For the rest of haplogroups, values of Hd were 0.89. Low nucleotide diversity index (π) and nucleotide polymorphism (Θ) were obtained for all analyzed haplogroups. Haplogroup I was the most variable based on π and Θ values obtained. The neutrality analysis based on Fús test was negative in all haplogroups, except in haplogroup II. However, was statistically significant ($p < 0.05$) only for haplogroup I (Table 3). Tajimás Test D was negative in all haplogroups, except in haplogroup II.

3.6. Haplotype networks and population connectivity based on shared haplotypes

For all the samples analyzed, 44 haplotypes were obtained, of which 40 were unique and 2 shared for the *ND4* gene matrix. The populations from Mexico State and Guerrero shared one haplotype, as did the populations of Jalisco and Colima (Fig. 3). Spatial segregation was consistent with the phylogenetic analysis. The haplogroups detected by the phylogeny were separated by at least six (and up to 16) mutational steps. We could not perform the connectivity analysis due to the small number

Table 1
Samples used for the phylogeographic analysis of *Triatoma pallidipennis* (Hemiptera: Reduviidae: Triatominae) in Mexico. Samples from GenBank are marked with*.

State	Municipality	Locality	Code	*ND4*samples	*ITS-2* samples
Morelos	Cuernavaca*	Cuernavaca	Tpal_1-8	8	-
	Jiutepec*	Jiutepec	Tpal_9-10	2	-
	Jantetelco*	Chalcatzingo	Tpal_11-15	5	1
	Puente de Ixtla*	Ahuehuetzingo	Tpal_16-17	2	-
	Puente de Ixtla*	Puente de Ixtla	Tpal_18	1	-
	Puente de Ixtla*	Vista Hermosa	Tpal_19	1	-
	Puente de Ixtla*	Xoxocotla	Tpal_20	1	-
	Axochiapan*	Quebrantadero	Tpal_21-22	2	-
	Axochiapan*	Atlacahualoya	Tpal_23	1	-
	Amacuzac	Teacalco	Tpal_24-26	3	-
Puebla	Jolalpan*	Jolalpan	Tpal_27-28	2	-
	Huatlatlauca	-	Tpal_29-30	2	2
State of México	Tlatlaya*	Juntas	Tpal_31-33	3	-
	Toluca	San Nicolás Tolentino	Tpal_34-36	3	3
	Ixtapan del Oro	Tutuapan	Tpal_37	1	1
	Ixtapan del Oro	Milpillas	Tpal_38-39	2	2
	Otzoloapan	-	Tpal_40	1	1
	Otzoloapan	Otzoloapan	Tpal_41-42	2	2
	Otzoloapan	San Martín	Tpal_43-44	2	2
	Zacazonapan	La Cañada	Tpal_45	1	1
	Sultepec	Laguna Seca	Tpal_46	1	1
	Tejupilco	La Labor	Tpal_47-48	2	2
	Santo Tomás	San Pedro	Tpal_49	1	1
	Santo Tomás	Santo Tomás	Tpal_50	1	1
	Luvianos	Caja de Agua	Tpal_51	1	1
Michoacán	Taretan*	Taretan	Tpal_52	1	-
	Turicato	Puruaran	Tpal_53	1	-
	Tacámbaro	Parocho	Tpal_54	1	-
Guerrero	Taxco	Joyas del Progreso	Tpal_55	1	1
	Pilcaya*	Cacahuamilpa	Tpal_56	1	-
	Chilpancingo	Chilpancingo	Tpal_57	1	1
	Chilpancingo	Colonia 21 de septiembre	Tpal_58	1	-
	Chilpancingo	Colonia Ángel Aguirre	Tpal_59-60	2	2
	E. Neri	Zumpango	Tpal_61	1	-
Jalisco	Autlán	Autlán	Tpal_62-64	3	3
Oaxaca	Mariscala de Juárez	Santa Frayle*	Tpal_65-66	2	-
Colima	Comala*	Comala	Tpal_67-68	2	-
	Comala	Comala	Tpal_69	1	1
	Cuauthemoc	Palmillas	Tpal_70	1	1
	Coquimatlán	Los Limones	Tpal_71	1	-
	Ixtlahuacán	La Tepamera	Tpal_72	1	X
	Tecomán	San Miguel del Ojo de Agua	Tpal_73	1	1
T. phyllosoma	Oaxaca			2	2

Table 2
Genetic distances (K2P) / genetic differentiation (Fst) between haplogroups of *Triatoma pallidipennis* (Hemiptera: Reduviidae: Triatominae) in Mexico.

	H-I	H-II	H-IIIA	H-IIIB	H-IV	H-V	Colima
H-I		0.349*	0.758*	0.929*	0.628*	0.931*	-
H-II	3.196		0.814*	0.934*	0.682*	0.946*	-
H-IIIA	6.258	6.215		0.969*	0.829*	0.975*	-
H-IIIB	6.618	6.760	2.946		0.928*	0.804*	-
H-IV	6.005	6.123	4.612	4.972		0.951*	-
H-V	4.911	5.882	6.459	6.143	5.464		-
Colima	4.744	5.395	6.108	5.905	5.081	3.414	
Jalisco	5.125	5.675	5.842	5.445	5.074	2.820	4.211

* Statistical significance ($p < 0.05$). H= Haplogroup.

of populations that shared haplotypes of this gene.

For the *ITS-2* matrix, there were 10 haplotypes, of which 8 were unique and 2 shared. Haplotype 10 was shared by four populations of *T. pallidipennis*, while haplotype 4 was shared between populations from Jalisco and Colima (Fig. 4), similar to the *ND4* gene.

The dispersal network obtained from the niche model (Fig. 5A) transformed to a friction layer (Fig. 5B) among sites based on shared *ITS-2* haplotypes did not show potential migration routes among the haplogroups delimited as species-level clades by STACEY (Fig. 5C). Within haplogroup V, there was a possible migration route between populations from Jalisco and Colima, but it was supported by relatively low

Table 3
Indices of genetic diversity among haplogroups of *Triatoma pallidipennis* (Hemiptera: Triatominae).

	H-I	H-II	H-III	H-V	Global
N	28	13	20	8	73
η	44	24	24	21	91
S	44	24	23	21	86
Su	574	596	596	597	527
k	10.33	8.744	6.495	5.714	21.087
h	18	8	10	6	44
Hd + sd	0.960 ± 0.020	0.897 ± 0.067	0.895 ± 0.043	0.893 ± 0.111	0.979 ± 0.006
π + sd	0.020 ± 0.003	0.017 ± 0.001	0.012 ± 0.002	0.009 ± 0.004	0.041 ± 0.001
Θ + sd	0.022 ± 0.007	0.015 ± 0.006	0.012 + 0.004	0.009 ± 0.006	0.034 ± 0.009
Fuś test Fs	-2.587*	0.79	-0.96	-0.208	-5.649*
Tajimaś Test D	-0.322	0.5654	-0.154	-1.536	0.428

Number of sequences (N), number of mutations (η), number of segregating sites (S), number of unique sites (Su), mean number of pair differences (k), number of haplotypes (h), haplotypic diversity (Hd), nucleotide diversity (π) and nucleotide polymorphism index (Θ), standard deviation (de). Fu (1996), Tajima Fs and D index (Tajima, 1989).

* Statistical significance ($p < 0.05$).

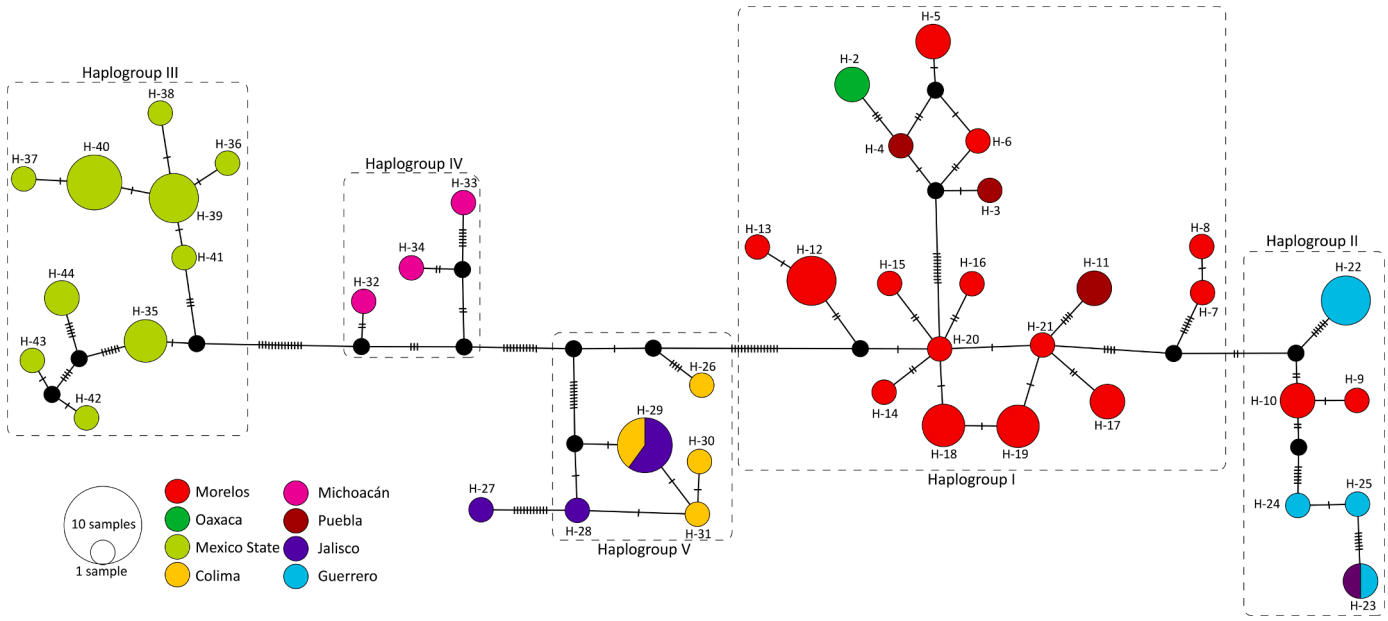

Fig. 3. Haplotype network (median joining) showing the relationships among the 44 haplotypes obtained from a genetic matrix for the *ND4* gene, detected for *Triatoma pallidipennis* (Hemiptera: Reduviidae: Triatominae). Each bar across the solid line represents a nucleotide difference between the haplotypes. Black dots are hypothetical vectors representing theoretical consensus sequences (not sampled or extinct).

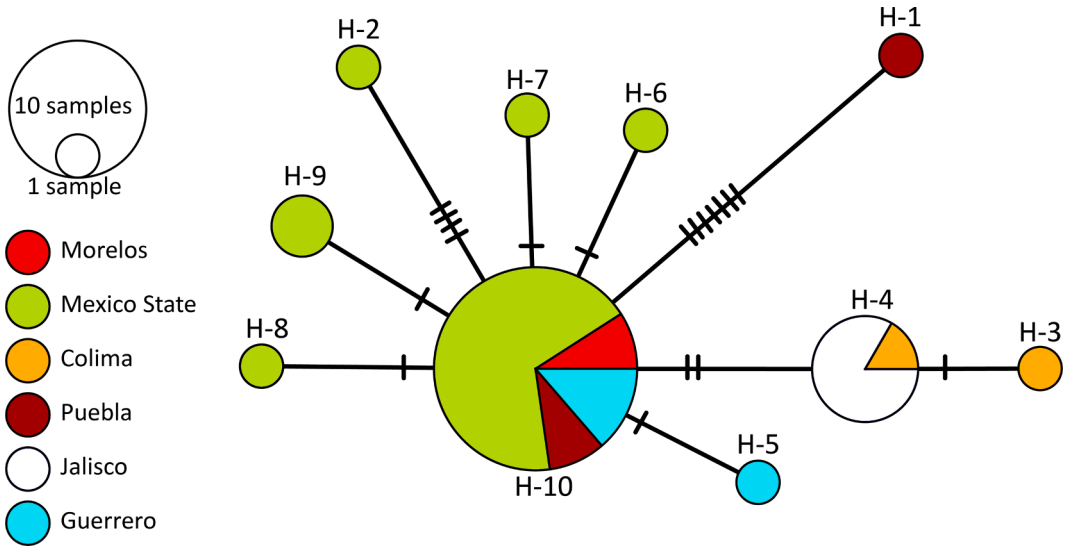

Fig. 4. Haplotype network (median joining) showing the relationships between the 10 haplotypes obtained from a genetic matrix for the *ITS-2* gene detected for *Triatoma pallidipennis* (Hemiptera: Reduviidae: Triatominae). Each bar across the solid line represents a nucleotide difference between the haplotypes.

connectivity values. High connectivity values were found towards the interior of haplogroup III (Mexico State). Among haplogroups, connectivity routes were observed between haplogroups III (Mexico State) and II (Guerrero) and between haplogroups I (Morelos-Oaxaca-Puebla) and III. However, in both cases, the routes had low to medium connectivity (Fig. 5C)

4. Discussion

4.1. Species delimitation

Our results demonstrate the presence of cryptic species in what has so far been considered a single taxonomic entity (Cortés-Jiménez et al., 1996; Ramsey et al., 2015) Lent and Wygodzinsky (1979). found important morphological variations between specimens of *T. pallidipennis*, to the point of doubting whether they were really the same taxonomic entity. More recently, the possibility that *T. pallidipennis* was a complex of cryptic species was previously addressed by Harris (2003) and Mayares (2014). However, previous studies did not have a high geographical representativeness of the species and did not use specific methods of cryptic species delimitation. Thus, our analysis is the most comprehensive phylogenetic reconstruction for this species so far, allowing us to achieve greater geographical representativeness over the known distribution of the species and implement specific analysis methods to answer the question of cryptic species.

There were inconsistencies in species delimitation between the mPTP (eight possible species), the bGMYC (six possible species), and the STACEY (six possible species). Despite these inconsistencies (which were restricted to differences in divisions within haplogroups III and V), it should be noted that all three delimitation methods agreed that the

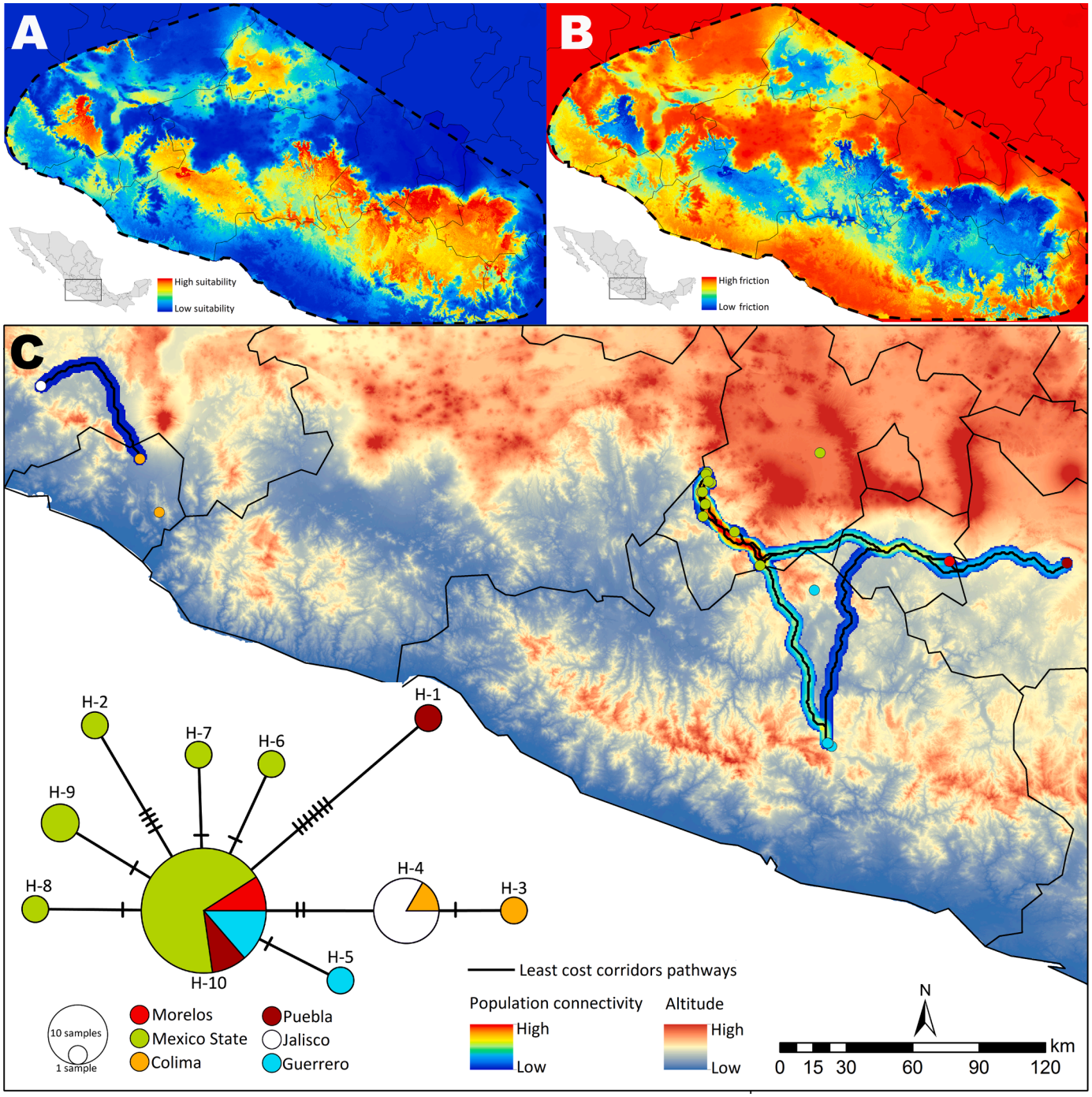

Fig. 5. Landscape connectivity analysis based on *ITS-2* shared haplotypes for *Triatoma pallidipennis*. (A) Ecological niche model. (B) Friction layer obtained from Ecological niche modeling. (C) *ITS-2* haplotype network and dispersal network among *Triatoma pallidipennis* populations. Dashed lines represent the calibration area of the ecological niche model.

five haplogroups constitute taxonomic entities (See Fig. 3; Supplementary Data S3). This is further supported by pairwise genetic distances greater than 3% and 6–16 mutational steps between haplogroups, suggesting important genetic differences among the haplogroups. Finally, the low connectivity values obtained from the *ITS-2* dispersal network among haplogroups provides another line of evidence that allows us to confirm that *T. pallidipennis* is indeed a complex of cryptic species.

Both the mPTP and STACEY methods proposed the separation of haplogroup III into two different taxonomic entities (while bGMYC did not). These two groups correspond to localities of Tlatlaya, Toluca, Ixtapán del Oro, Otzoloapan, Zacazonapan and Santo Tomás (H-IIIA), and Luvianos, Sultepec and Tejupilco (H-IIIB), respectively, all of them from Mexico state. When calculating the Gd between these two groups, this value was 2.946, just below the 3% threshold used in this study to support lineage divergence, based on previous work with *ND4* gene to delimit *Triatoma* haplogroups (Mayares, 2014; Pech-May et al., 2019). Also, there were high connectivity values in the *ITS-2* dispersal network among the populations in Mexico State, suggesting gene flow among those populations. For these reasons, we accept the proposal of the bGMYC method and considers haplogroup III as a single taxonomic entity. However, these populations may be undergoing a speciation event that is still unfinished (Futuyma, 2013), a hypothesis which is

supported by significant genetic differentiation (Fst) between them.

The other incongruity observed was between the specimens of Colima and Jalisco. The mPTP recognized three different taxonomic entities in these populations, separating two indviduals from the main clade into their own clades—one from Colima (Tpal 72) and one from Jalisco (Tpal 62). However, bGMYC and STACEY only separated Tpal 72 from the main clade, resulting in two (rather than three) taxonomic entities. Tpal 72 and Tpal 62 had Gd values of 3.414 and 2.820%, respectively, from the rest of the specimens from Haplogroup V. The value found for Tpal 62 remains below the 3% threshold we considered to validate new taxonomic entities, so we accept the proposal from the coalescent methods. Although Tpal_72 had a GD value greater than 3%, the Pp support for the position of this terminal on the tree obtained by BI with the *ND4* gene matrix was low (0.63). Therefore, caution should be taken to propose this specimen as a new taxonomic entity. Increased sampling of localities in the state of Colima and surrounding regions will clarify the taxonomic position of this individual.

According to Carstens et al. (2013), when delimiting cryptic species, it is advisable to apply different methods of delimitation and base decisions on the congruences between methods. The haplogroups detected in this work confirm the those reported by Harris (2003), and adds new lineages for the states of Michoacán and Mexico State. With respect to the proposal made by Harris (2003) to consider the specimens from Colima as a new species, our work reaffirms this decision and includes the individuals of Jalisco as part of this new taxonomic entity.

4.2. Divergence times

From the ultrametric tree constructed using the *ND4* gene, we estimate that *T. pallidipennis* diverged approximately 0.88 Mya ago (95% HPD = 0.44–1.38), which is relatively recently in evolutionary time. These results are similar to those reported by Harris (2003), who found that *T. pallidipennis* diverged approximately 1–2.3 million years ago. Although our results overlap with the range of dates proposed by Harris (2003), the values found in this study are more recent, which is likely due to our use of *T. phyllosoma,* the sister species of *T. pallidipennis*, as the outgroup. This allowed us to estimate divergence times with greater resolution than Harris (2003), since was used *T. dimidiata,* a more ancestral species, as the outgroup, which modifies the divergence time found. However, it has been shown that the accuracy of divergence time estimates is dependent on many factors, including evolutionary model selection and rate variation among lineages (Ho, 2014; Ho and Duchêne, 2014), among others. Our results therefore need to be considered with caution, since our divergence time estimates are based on a single locus (*ND4*), mostly because of the size sample.

Estimates of the divergence time of each of the defined haplogroups shows that they began to diverge about 0.5 Mya ago. This suggests the possible recent origin of these cryptic species in the mid-Pleistocene, specifically in the Ionian subperiod. This coincides with Ibarra-Cerdeña et al., (2014), who estimated that speciation events in Neotropical triatomines occurred mainly during the Pleistocene. This epoch was characterized by more than nine interglacial cycles of different magnitudes, recorded from approximately 0.97 Mya on the American continent, alternating between cold and semi-arid conditions during glaciations and warm and humid conditions during the interglacial or deglaciation periods (Clapperton, 1993; Benedetto, 2012) The divergence times found for these lineages are relatively similar to the divergence times found for other haplogroups in the genus *Triatoma,* for example, in *T. dimidiata* (Pech-May et al., 2019).

4.3. Diversity and genetic differentiation between haplogroups

The haplotypic diversity observed was only greater than 0.9 for Haplogroup I. In the rest of the haplogroups, the values were around 0.89. Nucleotide diversity values were low in all happlogroups, suggesting that populations underwent bottlenecks (Lowe et al., 2004). Both results together indicate that, although haplotypes are diverse, the differences between them are few, suggesting that they have arisen recently and therefore may be closely related. The large number of haplotypes found with a low differentiation between them is explained by a rapid accumulation of mutations over a short time, which has not been enough to allow them to be eliminated or fixed within populations (Grant and Bowen, 1998). The presence of high values of genetic differentiation (Fst) between haplogroups indicates that there are marked genetic differences, indicating a negligible or total absence of genetic exchange between them. Similar genetic differentiations have been previously reported for the *ND4* gene (Grisales et al., 2010; Gomez-Palacio and Triana, 2014; Pech-May et al., 2019).

4.4. Final considerations

Our results confirm that *T. pallidipennis* is a complex of cryptic species, an aspect that has been addressed previously but that, due to the lack of geographical representation and the absence of robust methods for the delimitation of species, could not be confirmed. Thus, this work finally updates the debated taxonomic status of *Triatoma pallidipennis.* Based on our results, we propose that each of the haplogroups of *T. pallidipennis* should be recognized as valid species. However, other studies that provide morphological and ecological elements in addition to the existing genetic information are necessary to formally describe these new species [based on integrative taxonomy (Alevi et al., 2021)].

An important aspect derived from our work is the usefulness of species delimitation methods to clarify species limits in the genus *Triatoma*. This is not common in studies similar to ours (see Bargues et al., 2008; Pech-May et al., 2019), and its use should be a good practice in the future, due to its usefulness and robustness to answer taxonomic and evolutionary questions in the genus.

On the other hand, the presence of this new complex of cryptic species opens new questions regarding its evolutionary position within the genus, and even more so within the *Phyllosoma* complex. Classic and recent phylogenetic reconstructions that have included *Triatoma pallidipennis* have lacked representation of specimens from different localities, with Morelos being the most used. (see Argues et al., 2000; Ibarra-Cerdeña et al., 2014; Justi et al., 2014, 2016). Therefore, future phylogenetic reconstructions should consider the presence of these new cryptic lineages and clarify their relationship with the rest of the species, or at least species distributed in Mexico.

Supporting information

Supplementary data S1

CRediT authorship contribution statement

Daryl D. Cruz: Conceptualization, Methodology, Formal analysis, Writing – original draft, Writing – review & editing. **Elizabeth Arellano:** Conceptualization, Methodology, Writing – review & editing.

Declaration of Competing Interest

The authors declare that they have no known competing financial interests or personal relationships that could have appeared to influence the work reported in this paper.

Acknowledgments

We would like to extend our thanks to Dr. María Magdalena Ramírez Martínez, Dr. Imelda Medina and the INDRE Entomology Laboratory for providing samples. This study was supported by the CONACYT scholarship program 2018-000012-01NACF-11846.

Supplementary materials

Supplementary material associated with this article can be found, in the online version, at doi:10.1016/j.actatropica.2022.106382.

References

Abad-Franch, F., Monteiro, F.A., 2005. Molecular research and the control of Chagas disease vectors. Anais Acad. Bras. Ciênc. 77 (3), 437–454.

Agapow, P.M., Bininda-Emonds, O.R., Crandall, K.A., Gittleman, J.L., Mace, G.M., et al., 2004. The impact of species concept on biodiversity studies. Q. Rev. Biol. 79 (2), 161–179.

Alevi, K.C.C., Mendonça, P.P., Pereira, N.P., Rosa, J.A., Azeredo-Oliveira, M.T.V., 2012. Karyotype of *Triatoma* melanocephala Neiva & Pinto (1923). Does this species fit in the Brasiliensis subcomplex? Infect. Genet. Evol. 12, 1652–1653.

Alevi, K.C.C., Oliveira, J., Azeredo-Oliveira, M.T.V., Rosa, J.A., 2017a. *Triatoma* vitticeps subcomplex (Hemiptera, Reduviidae, Triatominae): a new grouping of Chagas disease vectors from South America. Parasites Vectors 10, 180.

Alevi, K.C.C., Guerra, A.L., Imperador, C.H.L., Jurberg, J., Moreira, F.F.F., et al., 2017b. Mitochondrial gene confirms the specific status of *Triatoma* pintodiasi jurberg, cunha, and rocha, 2013 (Hemiptera, Triatominae), an endemic species in Brazil. Am. J. Trop. Med. Hyg. 96 (1), 200.

Alevi, K.C.C., Garcia, A.C.C., Guerra, A.L., Moreira, F.F.F., de Oliveira, J., et al., 2018. *Triatoma* vitticeps (Stal, 1859) (Hemiptera, Triatominae): a Chagas disease vector or a complex of vectors? Am. J. Trop. Med. Hyg. 99 (4), 954.

Alevi, K.C.C., Oliveira, J., Garcia, A.C.C., Cristal, D.C., Delgado, L.M.G., et al., 2020. *Triatoma* rosai sp. Nov. (Hemiptera, Triatominae): a new species of Argentinian Chagas disease vector described based on integrative taxonomy. Insects 11, 830.

Alevi, K.C.C., de Oliveira, J., Rocha, D.S., Galvão, C., 2021. Trends in taxonomy of Chagas disease vectors (Hemiptera, Reduviidae, Triatominae): from linnaean to integrative taxonomy. Pathogens 10, 1627.

Arbogast, B.S., Edwards, S.V., Wakeley, J., Beerli, P., Slowinski, J.B., 2002. Estimating divergence times from molecular data on phylogenetic and population genetic timescales. Annu. Rev. Ecol. Syst. 33, 707–740.

Argues, M.D., Marcilla, A., Ramsey, J.M., Dujardin, J.P., Schofield, C.J., Mas-Coma, S., 2000. Nuclear rDNA-based molecular clock of the evolution of Triatominae (Hemiptera: Reduviidae), vectors of Chagas disease. Mem. Inst. Oswaldo Cruz 95 (4), 567–573.

Bargues, M.D., Klisiowicz, D.R., Gonzalez-Candelas, F., Ramsey, J.M., Monroy, C., et al., 2008. Phylogeography and genetic variation of *Triatoma* dimidiata, the main Chagas disease vector in central America, and its position within the genus *Triatoma*. PLoS Negl. Trop. Dis. 2 (5), e233. https://doi.org/10.1371/journal.pntd.0000233.

Benedetto, J.L., 2012. The Continent of Gondwana Through Time, An Introduction to Historical Geology. National Academy of Sciences, Córdoba. Argentina.

Brown, J.L., Bennett, J.R., French, C.M., 2017. SDMtoolbox 2.0: the next generation python-based GIS toolkit for landscape genetic, biogeographic and species distribution model analyses. PeerJ 5, e4095.

Burmeister, H, 1835. Handbuch der Entomologie, 2. Berlin, pp. 1–400.

Bustamante, D.M., Monroy, C., Menes, M., Rodas, A., Salazar-Schettino, P.M., et al., 2004. Metric variation among geographic populations of the Chagas vector *Triatoma* dimidiata (Hemiptera: Reduviidae: Triatominae) and related species. J. Med. Entomol. 41, 296–301.

Caldecott, J.O., Jenkins, M.D., Johnson, T.H., Groombridge, B., 1996. Priorities for conserving global species richness and endemism. Biodivers. Conserv. 5 (6), 699–727.

Cardoso, A., Serrano, A., Vogler, A.P., 2009. Morphological and molecular variation in tiger beetles of the cicindela hybrida complex: is an 'integrative taxonomy' possible? Mol. Ecol. 18, 648–664.

Carstens, B.C., Pelletier, T.A., Reid, N.M., Satler, J.D., 2013. How to fail at species delimitation. Mol. Ecol. 22 (17), 4369–4383.

Cassens, I., Van Waerebeek, K., Best, P.B., Crespo, E.A., Reyes, J., Milinkovitch, M.C., 2003. The phylogeography of dusky dolphins (lagenorhynchus obscurus): a critical examination of network methods and rooting procedures. Mol. Ecol. 12 (7), 1781–1792.

Cesaretto, N.R., Oliveira, J., Ravazi, A., Madeira, F.F., Reis, Y.V., Oliveira, A.B.B., Vicente, R.D., Cristal, D.C., Galvão, C., Azeredo-Oliveira, M.T.V., Rosa, J.A., Alevi, K. C.C, 2021. Trends in taxonomy of triatomini (Hemiptera, Reduviidae, Triatominae): reproductive compatibility reinforces the synonymization of meccus Stål, 1859 with *Triatoma* laporte, 1832. Parasites Vectors 14, 340.

Chan, L.M., Brown, J.L., Yoder, A.D., 2014. Integrating statistical genetic and geospatial methods brings new power to phylogeography. Mol. Phylogenet. Evol. 59, 523–537.

Clapperton, C.M., 1993. Nature of environmental changes in South America at the last glacial maximum. Palaeogeogr. Palaeoclimatol. Palaeoecol. 101 (3-4), 189–208.

Cortés-Jiménez, M., Nogueda-Torres, B., Alejandre-Aguilar, R., Isita-Torneli, L., Ramírez-Moreno, E., 1996. Frequency of triatomines infected with trypanosoma cruzi collected in cuernavaca city, Morelos, Mexico. Rev. Latinoam. Microbiol. 38, 115–119.

Cracraft, J., 1989. Speciation and its ontology: the empirical consequences of alternative species concepts for understanding patterns and processes of differentiation. Speciat. Conseq. 28, 59.

Cruz, D.D., Nava-García, E., Arellano, E., 2020. An improved and low-cost protocol for high-quality DNA isolation for the Chagas disease vectors. Infect. Genet. Evol. 80, 104201.

De Queiroz, K., 2007. Species concepts and species delimitation. Syst. Biol. 56 (6), 879–886.

De Queiroz, K., Donoghue, M.J., 1990. Phylogenetic systematics or Nelson's version of cladistics? Cladistics 6, 61–75.

Dorn, P.L., Justi, S.A., Dale, C., Stevens, L., Galvão, C., et al., 2018. Description of *Triatoma* mopan sp. n. from a cave in belize (Hemiptera, Reduviidae, Triatominae). Zookeys (775), 69.

Dotson, E., Beard, C.B., 2001. Sequence and organization of the mitochondrial genome of the Chagas disease vector, *Triatoma* dimidiata. Insect Mol. Biol. 10, 205–215.

Drummond, A.J., Suchard, M.A., Xie, D., Rambaut, A., 2012. Bayesian phylogenetics with BEAUti and the BEAST 1.7. Mol. Biol. Evol. 29, 1969–1973.

Edgar, R.C., 2004. MUSCLE: multiple sequence alignment with high accuracy and high throughput. Nucl. Acids Res. 32, 1792–1797.

ESRI, 2011. ArcGIS Desktop Release 10. Environmental System Research Institute, Inc, Redlands, CA.

Excoffier, L., Lischer, H.E., 2010. Arlequin suite ver 3.5: a new series of programs to perform population genetics analyses under linux and windows. Mol. Ecol. Resour. 10 (3), 564–567.

Fetzner, J.W., 1999. Extracting high-quality DNA from shed reptile skins: a simplified method. BioTechniques 26 (6), 1052–1054.

Fick, S.E., Hijmans, R.J., 2017. WorldClim 2: new 1-km spatial resolution climate surfaces for global land areas. Int. J. Climatol. 37 (12), 4302–4315.

Flores, A., Magallón-Gastélum, E.M.F., Bosseno, R., Ordoñez, F.L., Kasten, B., et al., 2001. Isoenzyme variability of five principal triatomine vector species of Chagas disease in Mexico. Infect. Genet. Evol. 1, 21–28.

Fu, Y.X., 1997. Statistical test of neutrality of mutation against population growth, hitchhiking and background selection. Genetics 147 (2), 915–925.

Futuyma, D.J., 2013. Evolution, 3rd ed. Sinauer Associates Inc, Sunderland, MA.

Gadagkar, S.R., Rosenberg, M.S., Kumar, S., 2005. Inferring species phylogenies from multiple genes: concatenated sequence tree versus consensus gene tree. J. Exp. Zool. Part B Mol. Dev. Evol. 304, 64–74.

Garcia, A.C.C., Oliveira, J., Cristal, D.C, Delgado, L.M.G., Bittinelli, I.F., et al., 2021. Intraspecific and interspecific phenotypic differences confirm the absence of cryptic speciation in *Triatoma* sordida (Hemiptera, Triatominae). Am. J. Trop. Med. Hyg. 105, 1759–1766.

Gomez-Palacio, A., Triana, O., 2014. Molecular evidence of demographic expansion of the Chagas disease vector *Triatoma* dimidiata (Hemiptera, Reduviidae, Triatominae) in Colombia. PLoS Negl.Trop. Dis. 8 (3), e2734. https://doi.org/10.1371/journal.pntd.0002734. PMID: 24625572.

Gómez-Palacio, A., Arboleda, S., Dumonteil, E., Peterson, A.T., 2015. Ecological niche and geographic distribution of the Chagas disease vector, *Triatoma* dimidiata (Reduviidae: Triatominae): evidence for niche differentiation among cryptic species. Infect. Genet. Evol. 36, 15–22.

Grant, W.S., Bowen, B.W., 1998. Shallow population histories in deep evolutionary lineages of marine fishes: insights from sardines and anchovies and lessons for conservation. J. Hered. 89, 415–425.

Grisales, N., Triana, O., Angulo, V., Jaramillo, N., Parra-Henao, G., et al., 2010. Genetic differentiation of three colombian populations of *Triatoma* dimidiata (Latreille, 1811) by molecular analysis of the mitochondrial gene ND4. Biomedical 30, 207–214.

Gurgel-Goncalves, R., Ferreira, J.B.C., Rosa, A.F., Bar, M.E., Galvao, C., 2011. Geometric morphometrics and ecological niche modelling for delimitation of near-sibling triatomine species. Med. Vet. Entomol. 25 (1), 93, 84.

Harris, K., 2003. Taxonomy and Phylogeny of North American Triatominae: Public Health Implications. Moorehouse School of Medicine, Atlanta, GA. Doctoral Thesis.

Ho, S., 2014. The changing face of the molecular clock. Trends Ecol. Evol. 29, 496–503.

Ho, S., Duchêne, S., 2014. Molecular-clock methods for estimating evolutionary rates and timescales. Mol. Ecol. 23 (24), 5947–5965.

Huelsenbeck, J.P., Ronquist, F., 2001. MRBAYES: Bayesian inference of phylogenetic trees. Bioinformatics 17, 754–755 (Oxford, England).

Ibarra-Cerdeña, C.N., Zaldívar-Riverón, A., Peterson, A.T., Sánchez-Cordero, V., Ramsey, J.M., 2014. Phylogeny and niche conservatism in north and central American triatomine bugs (Hemiptera: Reduviidae: Triatominae), vectors of Chagas' disease. PLoS Negl.Trop. Dis. https://doi.org/10.1371/journal.pntd.0003266.

Jackson, J.K., Resh, V.H., 1998. Morphologically cryptic species confound ecological studies of the caddifishy genus gumaga (trichoptera: sericostomatidae) in Northern California. Aquat. Insect. 20, 69–84.

Jones, G., 2017. Algorithmic improvements to species delimitation and phylogeny estimation under the multispecies coalescent. J. Math. Biol. 74, 447–467.

Justi, S.A., Russo, C.A., Mallet, J.R., Obara, M.T., Galvao, C., 2014. Molecular phylogeny of triatomini (Hemiptera: Reduviidae: Triatominae). Parasite Vectors 7, 149.

Justi, S.A., Galvao, C., Schrago, C.G., 2016. Geological changes of the Americas and their influence on the diversification of the neotropical kissing bugs (Hemiptera: Reduviidae: Triatominae). PLoS Negl.Trop. Dis. 10 (4), e0004527.

Kalyaanamoorthy, S., Minh, B.Q., Wong, T.K., von Haeseler, A., Jermiin, L.S., 2017. ModelFinder: fast model selection for accurate phylogenetic estimates. Nat. Methods 14 (6), 587.

Kapli, P., Lutteropp, S., Zhang, J., Kobert, K., Pavlidis, P., et al., 2017. Multi-rate poisson tree processes for single-locus species delimitation under maximum likelihood and Markov chain Monte Carlo. Bioinformatics 33 (11), 1630–1638.

Kass, J.M., Vilela, B., Aiello-Lammens, M.E., Muscarella, R., Merow, C., Anderson, R.P., 2018. Wallace: a flexible platform for reproducible modeling of species niches and distributions built for community expansion. Methods Ecol. Evol. 9, 1151–1156.

Leigh, J.W., Bryant, D., 2015. POPART: full-feature software for haplotype network construction. Methods Ecol. Evol. 6, 1110–1116.

Lent, H., Wygodzinsky, P., 1979. Revision of Triatominae (Hemiptera: ruduviidae) and their significance as vector of Chagas' disease. Bull. Am. Mus. Nat. Hist. 163, 123–520.
Lima-Cordón, R.A., Monroy, M.C., Stevens, L., Rodas, A., Rodas, G.A., et al., 2019. Description of *Triatoma* huehuetenanguensis sp. n., a potential Chagas disease vector (Hemiptera, Reduviidae, Triatominae). ZooKeys 820 (820), 51.
Lowe, A., Harris, S., Ashton, P., 2004. Ecological Genetics: Designs, Analysis, and Application. Blackwell publishing, USA, p. 320 p.
Martínez-Hernandez, F., Villalobos, G., Martínez-Ibarra, J.A., 2021. Population structure and genetic diversity of *Triatoma* longipennis (usinger, 1939) (Heteroptera: Reduviidae: Triatominae) in Mexico. Infect. Genet. Evol. 89, 104718.
Mayares, D.I., 2014. Phylogeography of *Triatoma Pallidipennis* (Hemíptera: Reduviidae) in the State of Morelos. UAEM, Mexico. Master's thesis.
Mayr, E., 1982. The Growth of Biological Thought: Diversity, Evolution, and Inheritance. Harvard University Press.
Miller, M.A., Pfeiffer, W., Schwartz, T., 2012. The CIPRES science gateway: enabling high-impact science for phylogenetics researchers with limited resources. In: Stewart C., General Chair.. In: Proceedings of the 1st Conference of the Extreme Science and Engineering Discovery Environment: Bridging from the Extreme to the Campus and Beyond, XSEDE '12. Chicago, IL. NY. Association for Computing Machinery, pp. 1–8, 16–20 Jul 2012.
Minh, B.Q., Nguyen, M.A., von Haeseler, A., 2013. Ultrafast approximation for phylogenetic bootstrap. Mol. Biol. Evol. 30, 1188–1195.
Monteiro, F.A., Weirauch, C., Felix, M., Lazoski, C., Abad-Franch, F., 2018. Evolution, systematics, and biogeography of the Triatominae, vectors of Chagas disease. Adv. Parasitol. 99, 265–344.
Nguyen, L.T., Schmidt, H.A., Von Haeseler, A., Minh, B.Q., 2015. IQ-TREE: a fast and effective stochastic algorithm for estimating maximum-likelihood phylogenies. Mol. Biol. Evol. 32 (1), 268–274.
Nixon, K.C., Carpenter, J.M., 1993. On outgroups. Cladistics 9 (4), 413–426.
Okonechnikov, K., Golosova, O., Fursov, M., 2012. Unipro UGENE: a unified bioinformatics toolkit. Bioinformatics 28, 1166–1167 (Oxford, England).
Padial, J.M., Miralles, A., De la Riva, I., Vences, M., 2010. The integrative future of taxonomy. Front. Zool. 7 (1), 1–14.
Paiva, V.F, Belintani, T., de Oliveira, J., Galvão, C., da Rosa, J.A., 2022. A review of the taxonomy and biology of Triatominae subspecies (Hemiptera: Reduviidae). Parasitol. Res. https://doi.org/10.1007/s00436-021-07414-2.
Panzera, F., Pita, S., Nattero, J., Panzera, Y., Galvão, C., et al., 2015. Cryptic speciation in the *Triatoma* sordida subcomplex (Hemiptera, Reduviidae) revealed by chromosomal markers. Parasites Vectors 8 (1), 1–10.
Pech-May, A., Mazariegos-Hidalgo, C.J., Izeta-Alberdi, A., López-Cancino, S.A., Tun-Ku, E., De la Cruz-Félix, K., Ibarra-Cerdeña, C.N., González Ittig, R.E., Ramsey, J.M., 2019. Genetic variation and phylogeography of the *Triatoma* dimidiata complex evidence a potential center of origin and recent divergence of haplogroups having differential trypanosoma cruzi and DTU infections. PLoS Negl.Trop. Dis. 13 (1), e0007044.
Phillips, S.J., Anderson, R.P., Schapire, R.E., 2006. Maximum entropy modeling of species geographic distributions. Ecol. Model. 190, 231–259.
Pita, S.P., Nattero, J., Galvão, C., Alevi, K.C.C., Teves, S.C., et al., 2016. New arrangements on several species subcomplexes of *Triatoma* genus based on the chromosomal position of ribosomal genes (Hemiptera -Triatominae). Infect. Genet. Evol. 43, 225–231.
Rambaut, A. 2014. FigTree v 1.3.1. http://tree.bio.ed.ac.uk/software/figtree/. Accessed May 2015.
Rambaut, A., Drummond A.J.. 2007. Tracer v 1.5. http://tree.bio.ed.ac.uk/software/tracer/. Accessed February 2018.
Ramsey, J.M., Peterson, A.T., Carmona-Castro, O., Moo-Llanes, D.A., Nakazawa, Y., Butrick, M., Tun-Ku, E., de la Cruz-Félix, K., Ibarra-Cerdeña, C.N., 2015. Atlas of Mexican Triatominae (Reduviidae: Hemiptera) and vector transmission of Chagas disease. Mem. Inst. Oswaldo Cruz 110 (3), 339–352.
Reid, N.M., Carstens, B.C., 2012. Phylogenetic estimation error can decrease the accuracy of species delimitation: a Bayesian implementation of the general mixed yule-coalescent model. BMC Evol. Biol. 12 (1), 196.
Rengifo-Correa, L., Abad-Franch, F., Martínez-Hernández, F., Salazar-Schettino, P.M., Téllez-Rendón, J.L., et al., 2021. A biogeographic-ecological approach to disentangle reticulate evolution in the *Triatoma* phyllosoma species group (Heteroptera: Triatominae), vectors of Chagas disease. J. Zool. Syst. Evol. Res. 59 (1), 94–110.
Richards, B., Rua, N.M., Monroy, C., Stevens, L., Dorn, P.L., 2013. Novel polymerase chain reaction-restriction fragment length polymorphism assay to determine internal transcribed spacer-2 group in the Chagas disease vector, *Triatoma* dimidiata (latreille, 1811). Mem. Inst. Oswaldo Cruz 108, 395–398.
Rivera, P.C., González-Ittig, R., Robainas, A., Trimarchi, L.I, Levis, S., et al., 2018. Molecular phylogenetics and environmental niche modeling reveal a cryptic species in the oligoryzomys flavescens complex (rodentia, cricetidae). J. Mammal. 99 (2), 363–376.
Ronquist, F., Huelsenbeck, J.P., 2003. MrBayes 3: Bayesian phylogenetic inference under mixed models. Bioinformatics 19, 1572–1574.
Rozas, J., Ferrer-Mata, A., Sánchez-Del Barrio, J.C., Guirao-Rico, S., Librado, P., et al., 2017. DnaSP 6: DNA sequence polymorphism analysis of large data sets. Mol. Biol. Evol. 34 (12), 3299–3302.
Schofield, C.J., 1994. Triatominae: Biology and Control. Eurommunica Publications, W. Sussex, UK, p. 80.
Schonrogge, K., Barr, B., Wardlaw, J.C., Napper, E., Gardner, M.G., et al., 2002. When rare species become endangered: cryptic speciation in myrmecophilous hoverfishes. Biol. J. Linn. Soc. 75, 291–300.
Stal, C, 1872. Enumeratio Hemipterorum. Pars 2. Ibid. 10, 1–159.
Stuart, B.L., Inger, R.F., Voris, H.K., 2006. High level of cryptic species diversity revealed by sympatric lineages of Southeast Asian forest frogs. Biology letters 2 (3), 470–474.
Tajima, F., 1989. Statistical method for testing the neutral mutation hypothesis by DNA polymorphism. Genetics 123, 585–595.
Tamura, K., Stecher, G., Peterson, D., Filipski, A., Kumar, S., 2013. MEGA6: molecular evolutionary genetics analysis version 6.0. Mol. Biol. Evol. 30 (12), 2725–2729.
Vogler, To., Monaghan, M., 2007. Recent advances in DNA taxonomy. J. Zool. Syst. Evol. Res. 45, 1–10.
Williams, H.C., Ormerod, S.J., Bruford, M.W., 2006. Molecular systematics and phylogeography of the cryptic species complex baetis rhodani (ephemeroptera, baetidae). Mol. Phylogenet. Evol. 40, 370–382.
Wong, Y.Y., Macias, K.J.S., Martínez, D.G., Solorzano, L.F., Ramirez-Sierra, M.J., et al., 2016. Molecular epidemiology of trypanosoma cruzi and *Triatoma* dimidiata in costal ecuador. Infect. Genet. Evol. 41, 207–212.
Zhang, J., Kapli, P., Pavlidis, P., Stamatakis, A., 2013. A general species delimitation method with applications to phylogenetic placements. Bioinformatics 29, 2869–2876 (Oxford, England).

Supplementary Data S1

Article: Molecular data confirm *Triatoma pallidipennis* Stål, 1872 (Hemiptera: Reduviidae: Triatominae) as a novel cryptic species complex

Journal: Acta Tropica

Daryl D. Cruz, Elizabeth Arellano

Centro de Investigación en Biodiversidad y Conservación (CIByC), UAEM, Cuernavaca, Morelos, México

Tabla S1. Sequence data to ND4 gene obtained in this work with the GenBank Data Libraries Accession

Country	State	Municipality	Locality	Accession
Mexico	Puebla	Huatlatlauca	-	OM158086
Mexico	Puebla	Huatlatlauca	-	OM158087
Mexico	Morelos	Amacuzac	Teacalco	OM158088
Mexico	Morelos	Amacuzac	Teacalco	OM158089
Mexico	Morelos	Amacuzac	Teacalco	OM158090
Mexico	Guerrero	Taxco	Joyas del Progreso	OM158091
Mexico	Guerrero	Taxco	Joyas del Progreso	OM158092
Mexico	Guerrero	Chilpancingo	Chilpancingo	OM158093
Mexico	Guerrero	Chilpancingo	Colonia 21 de septiembre	OM158094
Mexico	Guerrero	Chilpancingo	Colonia Ángel Aguirre	OM158095
Mexico	Guerrero	Chilpancingo	Colonia Ángel Aguirre	OM158096
Mexico	Colima	Ixtlahuacán	La Tepamera	OM158097
Mexico	Jalisco	Autlán	Autlán	OM158098
Mexico	Jalisco	Autlán	Autlán	OM158099
Mexico	Colima	Comala	Comala	OM158100
Mexico	Jalisco	Autlán	Autlán	OM158101
Mexico	Colima	Cuauthemoc	Palmillas	OM158102
Mexico	Colima	Coquimatlán	Los Limones	OM158103
Mexico	Colima	Tecomán	San Miguel del Ojo de Agua	OM158104
Mexico	Michoacán	Turicato	Puruaran	OM158105
Mexico	Michoacán	Tacámbaro	Parocho	OM158106
Mexico	State of México	Ixtapan del Oro	Milpillas	OM158107
Mexico	State of México	Santo Tomás	San Pedro	OM158108
Mexico	State of México	Otzoloapan	-	OM158109
Mexico	State of México	Otzoloapan	San Martín	OM158110
Mexico	State of México	Toluca	San Nicolás Tolentino	OM158111
Mexico	State of México	Toluca	San Nicolás Tolentino	OM158112
Mexico	State of México	Otzoloapan	Otzoloapan	OM158113
Mexico	State of México	Toluca	San Nicolás Tolentino	OM158114
Mexico	State of México	Ixtapan del Oro	Tutuapan	OM158115
Mexico	State of México	Otzoloapan	Otzoloapan	OM158116
Mexico	State of México	Zacazonapan	La Cañada	OM158117
Mexico	State of México	Ixtapan del Oro	Milpillas	OM158118
Mexico	State of México	Santo Tomás	Santo Tomás	OM158119
Mexico	State of México	Otzoloapan	San Martín	OM158120
Mexico	State of México	Luvianos	Caja de Agua	OM158121
Mexico	State of México	Sultepec	Laguna Seca	OM158122
Mexico	State of México	Tejupilco	La Labor	OM158123
Mexico	State of México	Tejupilco	La Labor	OM158124

Tabla S2. Sequence data to ITS-2 gene obtained in this work with the GenBank Data Libraries Accession

Country	State	Municipality	Locality	Accession
Mexico	Puebla	Huatlatlauca	-	OM135344
Mexico	Estado de México	Otzoloapan	San Martín	OM135345
Mexico	Colima	Tecomán	San Miguel del Ojo de Agua	OM135346
Mexico	Colima	Cuauthemoc	Palmillas	OM135347
Mexico	Jalisco	Autlán	Autlán	OM135348
Mexico	Jalisco	Autlán	Autlán	OM135349
Mexico	Jalisco	Autlán	Autlán	OM135350
Mexico	Colima	Comala	Comala	OM135351
Mexico	Guerrero	Chilpancingo	Chilpancingo	OM135352
Mexico	State of México	Zacazonapan	La Cañada	OM135353
Mexico	State of México	Toluca	San Nicolás Tolentino	OM135354
Mexico	State of México	Toluca	San Nicolás Tolentino	OM135355
Mexico	State of México	Ixtapan del Oro	Milpillas	OM135356
Mexico	State of México	Otzoloapan	Otzoloapan	OM135357
Mexico	State of México	Santo Tomás	San Pedro	OM135358
Mexico	State of México	Sultepec	Laguna Seca	OM135359
Mexico	State of México	Tejupilco	La Labor	OM135360
Mexico	State of México	Ixtapan del Oro	Tutuapan	OM135361
Mexico	Guerrero	Chilpancingo	Colonia Ángel Aguirre	OM135362
Mexico	Guerrero	Taxco	Joyas del Progreso	OM135363
Mexico	Puebla	Huatlatlauca		OM135364
Mexico	Guerrero	Chilpancingo	Colonia Ángel Aguirre	OM135365
Mexico	State of México	Otzoloapan		OM135366
Mexico	State of México	Tejupilco	La Labor	OM135367
Mexico	State of México	Otzoloapan	Otzoloapan	OM135368
Mexico	State of México	Santo Tomás	Santo Tomás	OM135369
Mexico	State of México	Luvianos	Caja de Agua	OM135370
Mexico	State of México	Ixtapan del Oro	Milpillas	OM135371
Mexico	State of México	Toluca	San Nicolás Tolentino	OM135372
Mexico	State of México	Otzoloapan	San Martín	OM135373

Tabla S3. Sequence data from GenBank used in this work.

State	Municipality	Locality	Accession
Morelos	Cuernavaca	Cuernavaca*	MW620916, MW620960; AF436862; AF436861; AF436876; AF436869; AF436865; AF436866; AF436868; AF436871
	Jiutepec	Jardín Juárez	MW620919; AF436877
	Puente de Ixtla	Ahuehuetzingo	MW620892, MW620893
	Puente de Ixtla	Puente de Ixtla	MW620885
	Puente de Ixtla	Vista Hermosa	MW620886
	Puente de Ixtla	Xoxocotla	MW620937
	Jantetelco	Chalcatzingo*	AF436873; AF436875; AF436878; AF436872; AF436867
	Axochiapan	Quebrantadero	MW620882, MW620883
	Axochiapan	Atlacahualoya	MW620884
Puebla	Jolalpan	Jolalpan	MW620890, MW620889
State of México	Tlatlaya	Juntas	MW620962, MW620887, MW620961
Michoacán	Taretan	Taretan	MW620963
Guerrero	Pilcaya	Cacahuamilpa	MW620888
Oaxaca	Mariscala de Juárez	Santa Frayle*	AF436863; AF436864
Colima	Comala	Comala*	AF436861; AF436862

Supplementary Data S2

Article: Molecular data confirm *Triatoma pallidipennis* Stål, 1872 (Hemiptera: Reduviidae: Triatominae) as a novel cryptic species complex

Journal: Acta Tropica

Daryl D. Cruz, Elizabeth Arellano

Centro de Investigación en Biodiversidad y Conservación (CIByC), UAEM, Cuernavaca, Morelos, México

Table S1. Bioclimatic variables used to develop a model predicting the potential geographic distribution of *Triatoma pallidipennis* in Mexico.

Variable	Description
BIO2	Mean Diurnal Range (Mean of monthly (max temp - min temp))
BIO3	Isothermality (BIO2/BIO7) (×100)
BIO4	Temperature Seasonality (standard deviation ×100)
BIO13	Precipitation of Wettest Month
BIO15	Precipitation Seasonality (Coefficient of Variation)
BIO17	Precipitation of Driest Quarter

Table S2. Parameter settings selected during model calibration, used for creating ecological niche models of the species. R. M. = regularization multiplier; F. C. = feature classes; AICc = Akaike Information Criterion corrected; w=weith.

R. M.	F. C	AICc	delta.AICc	w.AIC
2	LQHP	3361.863834	0	0.314422793
1.5	LQHP	3361.866941	0.003106877	0.313934736
0.5	LQ	3362.284919	0.421085466	0.254727876
1	LQ	3364.273215	2.409381462	0.094259143
3	LQHP	3369.866337	8.00250318	0.005751651
1.5	LQ	3369.982797	8.118963298	0.005426297
3	LQH	3371.604273	9.740439259	0.002412151
3.5	LQH	3372.184682	10.32084855	0.001804555
1.5	H	3372.278993	10.41515914	0.001721436
2.5	LQHP	3372.53173	10.66789664	0.001517084
4	LQH	3372.678772	10.81493877	0.001409548
2	LQH	3374.728173	12.86433915	0.000505893
2.5	LQH	3375.009603	13.14576923	0.000439487
3	H	3375.069631	13.20579692	0.000426493
3.5	LQHP	3376.049245	14.18541164	0.000261331
4.5	LQH	3376.083336	14.21950262	0.000256914
2	LQ	3377.02469	15.16085609	0.000160463
5	LQH	3377.189073	15.3252392	0.000147802
2.5	H	3377.255919	15.39208494	0.000142944
3.5	H	3378.264264	16.40043017	8.63E-05
2	H	3378.810494	16.94665991	6.57E-05
4	LQHP	3378.810799	16.94696493	6.57E-05
1	LQH	3381.919974	20.05614072	1.39E-05
1.5	LQH	3382.943719	21.0798854	8.32E-06
5.5	LQH	3382.983295	21.11946098	8.16E-06
4	H	3383.773609	21.90977536	5.49E-06
1	H	3383.781676	21.9178422	5.47E-06
4.5	LQHP	3384.154391	22.2905577	4.54E-06
2.5	LQ	3385.092296	23.22846202	2.84E-06
6	LQH	3386.772811	24.90897775	1.23E-06
4.5	H	3388.139431	26.2755973	6.19E-07

6	LQHP	3388.31143	26.44759673	5.68E-07
3	LQ	3388.338562	26.47472856	5.61E-07
6.5	LQHP	3388.909772	27.04593821	4.21E-07
3.5	LQ	3389.003913	27.14007957	4.02E-07
4.5	LQ	3390.016444	28.15261063	2.42E-07
4	LQ	3390.6587	28.79486652	1.76E-07
6.5	LQH	3390.753391	28.88955733	1.68E-07
5.5	H	3391.280591	29.41675739	1.29E-07
5.5	LQHP	3391.785515	29.92168164	1.00E-07
5	H	3392.03872	30.17488657	8.81E-08
6	H	3392.975757	31.11192322	5.52E-08
5	LQHP	3393.407409	31.543575	4.45E-08
5	LQ	3393.837637	31.97380371	3.59E-08
7	LQHP	3394.438468	32.57463412	2.65E-08
7	LQH	3394.916106	33.05227279	2.09E-08
7.5	LQHP	3395.232117	33.3682838	1.79E-08
8	LQHP	3395.437446	33.57361271	1.61E-08
6.5	H	3396.472595	34.60876149	9.60E-09
0.5	L	3396.761926	34.89809244	8.31E-09
9	LQHP	3397.517697	35.6538633	5.69E-09
7	H	3397.814715	35.95088148	4.91E-09
5.5	LQ	3397.914698	36.05086479	4.67E-09
1	L	3399.164646	37.30081199	2.50E-09
7.5	LQH	3399.381864	37.51803011	2.24E-09
9.5	LQHP	3399.534378	37.67054388	2.08E-09
8.5	LQHP	3400.094934	38.2311004	1.57E-09
7.5	H	3401.438081	39.57424733	8.02E-10
10	LQHP	3401.620974	39.75714029	7.32E-10
8	LQH	3401.915835	40.05200109	6.31E-10
8	H	3402.967276	41.10344209	3.73E-10
1	LQHP	3403.26149	41.39765646	3.22E-10
6	LQ	3404.971527	43.10769368	1.37E-10
8.5	H	3406.777221	44.91338689	5.56E-11
8.5	LQH	3407.069673	45.2058391	4.80E-11
1.5	L	3410.516048	48.65221462	8.57E-12

6.5	LQ	3410.573098	48.7092647	8.33E-12
9	H	3410.716786	48.85295185	7.75E-12
9	LQH	3411.898691	50.03485721	4.29E-12
2	L	3412.417421	50.55358685	3.31E-12
9.5	LQH	3412.905873	51.04203957	2.59E-12
10	LQH	3413.817158	51.95332459	1.64E-12
10	H	3414.060138	52.19630465	1.46E-12
9.5	H	3414.784232	52.92039871	1.01E-12
2.5	L	3415.535806	53.67197225	6.96E-13
7	LQ	3416.362252	54.49841824	4.61E-13
7.5	LQ	3416.455524	54.59169039	4.40E-13
3	L	3419.923778	58.05994416	7.76E-14
8	LQ	3420.330497	58.46666318	6.33E-14
3.5	L	3421.559733	59.69589921	3.43E-14
4	L	3421.935983	60.07214891	2.84E-14
8.5	LQ	3424.313366	62.44953264	8.65E-15
4.5	L	3424.887332	63.02349841	6.49E-15
5	L	3425.72295	63.85911602	4.27E-15
5.5	L	3426.648053	64.78421883	2.69E-15
9	LQ	3428.39906	66.53522598	1.12E-15
6	L	3429.029874	67.16604052	8.18E-16
6.5	L	3431.60649	69.74265635	2.25E-16
9.5	LQ	3432.58206	70.71822658	1.38E-16
7	L	3434.043337	72.17950295	6.67E-17
0.5	H	3434.460579	72.59674515	5.41E-17
10	LQ	3436.8545	74.99066614	1.63E-17
7.5	L	3437.003777	75.1399438	1.52E-17
8	L	3440.109639	78.24580569	3.21E-18
9	L	3442.576306	80.71247221	9.35E-19
9.5	L	3442.884035	81.02020091	8.02E-19
10	L	3443.207503	81.34366934	6.82E-19
8.5	L	3443.316138	81.45230404	6.46E-19
0.5	LQH	3465.879354	104.0155204	8.14E-24
0.5	LQHP	3479.819454	117.95562	7.65E-27

Supplementary Data S3

Article: Molecular data confirm *Triatoma pallidipennis* Stål, 1872 (Hemiptera: Reduviidae: Triatominae) as a novel cryptic species complex

Journal: Acta Tropica

Daryl D. Cruz, Elizabeth Arellano

Centro de Investigación en Biodiversidad y Conservación (CIByC), UAEM, Cuernavaca, Morelos, México

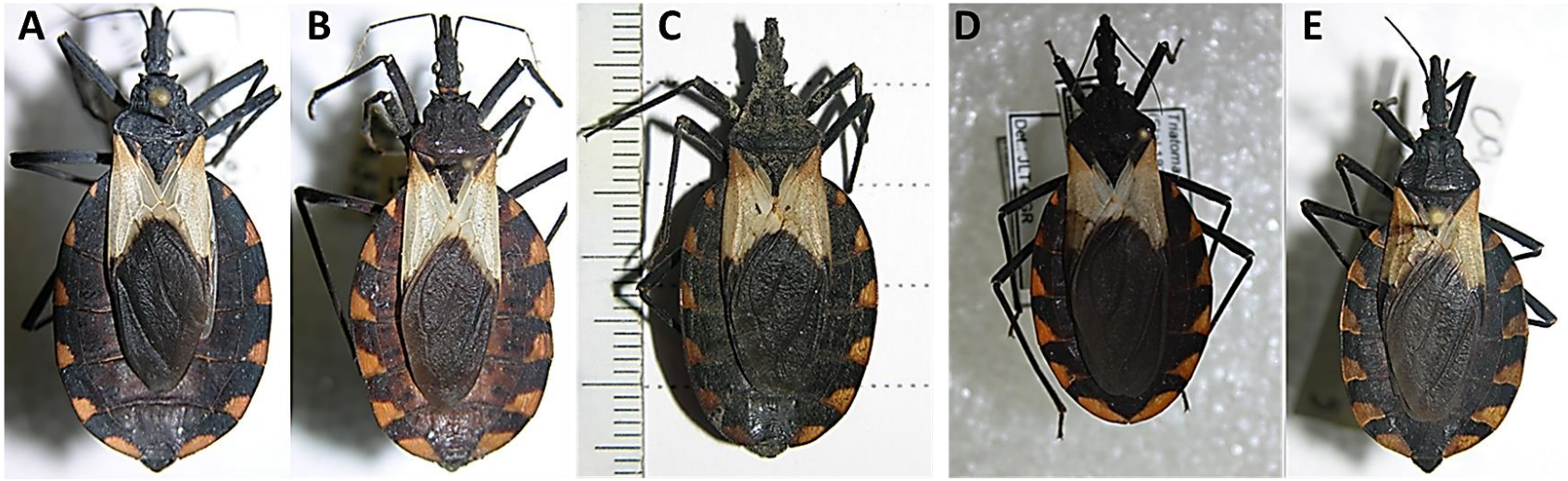

Figure S3. Representation of haplogroups detected from phylogenetic analyses using the mitochondrial gene ND4 and the nuclear gene ITS-2. Haplogroup I (A), Haplogroup II (B), Haplogroup III (C), Haplogroup IV (D) and Haplogroup V (E).

Capítulo III.

Geometric morphometrics and ecological niche modelling for delimitation of *Triatoma pallidipennis* haplogroups

GEOMETRIC MORPHOMETRICS AND ECOLOGICAL NICHE MODELLING FOR DELIMITATION OF *TRIATOMA PALLIDIPENNIS* HAPLOGROUPS

Daryl D. Cruz[1]*, Sandra Milena Ospina-Garces[2], Elizabeth Arellano[1], Carlos N. Ibarra-Cerdeña[3], Elizabeth Nava-García[4] and Raúl Alcalá[1]

[1]Centro de Investigación en Biodiversidad y Conservación (CIByC), Universidad Autónoma del Estado de Morelos, Av. Universidad 1001 Col. Chamilpa, CP. 62209, Cuernavaca, Morelos, México.

[2]Centro de Investigaciones Tropicales, Universidad Veracruzana, José María Morelos No. 44 y 46. Col. Centro, C.P. 91000 Xalapa, Veracruz, México.

[3]Departamento de Ecología Humana, Centro de Investigación y de Estudios Avanzados del IPN (CINVESTAV), Unidad Mérida, Yucatán, México.

[4]Facultad de Ciencias Biológicas, Universidad Autónoma del Estado de Morelos, Av. Universidad 1001 Col. Chamilpa, CP. 62209, Cuernavaca, Morelos, México

Abstract

One of the most epidemiologically important and most widely distributed endemic triatomines in Mexico is *Triatoma pallidipennis.* A recent phylogenetic analysis of *T. pallidipennis* using mathematical methods for species delimitation based on the mitochondrial ND4 gene and ribosomal gene ITS-2 revealed five monophyletic haplogroups with potential validity as cryptic species. The goal of this study is to compare *T. pallidipennis* haplogroups that may constitute cryptic species using head and pronotum features, environmental characteristics of their habitats, and ecological niche modeling, based on the premise that they constitute genetically well-differentiated species. Morphometric and ecological analysis was performed on four and three of the five haplogroups, based on the amount of data available for each analysis. To analyze variation in shape, images of the head and pronotum of the specimens were obtained and analyzed using methods based on landmarks and semilandmarks. The ecological niche models were obtained from occurrence data for each analyzed haplogroup, as well as a set of bioclimatic variables that characterized the environmental niche of each one. Statistical significance tests and multivariate methods were used to detect differences between haplogroups, both for morphometric and ecological analyses. Important differences were found, both in the shape of the analyzed structures and the environmental characteristics of the distribution areas of the analyzed haplogroups. Our results show how the analysis of morphometric variation and the characterization of the environmental conditions that define the climatic niche can be used to improve the delimitation of *Triatoma pallidipennis* haplogroups that may constitute cryptic species.

Keywords: Morphometry, *Triatoma*, Cryptic species, Maxent

Introduction

The correct estimation and characterization of biodiversity are key elements for the conservation and use of natural entities. Since "species" is the operative unit in Biology, defining species limits is a pillar of the quantification and management of biodiversity. For this reason, its conceptualization has been the subject of considerable intellectual effort (Sites and Marshall, 2003; de Queiroz, 2007).

Historically, diagnostic phenotypic characters have been used to carry out taxonomic delimitations, classifying distinct populations into species and subspecies, known as the "traditional taxonomic approach" (Matos-Maraví *et al.*, 2019). In entomology, specifically, much attention has been paid to the morphology of various body parts to identify, name, and classify organisms. Thus, traditional taxonomy and systematics have used the specific external morphological characteristics as diagnostic characters for the identification of taxa (Tatsuta *et al.*, 2018). However, some entities are recognized as distinct species under other criteria (mainly phylogenetic) but are not (at least superficially) distinguishable based on external morphology and have therefore been recognized as a single species; these are known as cryptic species (Bickford *et al.*, 2007) and are a case in which the traditional taxonomic approach fails to delimit taxa that should be considered separate species. Failure to correctly detect and delimit species results in an underestimation of true levels of biodiversity (Lefébure *et al.*, 2006; Padial *et al.*, 2010). Cryptic species have been shown to occur in many groups (Bickford *et al.*, 2007; Pfenninger and Schwenk, 2007).

Recently, the integrative taxonomy approach has been widely proposed in systematics studies (Dayrat, 2005; Sangster, 2018). Lines of evidence such as geometric morphometrics and ecological analyses have been useful to discriminate between genetically well-differentiated species (Martinez-Borrego *et al.*, 2022). These integrative approaches are particularly useful in cases where traditional methods are insufficient (MacGuigan *et al.*, 2017, Freitas *et al.*, 2018).

Leaché *et al.*, (2009) argued that the use of morphological and ecological data, in addition to molecular data, allows better discrimination among species. Geometric morphometrics analysis is a robust tool to highlight interspecific variation and corroborate

the phylogenetic relationships within animal groups (e. g., Bogdanowicz, *et al.*, 2005; Pavan and Marroig, 2016). In addition, ecological niche studies are being increasingly used for these same purposes (e. g., Rissler and Apodaca 2007; Rivera *et al.*, 2018; Zhao *et al.*,2019; Masonick and Weirauch 2020), as well as for inferences related to evolutionary questions of both historical distributions and speciation processes (Graham *et al.*, 2004).

The genus *Triatoma* (Hemiptera: Reduviidae) is one of the most important epidemiological insects since they are the main vectors of Chagas disease on the American continent. Aside from their relevance as vectors, *Triatoma* is highly scientifically valuable because many species in the genus have high rates of speciation, making the genus an interesting model to evaluate recent speciation processes. The cryptic speciation phenomenon within *Triatoma* seems to be a relatively common process, detected mainly by molecular techniques (Bargues *et al.*, 2008, Ibarra-Cerdeña *et al.*, 2014, Justi *et al.*, 2014, Pech-May *et al.*, 2019). However, geometric morphometry has been repeatedly used as a tool to delimit species within the Triatominae subfamily (Gurgel-Gonçalves *et al.*, 2011, Dujardin, 2011, Vendrami *et al.*, 2017, Cruz *et al.*, 2020).

Ecological segregation could also play an important role in the process of lineage divergence in *Triatoma* (Gurgel-Gonçalves *et al.*, 2011). When two subsets of conspecific individuals succeed in adapting to distinct ecological niches, their evolutionary fates can become independent, often because of divergent selection, leading to speciation (Schluter, 2001). Consequently, many sister taxa exploit contrasting niches. This makes quantitative approaches like ecological niche modeling (ENM) useful to investigate recent speciation events that are likely to have been driven by ecological divergence (Warren *et al.*, 2008).

One of the most epidemiologically important and most widely distributed endemic triatomines in Mexico is *Triatoma pallidipennis* Stal, 1872 (Lent and Wygodzinsky 1979, Martínez-Ibarra *et al.*, 1999, Ramsey *et al.*, 2015). Lent and Wygodzinsky (1979), after examining several specimens from different locations, concluded that this species does not present significant morphological variations among its populations. As a result of this wide geographic distribution, a large niche breadth has been reported for the species (Ramsey *et al.*, 2015), which can be assumed to represent high ecological plasticity. However, a recent phylogenetic analysis of *T. pallidipennis* using mathematical methods for species

delimitation based on the mitochondrial ND4 gene from 73 specimens and ribosomal gene ITS-2 from 33 specimens from different locations throughout its geographic distribution revealed five monophyletic haplogroups with potential validity as cryptic species (Cruz and Arellano, 2022).

It is therefore desirable to broaden the understanding of the genetic distinction between *Triatoma pallidipennis* haplogroups by following an integrative taxonomy approach using alternative data sources such as geometric morphometrics and ecological attributes. The goal of this study is to compare *Triatoma pallidipennis* haplogroups that may constitute cryptic species using head and pronotum features, environmental characteristics of their habitats, and ecological niche modeling, based on the premise that they constitute genetically well-differentiated species.

Material and methods

Haplogroups analyzed

Morphometric and ecological analysis was performed on four and three of the five haplogroups (potential cryptic species) that were detected in the phylogenetic analysis of *T. pallidipennis* by Cruz and Arellano (2022) (Fig. S1). The possible cryptic species analyzed were: Haplogroup I: specimens from Morelos, Oaxaca, and eastern Puebla, Haplogroup II: specimens from southern Morelos, southwestern Mexico State, and eastern Guerrero, Haplogroup III: specimens from Mexico State and Haplogroup V: specimens from Colima and Jalisco. The individuals of *T. pallidipennis* used in the phylogenetic analysis were obtained through direct donations from the National Institute of Diagnosis and Reference (INDRE), the Ministry of Health of Mexico State, the State Laboratory of Medical Entomology (LEEM) of Mexico State, as well as direct collections made by LEEM personnel in the state of Guerrero.

Geometric morphometrics data.

To analyze variation in shape, images of the head and pronotum (Fig. 1A) of the specimens were obtained and analyzed using methods based on landmarks and semilandmarks (Bookstein, 1991; Zelditch *et al.*, 2004; Mitteroecker and Gunz, 2009; Adams and Otárola-Castillo, 2013). The relevance of the head as a structure for

morphometric analysis has been repeatedly evaluated in the genus *Triatoma* (Gurgel-Gonçalves *et al.*, 2011; Hernández *et al.*, 2013; Oliveira *et al.*, 2017; Nattero *et al.*, 2017). The pronotum, on the other hand, has been little explored in morphometric terms. In the context of species delimitation, the only known work that studies its potential to discriminate between cryptic *Triatoma* species is the study by Nattero *et al.*, (2017). Table S1 shows the total number of specimens, as well as the number of females and males obtained for each haplogroup analyzed. These included the specimens used in the phylogenetic analysis and others from the same localities. The final total sample size was 113 individuals.

All individuals were photographed under the same magnification and exposure settings and with a millimeter scale. To describe the shape of the head, we used 14 landmarks (Fig. 1B) that were a combination of those suggested by Gurgel-Gonçalves *et al.*, (2011) and Oliveira *et al.*, (2017). Six landmarks and 38 semi-landmarks were used for the pronotum (Fig. 1C) to describe the right pronotal contour of the specimens. As a result of digitization in TPS software (Rohlf, 2015), a matrix of coordinates (x; y) was obtained for each set of morphological points for each image processed for both structures. All landmarks used are listed in Table 2.

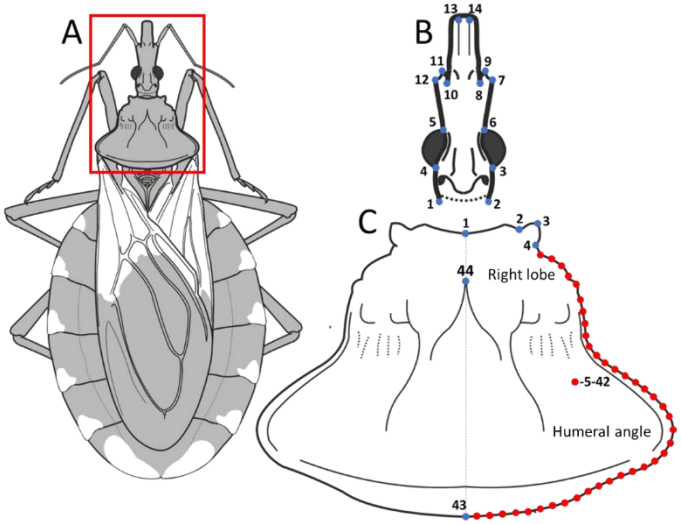

Figure 1. Location of the structures analyzed (A) and the landmarks and semilandmarks used for the description of the shape of the head (B) and pronotum (C) in haplogroups of *Triatoma pallidipennis*. Blue dots represent landmarks. Red dots represent semi- landmarks.

Table 2. Definition of the landmarks used for the morphometric characterization of the head and pronotum in haplogroups of *Triatoma pallidipennis*.

Structure	Landmarks
Head	1. Intersection point between head and neck on the left side
	2. Intersection between head and neck on the right side
	3. Left side post-ocular point
	4. Right side post-ocular point
	5. Pre-ocular point on left side
	6. Pre-ocular point on right side
	7. External region of the right antenniferous tubercle
	8. Insertion of the right antenniferous tubercle
	9. Internal region of the right antenniferous tubercle
	10. Insertion of the left antenniferous tubercle
	11. Internal region of the left antenniferous tubercle
	12. External region of the left antenniferous tubercle
	13. Left intersection between the gena and antecapeum
	14. Right intersection between the gena and antecapeum
Pronotum	1. Middle insertion of the upper pronotal border
	2. Inner base of the right spine
	3. Upper end of the right spine
	4. External base of the right spine
	43. Middle insertion of the lower pronotal border
	44. Intersection point between pronotal lobes

The morphometric analysis was performed using the package geomorph version 3.3.1 (Adams and Otarola-Castillo, 2013) of the R library (R Core Team 2017). Using the "define.sliders" function, we defined which points constitute the semi-landmarks that characterized the right edge of the pronotum. Generalized Procrustes Analysis (GPA) (Rohlf and Slice, 1990) was performed to superimpose the obtained coordinates and extract the shape variables. During this procedure, all samples are translated about a common origin to remove the effect of position, scaled through centroid sizes, and finally rotated (using a least-squares criterion) until the coordinates of the corresponding points align as closely as possible, to minimize the effect of differences in orientation. In the case of the pronotum configuration, semilandmarks were allowed to slide along their tangent vectors until reaching the minimum point of bending energy (Bookstein, 1997; Zelditch *et al.*, 2004; Gunz *et al.*, 2005; Gunz and Mitteroecker, 2013). As a result of the GPA, the Procrustes coordinates and the Procrustes distances were obtained, which were used as form variables. In addition, the centroid size (CS) was estimated to obtain a shape-independent measure of size.

Statistical data processing

Principal Component Analyses (PCA) of the geometric configurations of head and pronotum were performed to reduce their dimensionality. From this analysis, the scores of the first 10 principal components (PC) were extracted, which were used for the rest of the statistical analyses as shape variables. The mean shape variation in the positive and negative directions along the first two PC was visualized using deformation grids.

As part of the exploratory analysis, the presence or absence of sexual dimorphism was determined by considering the shape variables and the CS of both structures (head and pronotum). To detect whether there were significant differences between sexes, a Procrustes ANOVA (Goodall, 1991; Anderson, 2001) was performed for head and pronotum shape using the function "ProcD.lm", and a factorial design with shape as the dependent variable, sex as the main factor, and CS as a covariate. Significant differences ($p \leq 0.05$) in head and pronotum size between sexes were tested using the function "lm.rrpp" in the R package RRPP (Collyer and Adams, 2018). We found no significant sexual dimorphism in the size or shape of any structure analyzed; therefore, we pooled males and females in our analyses of interspecific differentiation. The allometric component (possible effect of size on shape variation) was analyzed using a Procrustes ANOVA and the same factorial design previously declared. However, this allometric effect was relatively low for both the head and the pronotum, with values of 5.7% and 2.0%, respectively.

Differences in size and shape between haplogroups were evaluated for the head and pronotum separately, using a Procrustes ANOVA. A factorial design was used with shape as the dependent variable, haplogroups as the main factor, and CZ as a covariate. The mean head/pronotum shape differences between species were quantified (Procrustes distances) and tested for statistical significance using a pairwise permutation test ($p \leq 0.05$; resampling = 1000; function "permudist") in the R package Morpho 2.4 (Schlager, 2017).

Based on the scores of the first 10 PCs, a Linear Discriminant Function Analysis was performed with the mass library (Ripley *et al.*, 2020) to estimate the percentage of correct discrimination. Finally, an Analysis of Canonical Variables was performed and, as with the PCs, the variation of the mean shape in the positive and negative directions along each canonical axis was visualized using deformation grids.

Ecological niche data

The occurrence data used for the ecological analyses were the coordinates of the localities where the individuals of each haplogroup were collected. We obtained additional data to reach the minimum number of locations (30) from the database published by Ramsey *et al.*, (2015), which is freely available (https://doi.org/10.5061/dryad.rq120), and the international database GIBIF (Global Information Biodiversity Facility, www.gbif.org). We used only occurrence data collected after 1950, and specimens with inconsistent information were not included in the analysis. Bioclimatic variables from the Worldclim 2.0 database (Fick and Hijmans, 2017) were used as descriptive variables (temperature and rainfall), with a spatial resolution of approximately $1km^2$.

Data processing and generation of ecological niche models

To detect differences between the ecological niches of the haplogroups previously defined by the phylogenetic analysis, ENM was performed for each one of them in the Maxent program ver.3.4.1 (Phillips *et al.*, 2006; 2017). The subset of bioclimatic variables was composed of those that were not strongly correlated ($r < 0.8$, following Moo-Llanes *et al.*, 2020; Tarquino-Carbonell *et al.*, 2020). Based on this previous analysis, the variables selected to obtain the ENMs were Bio2 = Mean Diurnal Range, Bio3 = Isothermality, BIO4 = Temperature Seasonality, Bio13 = Precipitation of Wettest Month, Bio15 = Precipitation Seasonality, and Bio16 = Precipitation of Wettest Quarter.

Since the performance of ENM is sensitive to the specifications of the modeling process (Araújo and Guisan, 2006; Araújo and Peterson, 2012; Radosavljevic and Anderson, 2014), before the generation of the ENM, we evaluated the program settings for each haplogroup. We used the Wallace package (Kass *et al.*, 2018) for R (R Core Team, 2017) to clean occurrence data, reduce spatial autocorrelation, and select the calibration area and the background samples. Spatial filtering of the occurrence data was carried out for each haplogroup to be modeled using the "spThing" package for R (Aiello-Lammens *et al.*, 2015). The minimum distance for filtering was 5 km. Calibration areas were determined by a convex minimum polygon of the presence points resulting from spatial filtering. From these, 10,000 background points were generated to obtain the ENM.

To define an appropriate level of complexity, we evaluated Maxent configurations to compare the performances of different test models. These models were created using the checkerboard method to partition the training and test data. In addition, 12 values were used for the regularization multiplier (0.5-6, with steps of 0.5) and six configurations of feature classes: L, LQ, H, LQH and LQHP (where L = linear, Q = quadratic, H = "hinge" and P = product). These analyses were performed using the "ENMeval" package of R (Muscarella *et al.*, 2014). The best configurations were selected based on the lowest values of the corrected Akaike Information Criterion (AICc).

The final models were calibrated with the full set of filtered records and the selected set of variables. We performed 50 replicates per modeled haplogroup using the best configurations obtained during the evaluation process. In addition, they were projected onto the entire Mexican territory to estimate new areas of environmental suitability for each of the lineages.

Ecological segregation between phylogenetic lineages

To estimate whether there is ecological segregation between haplogroups, we obtained the ellipsoids and centroids that characterize the environmental space of each one (Van Aelst and Rousseeuw, 2009). We did this using a Principal Components Analysis with 15 bioclimatic variables (excluding Bio8, Bio9, Bio18, and Bio19), to characterize the environmental space in which each haplogroup is distributed. From this analysis, the fundamental niche of *Triatoma pallidipennis* was obtained. In this fundamental niche, we then represented the realized niche of the populations composing each haplogroup using their presence data. All analyses were performed in the NicheA program (Qiao *et al.*, 2015).

From the Principal Components Analysis, the scores of the components with the highest contribution to the total variance were used to compare the environmental niche of each haplogroup using Kruskal-Wallis tests, since the data did not meet the assumptions of normality and homogeneity of variance. This analysis was performed in the program Statistica ver. 8.

Results

Geometric morphometrics

The ordination based on the exploratory analysis of PCA was not consistent with the separation between haplogroups for any of the structures analyzed (Fig. 4A-B). The first two PCs explained approximately 50 and 60% of the total cumulative variance for the head and pronotum, respectively. In the deformation grids for the head in the first two PCs, a slight displacement towards the posterior region of the head of the landmarks characterizing the pre-ocular region at the negative end of PC1 was observed. This shift was more evident at the negative end of PC2. For the positive ends of both axes, the greatest change in shape was observed in PC2, which showed a strong displacement towards the anterior region of the head of the landmarks that characterize the antenniferous tubercle.

The changes in the shape of the pronotum were most evident at the negative extremes of the PC, associated with the right lobe. At the negative end of PC1, there was a marked contraction of the points that characterize this region. This is different from the negative end of PC2, in which there was a displacement of these points towards the anterior region of the pronotum (Fig. 4B).

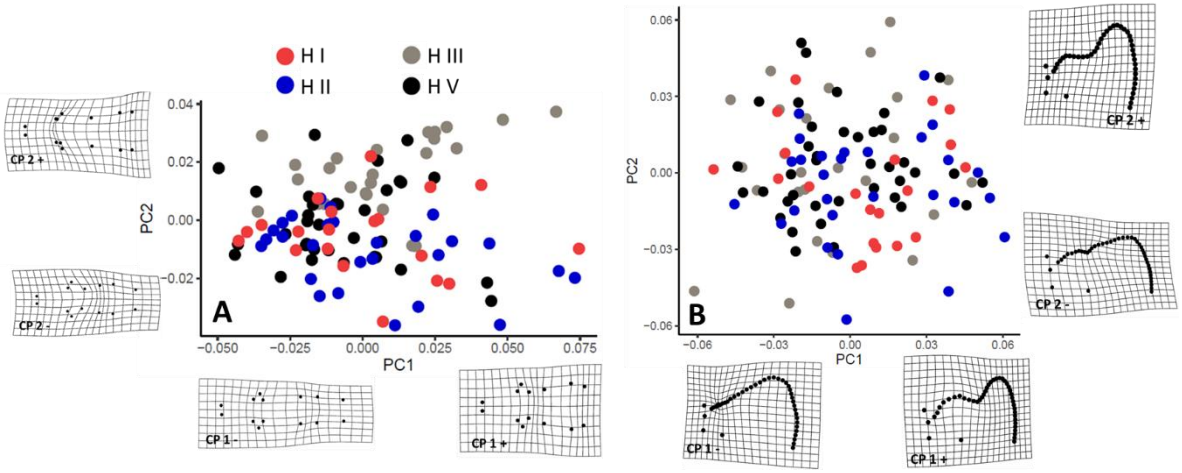

Figure 4. Principal Component Analysis for the head (A) and pronotum (B) shape among haplogroups of *Triatoma pallidipennis*. Deformation grids show the minimum and maximum variation in shape along the axis. PC: Principal Component. H: Haplogroup.

Differences in shapes and centroid size between haplogroups

The Procrustes ANOVA (Table 4) and pairwise comparisons showed differences in mean head shape among all haplogroups except between haplogroups II-III and II-V (Fig. 5A-D). Pairwise comparisons of mean pronotum shape only showed differences between haplogroups III-V and III-V, (Fig. 5E-F).

Table 4. Differences in head shape and pronotum shape between haplogroups of *Triatoma pallidipennis* using Analysis of Variance (ANOVA). $\alpha \leq 0.05$. SS: Sum of squares; MS: Mean squares.

		SS	MS	R2	F	Z	P-value
Head	Haplogroups	0,0198	0,0066	0,0930	3,5215	5,0964	0,001*
	Residuals	0,1934	0,0018	0,9069			
	Total	0,2132					
Pronotum	Haplogroups	0,0129	0,0043	0,0566	2,1825	2,7106	0,01*
	Residuals	0,2153	0,0019	0,9433			
	Total	0,2283					

The greatest differences in the shape of the head were mainly from the region of the antenniferous tubercle, which was smaller in haplogroup III than in haplogroups I and II (Fig. 5A-B). However, concerning haplogroup III, this region was larger (Fig. 5C). The ocular region and the base of the head were broader in haplogroup III than in haplogroups I and II but smaller than in haplogroup V. Finally, the most similar heads in shape were the middle forms of haplogroups II and V; the greatest differences between them were in the insertion of the antenniferous tubercle and the post-ocular region.

For the pronotum, there were differences in the shape of the right dorsal spine, in the middle insertion of the upper pronotal edge, in the insertion point of the pronotal lobes, and the shape of the right lobe, for the two paired comparisons made (Fig. 5E and F). The main differences in the mean shapes of the pronotum between haplogroups II and III were in the right lobe, the humeral angle, and the lower margin of the pronotum (Fig. 5E). The right lobe in haplogroup V was wider than in haplogroup II. The humeral angle was markedly truncated relative to the humeral angle of haplogroup II, which had a more pointed shape. Significant variation in the lower margin of the pronotum was also observed

between these haplogroups. The differences in the mean shape of the posterior lobe of the pronotum between haplogroups II and V were not as marked as in the previous comparison. However, haplogroup V presented a wider right lobe. As for the lower margin, the variation was much smaller (Fig. 5F).

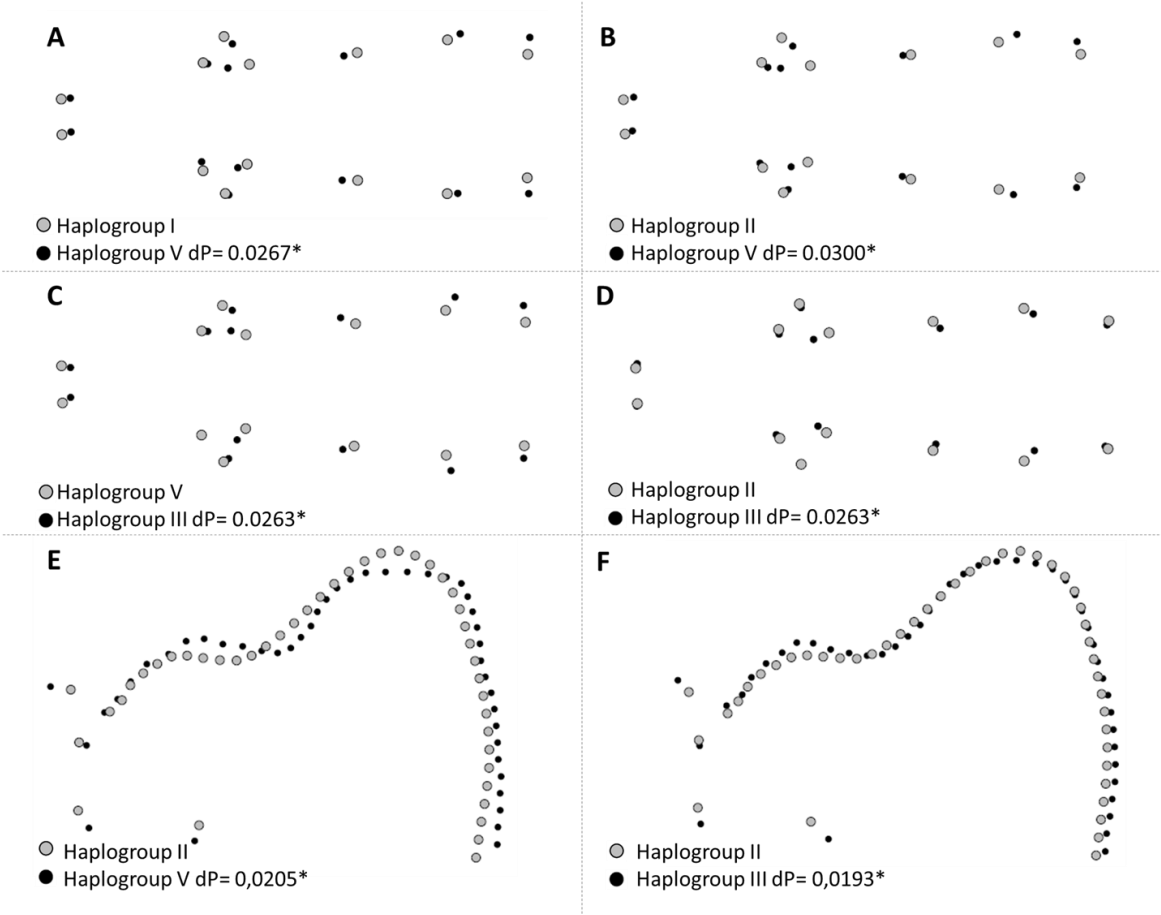

Figure 5. Differences in mean shape (Procrustes distances) between haplogroups of *Triatoma pallidipennis*. Differences were magnified by a factor of 3. dP = Procrustes distances between the mean shape of each pairwise comparison. * Indicate significant dP ($\alpha \leq 0.05$), based on pairwise permutation tests. A-D corresponds to the head. E and F correspond to the pronotum. Haplogroup I: specimens from Morelos, Haplogroup II: specimens from Mexico State and Guerrero, Haplogroup III: specimens from Mexico State and Haplogroup V: specimens from Colima and Jalisco.

Although there were differences in shape between haplogroups, there were no differences in the size of either the head or the pronotum (Fig. 6A and B).

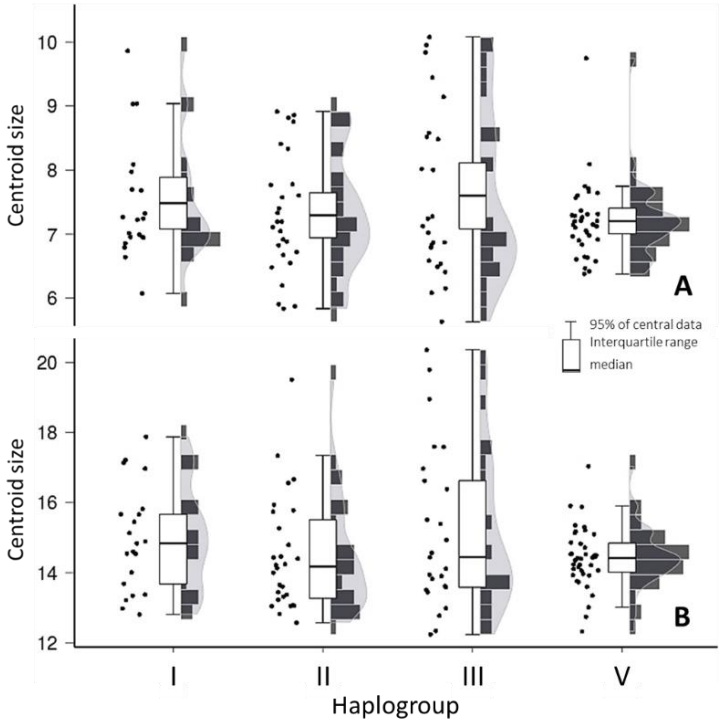

Figure 6. Comparison of Centroid size for the head (A) and pronotum (B) between haplogroups of *Triatoma pallidipennis*. Haplogroup I: specimens from Morelos, Haplogroup II: specimens from Mexico State and Guerrero, Haplogroup III: specimens from Mexico State and Haplogroup V: specimens from Colima and Jalisco.

Discrimination of haplogroups

It was not possible to correctly discriminate any of the haplogroups analyzed using the LDFA. The global discrimination percentages obtained for both structures were similar, with 49.5% overall discrimination for the head and 50.4% for the pronotum. However, the percentage of specific discrimination in some haplogroups was relatively high. For the head, the best-discriminated haplogroups were III and V, while for the pronotum, the best discriminated were II and III (Table 6).

Table 6. Result of Linear Discriminant Function Analysis to classify haplogroups of *Triatoma pallidipennis*, using shape information for the head and pronotum. % CD= Correct Discrimination Percentage.

	Haplogroup	I	II	V	III	Total	% CD
Head	I	3	8	4	5	20	15,0
	II	7	9	1	10	27	33,3
	V	3	2	17	3	25	**68,0**
	III	2	6	3	24	35	**68,5**
Pronotum	I	8	6	4	3	21	38,1
	II	1	18	5	4	28	**64,3**
	V	8	2	9	6	25	36,0
	III	2	8	7	22	39	56,4

In the ordination graph of the Analysis of Canonical Variables for the shape of the head considering 20 PC, haplogroup V was the most separated from the rest (Fig. 7A-B). The rest of the haplogroups analyzed showed high overlap. The deformation grids obtained for each canonical axis showed variations in head shape, mostly towards the negative end of the axis of Canonical Variable 1. These variations were mainly due to contractions in the pre-ocular regions and the antenniferous tubercles. In canonical axis 2, the variations in shape were subtler, given by contractions in the ocular region of the head (Fig. 7A).

In the case of the pronotum, the haplogroups overlapped almost completely in the Analysis of Canonical Variables (Fig. 7B). The shape did not present marked variations, as evidenced by the deformation grids obtained for both canonical axes. The slight variations observed were mainly in the shape of the right lobe and the humeral angle.

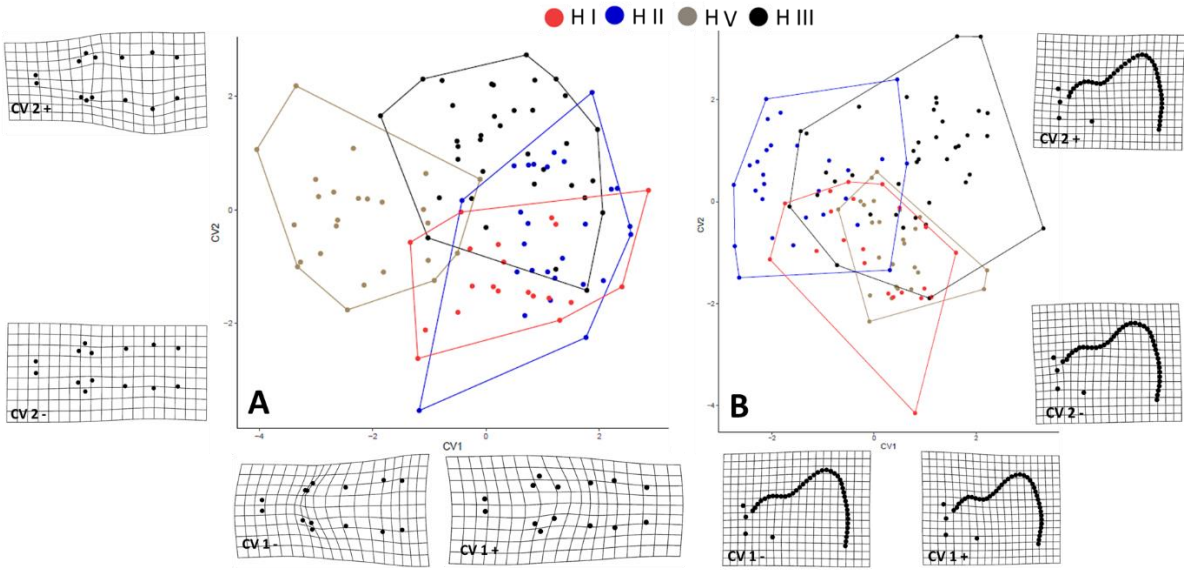

Figure 7. Ordination plot of the first two canonical axes for head shape (A) and (B) pronotum, among haplogroups of *Triatoma pallidipennis*. Deformation grids represent the minimum and maximum variation in shape along the axis. Haplogroup II: specimens from Morelos, Haplogroup III: specimens from Mexico State and Guerrero, Haplogroup V: specimens from Colima and Jalisco, Haplogroup VI: specimens from Mexico State.

Ecological niche modeling

When obtaining the ecological niche models, the climatic suitability areas (CSA) were recovered for each evaluated haplogroup (Fig. 8). Haplogroup V had a larger potential distribution (shown in Fig. 8C) than haplogroups I and III (shown in Fig. 8A and B, respectively). When projecting the conditions of these regions onto all of Mexico, the ecological niche of each haplogroup did not predict the CSA of the rest in the same way. Haplogroup V predicted a large part of the CSA obtained for haplogroup I, but only a small part of the known distribution area for haplogroup III (Fig. 8C). The models for haplogroup I and haplogroup III very poorly predicted the CSA of haplogroup V (Fig. 8A and B). In turn, the models of these last two haplogroups predict very few CSA of each other.

The ellipsoids that describe the environmental space of the populations for each haplogroup showed that haplogroup V has a broader environmental niche than the rest of the analyzed haplogroups (Fig. 8D). In addition, part of the environmental niche of haplogroup I and II overlapped with those of haplogroup V. The greatest differentiation

between ecological niches was observed between haplogroup I and II, where only a small part of the environmental conditions of the distribution of both overlaps.

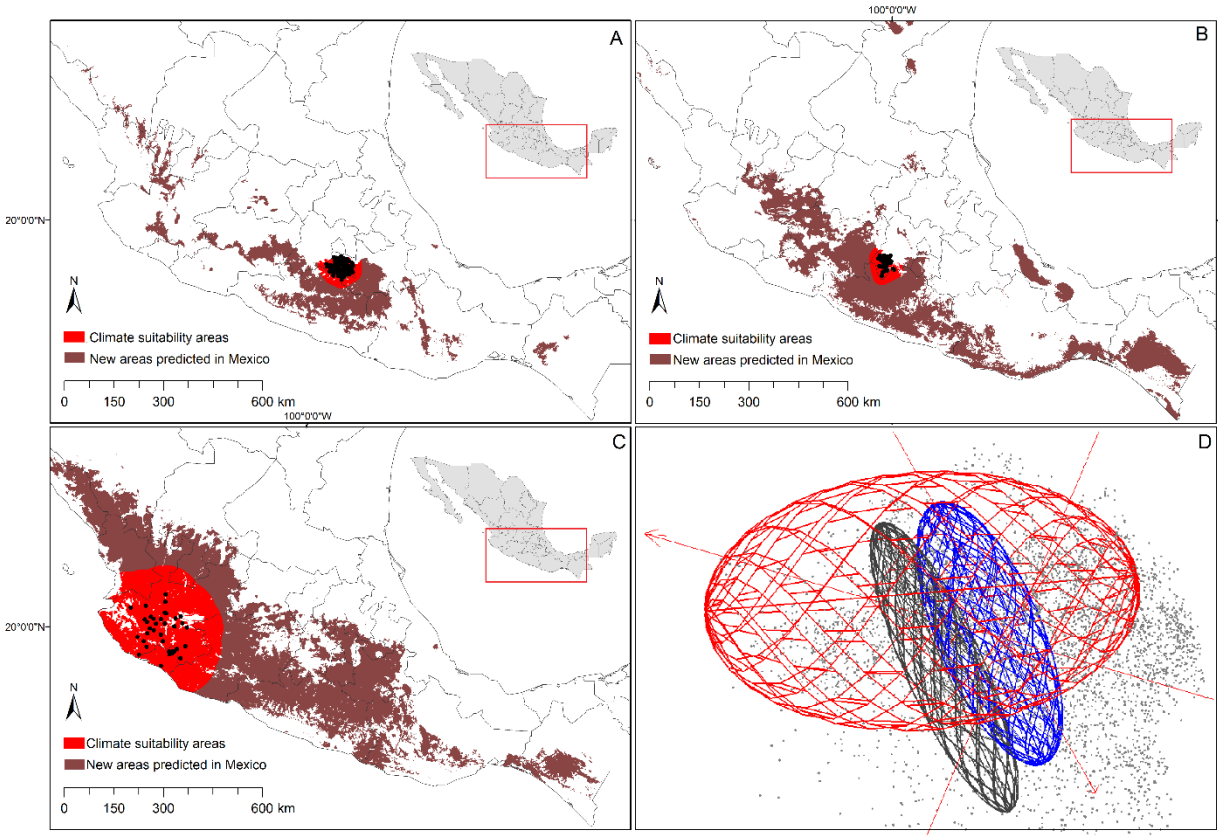

Figure 8. Climatic Suitability Areas and three-dimensional models in the environmental space of the presence records for three phylogenetic haplogroups of *Triatoma pallidipennis* (Hemiptera: Reduviidae). A: Haplogroup V. B: Haplogroup III. C: Haplogroup I. Blue ellipsoids correspond to the populations of Haplogroup I. Black ellipsoids correspond to the populations of Haplogroup III. Red ellipsoids correspond to the populations of Haplogroup V.

In the Principal Components Analysis, the first two components explained more than 95% of the variance of the environmental data. There were significant differences between at least two haplogroups in the first two components (Fig. 9).

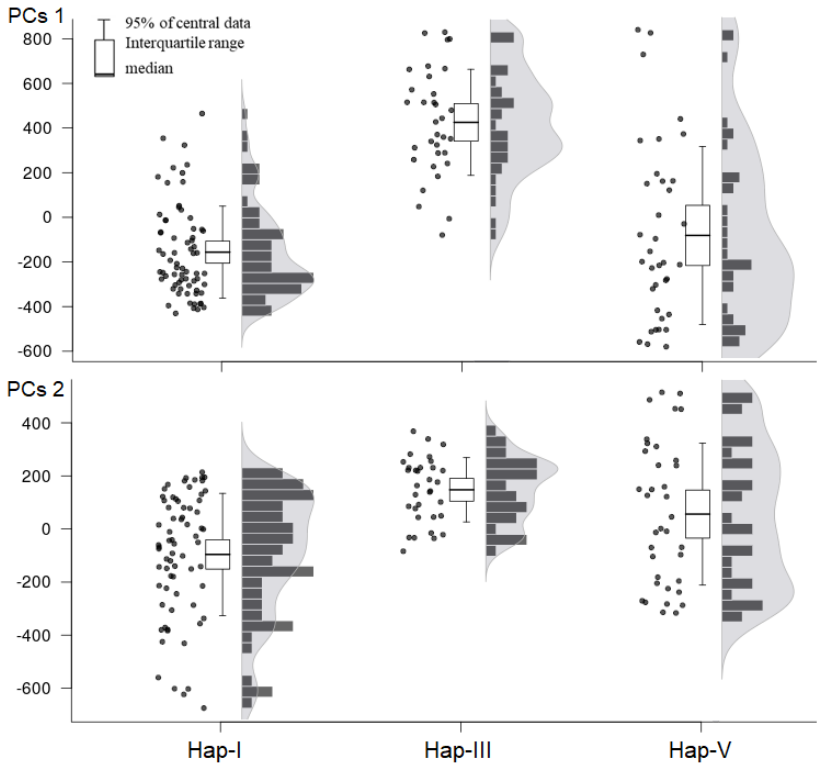

Figure 9. Statistical differences in the scores of the first two principal components among haplogroups of *Triatoma pallidipennis* (Hemiptera: Reduviidae), obtained by Kruskal-Wallis tests. A: Differences between haplogroups in Principal Component 1 score. B: Differences between haplogroups in Principal Component 2 score. Histograms, data density polygon, and data points (data used for statistical analysis) are plotted.

Discussion

Geometric morphometry

Species delimitation is frequently a controversial and complicated task, especially when the focal organisms are considered cryptic taxa (Tatsuta *et al.*, 2018). In the genus *Triatoma*, the presence of cryptic species has been extensively addressed, mainly using molecular methods (Bargues *et al.*, 2008; Ibarra-Cerdeña *et al.*, 2014; Justi *et al.*, 2014; Pech-May *et al.*, 2019). Geometric morphometrics has proven to be a useful tool in the context of species delimitation and taxonomic studies in triatomines (Dujardin *et al.*, 1999; Matias *et al.*, 2001; Jaramillo *et al.*, 2002; Villegas *et al.*, 2002; Gumiel *et al.*, 2003; Lehmann *et al.*, 2005; Vargas *et al.*, 2006; Feliciangeli *et al.*, 2007; Nattero *et al.*, 2017;

Cruz *et al.,* 2020). The use of morphological characters derived from novel techniques such as geometric morphometrics, as a reflection of genetic variability, is an efficient way to estimate the differentiation between phylogenetically differentiated groups (Patterson *et al.,* 2001).

Our results show significant differences in shape (but not size, as characterized by the CZ) among haplogroups. Previous studies have shown differences in head size between species (Gurgel-Gonçalves *et al.,* 2011, Oropeza *et al.*, 2017). Patterson (2007) hypothesized that differences in the head may have an evolutionary cause related to feeding strategies, with different morphologies allowing the ingestion of blood from different specific food sources, as well as different growth patterns. If we consider the hypothesis of Patterson (2007), a possible explanation for the fact that there is no difference in the size of the head between haplogroups is that the recent speciation processes that have occurred in the populations of *T. pallidipennis* may not have led to a segregation of feeding niches. For these reasons, the general size pattern of *T. pallidipennis* may be maintained in each of the haplogroups analyzed.

Although significant differences were found in the shape (Procrustes distances) of the head among almost all the haplogroups, there was relatively low discrimination among haplogroups using the LDA. Thus, the differences found in the shape of the head and the pronotum should be considered an indication that the haplogroups of *T. pallidipennis* are following different evolutionary divergences in which geographic isolation seems to be having an important effect. This phenomenon has been described for other triatomines, as is the case of the *dimidiata* species complex, in which morphological differences in head shape were a phenotypic consequence of isolation among their populations (Bustamante *et al.,* 2004).

The fact that the best-discriminated haplogroup based on head shape was from Colima and Jalisco (Haplogroup V) may be an indication that the geographic isolation between the populations of *T. pallidipennis* is acting as a modulator of the expression of differentiated morphological characters, concerning the other haplogroups. Geometric morphometrics is a complement to molecular methods since genetic differentiation very

often results in morphometric variations that allow groups from different regions to be distinguished (Bradshaw *et al.*, 2000; Stacey and Fellowes, 2002).

The capacity of geometric morphometrics to discriminate phylogenetically differentiated groups has been demonstrated for other groups of insects (De la Riva *et al.*, 2001). In our previous phylogenetic results (Cruz and Arellano, 2022), haplogroup V presents high values of genetic distances (K2P) based on the ND4 gene, concerning the other haplogroups analyzed (4.91, 5.82, and 6.45% with haplogroups I, II and III, respectively). Therefore, the geometric morphometrics analysis was able to differentiate this evolutionary unit from the others 68.0 % of the time. This was also the case of haplogroup III, which had similar correct discrimination values (68.5 %) to haplogroup V, and like these, had high genetic distances concerning the other haplogroups analyzed (6.61 and 6.76 % with haplogroups I and II, respectively). At the same time, the near-total overlap between haplogroups I and II in terms of head shape reflects the smaller genetic distance between these two haplogroups (3.19 %) (see Cruz and Arellano, 2022).

Regarding the pronotum, the global values of correct discrimination were lower than those found for the head. However, haplogroup II was the best discriminated against based on pronotum shape, reaching 64.3% correct discrimination. Although statistically significant differences were only found in the shape of the pronotum in the paired comparison between haplogroups II-III and II-V, these differences were marked, as can be seen in figure 5. Similar results were obtained by Nattero *et al*., (2017); they analyzed the morphological variability of the *Sordida* species subcomplex and obtained the lowest discrimination values between species from the pronotum shape information. These authors only used four landmarks for the morphometric characterization of this structure, which could explain their low discrimination values. The pronotum has been very seldom used in the context of geometric morphometrics (Nattero *et al.*, 2017), and in triatomines, it has mainly been used in traditional morphological descriptions (Lent and Wygodzinsky, 1979).

In this investigation, the greatest differences in pronotum shape were in the right posterior lobe and the humeral angle, which partially coincides with the results obtained by Cruz *et al.*, (2020) using elliptic Fourier descriptors to discriminate haplogroups of the *dimidiata* complex. Therefore, even in this study, we did not find a high percentage of

discrimination using the pronotum, the exploration of this structure constitutes an important step in any protocol of geometric morphometrics in triatomines to achieve a better characterization of its variation in this group of insects. It is possible that by describing the shape of the entire structure, either using landmarks and semilandmarks, as well as other morphometric methods such as Fourier elliptic descriptors, better discrimination percentages could be achieved. Fourier elliptic descriptors have been particularly efficient in discriminating species and haplogroups within the *Triatoma* genus (Santillán-Guayasamín *et al.*, 2017, Cruz *et al.*, 2020).

Ecological niche

In this study, environmental constraints for the current distribution of members of three *T. pallidipennis* haplogroups were identified by applying ecological niche modeling techniques. The distribution range of these haplogroups in Mexico reflects the diverse environmental conditions to which they have probably adapted. They may also reflect physiological differences among them (Zhao *et al.*, 2019).

The ENM for each haplogroup, both in their strict distribution areas and in the projections obtained for the rest of Mexico, shows considerable independence from environmental conditions. However, the prediction of some CAAs of one haplogroup from the occurrence data of another demonstrates a certain degree of niche conservatism, especially between the haplogroups I and V.

Our results have shown that the distribution of each haplogroup analyzed is limited by a set of environmental conditions. This was corroborated by obtaining the environmental space occupied by each hypervolume. Although there is still some overlap in the environmental conditions related to the distribution of the haplogroups, this is not of equal intensity for all. This could be an indication that ecological segregation has indeed played an important role in the differentiation of these monophyletic lineages, which is supported by the significant differences found for at least two of the haplogroups analyzed.

The ellipsoids showed clear differences in the use of the existing environmental space among the three haplogroups analyzed. This differentiation pattern has been reported for *Triatoma dimidiata* haplogroups (Gómez-Palacio *et al.*, 2015), so this phenomenon may

be more common in triatomines than currently recognized. However, although these results partially corroborate the role of ecological segregation as a speciation phenomenon in at least these two species complexes, for the *Triatoma pallidipennis* haplogroups it is necessary to evaluate hypotheses of niche conservatism to reach more solid conclusions.

Allopatric divergence has been considered the predominant mode of geographic speciation for most animal taxa (Barraclough *et al.*, 1999; Schluter, 2001; Levin, 2004) and does not account for significant niche divergence between closely related taxa. (Peterson *et al.*, 1999; Graham *et al.*, 2004; Kozak and Wiens, 2006; Broennimann *et al.*, 2007; Peterson and Nyári, 2008; Warren *et al.*, 2008). However, the distribution of the populations of the haplogroups analyzed in different biogeographical provinces is an important element to have in mind when considering ecological segregation. According to the classification of biogeographic provinces (Morrone, 2005), the populations belonging to haplogroup V are distributed in the Pacific Coast and Volcanic Axis provinces. Being present in two biogeographic provinces with different environmental characteristics explains the fact that this haplogroup presented a broader environmental niche than the rest. Haplogroup III has populations in the Balsas Depression and a small part of Volcanic Axis provinces, while the haplogroup I am only distributed within the Balsas Depression. The presence of shared populations in the Balsas Depression between haplogroups I and III could explain the slight overlap observed between ellipsoids of these haplogroups.

Although all these results suggest that the genetic differentiation between haplogroups of *T. pallidipennis* could reflect recent ecological segregation processes, the potential effect of genetic isolation of the populations of each haplogroup cannot be denied. Future analyses should be aimed at resolving this question, to provide more elements to elucidate the speciation processes that are occurring within *T. pallidipennis*. However, these results provide support from an ecological perspective that this species should be considered a complex of cryptic species.

Final considerations

Our results show how the analysis of morphometric variation and the characterization of the environmental conditions that define the climatic niche can be used to improve the delimitation of haplogroups that may constitute cryptic species. Analysis of

multiple lines of evidence (i.e., the integrative taxonomy approach) can increase our ability to detect intraspecific variation and provide strong evidence for species separation. In the case of triatomine species and other disease vectors, this information has implications for epidemiology, management, and vector control.

References

1. Adams, D. C., Rohlf, F. J., & Slice, D. E. (2004). Geometric morphometrics: ten years of progress following the 'revolution'. Italian Journal of Zoology, 71(1), 5-16.
2. Adams, D. C., & Otárola-Castillo, E. (2013). geomorph: an R package for the collection and analysis of geometric morphometric shape data. Methods in ecology and evolution, 4(4), 393-399.
3. Aiello-Lammens, M. E., Boria, R. A., Radosavljevic, A., Vilela, B., & Anderson, R. P. (2015). spThin: an R package for spatial thinning of species occurrence records for use in ecological niche models. Ecography, 38(5), 541-545.
4. Anderson, M. J. (2001). A new method for non-parametric multivariate analysis of variance. Austral ecology, 26(1), 32-46.
5. Araujo, M. B., & Guisan, A. (2006). Five (or so) challenges for species distribution modelling. Journal of biogeography, 33(10), 1677-1688.
6. Araújo, M. B., & Peterson, A. T. (2012). Uses and misuses of bioclimatic envelope modeling. Ecology, 93(7), 1527-1539.
7. Bargues, M. D., Klisiowicz, D. R., Gonzalez-Candelas, F., Ramsey, J. M., Monroy, C., Ponce, C., ... & Mas-Coma, S. (2008). Phylogeography and genetic variation of *Triatoma dimidiata*, the main Chagas disease vector in Central America, and its position within the genus *Triatoma*. PLoS neglected tropical diseases, 2(5), e233.
8. Barraclough, T. G., Hogan, J. E., & Vogler, A. P. (1999). Testing whether ecological factors promote cladogenesis in a group of tiger beetles (Coleoptera: Cicindelidae). Proceedings of the Royal Society of London. Series B: Biological Sciences, 266(1423), 1061-1067.
9. Bickford, D., Lohman, D. J., Sodhi, N. S., Ng, P. K., Meier, R., Winker, K., ... & Das, I. (2007). Cryptic species as a window on diversity and conservation. Trends in ecology & evolution, 22(3), 148-155.

10. Bogdanowicz, W., Juste, J., Owen, R. D., & Sztencel, A. (2005). Geometric morphometrics and cladistics: testing evolutionary relationships in mega-and microbats. Acta Chiropterologica, 7(1), 39-49.
11. Bookstein, F. L. (1997). Morphometric tools for landmark data (p. 455). Geometry and biology. Cambridge University Press. New York, EE. UU.
12. Bradshaw, W. E., Fujiyama, S., & Holzapfel, C. M. (2000). Adaptation to the thermal climate of North America by the pitcher-plant mosquito, *Wyeomyia smithii*. Ecology, 81(5), 1262-1272.
13. Broennimann, O., Treier, U. A., Müller-Schärer, H., Thuiller, W., Peterson, A. T., & Guisan, A. (2007). Evidence of climatic niche shift during biological invasion. Ecology letters, 10(8), 701-709.
14. Bustamante, D. M., Monroy, C., Menes, M., Rodas, A., Salazar-Schettino, P. M., Rojas, G., ... & Dujardin, J. P. (2004). Metric variation among geographic populations of the Chagas vector *Triatoma dimidiata* (Hemiptera: Reduviidae: Triatominae) and related species. Journal of Medical Entomology, 41(3), 296-301.
15. Collyer, M. L., & Adams, D. C. (2018). RRPP: An r package for fitting linear models to high-dimensional data using residual randomization. Methods in Ecology and Evolution, 9(7), 1772-1779.
16. Cruz, D. D., Arellano, E., Denis Ávila, D., & Ibarra-Cerdeña, C. N. (2020). Identifying Chagas disease vectors using elliptic Fourier descriptors of body contour: a case for the cryptic *dimidiata* complex. Parasites & vectors, 13(1), 1-12.
17. Cruz, D. D., & Arellano, E. (2022). Molecular data confirm *Triatoma pallidipennis* Stål, 1872 (Hemiptera: Reduviidae: Triatominae), as a novel cryptic species complex. Acta Tropica, 106382.
18. Dayrat, B. (2005). Towards integrative taxonomy. Biological journal of the Linnean society, 85(3), 407-417.
19. De la Riva, J., Le Pont, F., Ali, V., Matias, A., Mollinedo, S., & Dujardin, J. P. (2001). Wing geometry as a tool for studying the *Lutzomyia longipalpis* (Diptera: Psychodidae) complex. Memórias do Instituto Oswaldo Cruz, 96(8), 1089-1094.
20. De Queiroz, K. (2007). Species concepts and species delimitation. Systematic biology, 56(6), 879-886.

21. Dujardin, J. P. (2011). Modern morphometrics of medically important insects. In Genetics and evolution of infectious disease (pp. 473-501). Elsevier.
22. Dujardin, J. P., Panzera, P., & Schofield, C. J. (1999). Triatominae as a model of morphological plasticity under ecological pressure. Memórias do Instituto Oswaldo Cruz, 94, 223-228.
23. Feliciangeli, M. D., Sanchez-Martin, M., Marrero, R., Davies, C., & Dujardin, J. P. (2007). Morphometric evidence for a possible role of *Rhodnius prolixus* from palm trees in house re-infestation in the State of Barinas (Venezuela). Acta tropica, 101(2), 169-177.
24. Fick, S. E., & Hijmans, R. J. (2017). WorldClim 2: new 1-km spatial resolution climate surfaces for global land areas. International journal of climatology, 37(12), 4302-4315.
25. Freitas, F. V., Santos Júnior, J. E., Santos, F. R., & Silveira, F. A. (2018). Species delimitation and sex associations in the bee genus *Thygater*, with the aid of molecular data, and the description of a new species. Apidologie, 49(4), 484-496.
26. Gómez-Palacio, A., Arboleda, S., Dumonteil, E., & Peterson, A. T. (2015). Ecological niche and geographic distribution of the Chagas disease vector, *Triatoma dimidiata* (Reduviidae: Triatominae): Evidence for niche differentiation among cryptic species. Infection, genetics and evolution, 36, 15-22.
27. Goodall, C. (1991). Procrustes methods in the statistical analysis of shape. Journal of the Royal Statistical Society: Series B (Methodological), 53(2), 285-321.
28. Graham, C. H., Ron, S. R., Santos, J. C., Schneider, C. J., & Moritz, C. (2004). Integrating phylogenetics and environmental niche models to explore speciation mechanisms in dendrobatid frogs. Evolution, 58(8), 1781-1793.
29. Gumiel, M., Catalá, S., Noireau, F., Rojas de Arias, A., Garcia, A., & Dujardin, J. P. (2003). Wing geometry in *Triatoma infestans* (Klug) and *T. melanosoma* Martinez, Olmedo & Carcavallo (Hemiptera: Reduviidae). Systematic Entomology, 28(2), 173-180.
30. Gunz, P., & Mitteroecker, P. (2013). Semilandmarks: a method for quantifying curves and surfaces. Hystrix, the Italian journal of mammalogy, 24(1), 103-109.

595 31. Gunz, P., Mitteroecker, P., & Bookstein, F. L. (2005). Semilandmarks in three
596 dimensions. In Modern morphometrics in physical anthropology (pp. 73-98).
597 Springer, Boston, MA.
598 32. Gurgel-Gonçalves, R., Ferreira, J. B. C., Rosa, A. F., Bar, M. E., & Galvão, C.
599 (2011). Geometric morphometrics and ecological niche modelling for delimitation
600 of near-sibling triatomine species. Medical and Veterinary Entomology, 25(1), 84-
601 93.
602 33. Hernández, M. L., Dujardin, J. P., Gorla, D. E., & Catalá, S. S. (2013). Potential
603 sources of *Triatoma infestans* reinfesting peridomiciles identified by morphological
604 characterization in Los Llanos, La Rioja, Argentina. Memórias do Instituto Oswaldo
605 Cruz, 108(1), 91-97.
606 34. Ibarra-Cerdeña, C. N., Zaldívar-Riverón, A., Peterson, A. T., Sánchez-Cordero, V.,
607 & Ramsey, J. M. (2014). Phylogeny and niche conservatism in North and Central
608 American triatomine bugs (Hemiptera: Reduviidae: Triatominae), vectors of
609 Chagas' disease. PLoS neglected tropical diseases, 8(10), e3266.
610 35. Jaramillo O, N., Castillo, D., & Wolff E, M. (2002). Geometric morphometric
611 differences between *Panstrongylus geniculatus* from field and laboratory. Memórias
612 do Instituto Oswaldo Cruz, 97, 667-673.
613 36. Justi, S. A., Russo, C. A., Mallet, J. R. D. S., Obara, M. T., & Galvão, C. (2014).
614 Molecular phylogeny of Triatomini (Hemiptera: Reduviidae: Triatominae).
615 Parasites & vectors, 7(1), 1-12.
616 37. Kass, J. M., Vilela, B., Aiello-Lammens, M. E., Muscarella, R., Merow, C., &
617 Anderson, R. P. (2018). Wallace: A flexible platform for reproducible modeling of
618 species niches and distributions built for community expansion. Methods in
619 Ecology and Evolution, 9(4), 1151-1156.
620 38. Kozak, K. H., Graham, C. H., & Wiens, J. J. (2008). Integrating GIS-based
621 environmental data into evolutionary biology. Trends in ecology & evolution, 23(3),
622 141-148.
623 39. Leaché, A. D., Koo, M. S., Spencer, C. L., Papenfuss, T. J., Fisher, R. N., &
624 McGuire, J. A. (2009). Quantifying ecological, morphological, and genetic variation

to delimit species in the coast horned lizard species complex (*Phrynosoma*). Proceedings of the National Academy of Sciences, 106(30), 12418-12423.

40. Lefébure, T., Douady, C. J., Gouy, M., & Gibert, J. (2006). Relationship between morphological taxonomy and molecular divergence within Crustacea: proposal of a molecular threshold to help species delimitation. Molecular phylogenetics and evolution, 40(2), 435-447.
41. Lehmann, P., Ordoñez, R., Ojeda-Baranda, R., Lira, J., Hidalgo-Sosa, L., Monroy, C., & Ramsey, J. M. (2005). Morphometric analysis of *Triatoma dimidiata* populations (Reduviidae: Triatominae) from Mexico and northern Guatemala. Memórias do Instituto Oswaldo Cruz, 100(5), 477-486.
42. Lent, H., & Wygodzinsky, P. (1979). Revision of the Triatominae (Hemiptera, Reduviidae), and their significance as vectors of Chagas' disease. Bulletin of the American museum of Natural History, 163(3), 123-520.
43. Levin, D. A. (2004). The ecological transition in speciation. New Phytologist, 161(1), 91-96.
44. MacGuigan, D. J., Geneva, A. J., & Glor, R. E. (2017). A genomic assessment of species boundaries and hybridization in a group of highly polymorphic anoles (*distichus* species complex). Ecology and Evolution, 7(11), 3657-3671.
45. Martínez-Borrego, D., Arellano, E., Cruz, D. D., González-Cózatl, F. X., Nava-García, E., & Rogers, D. S. (2021). Morphological and ecological data confirm *Reithrodontomys cherrii* as a distinct species from *Reithrodontomys mexicanus*. THERYA, 13(1), 115.
46. Martínez-Ibarra, J. A., & Katthain-Duchateau, G. (1999). Biology of *Triatoma pallidipennis* Stal 1945 (Hemiptera: Reduviidae: Triatominae) under laboratory conditions. Memórias do Instituto Oswaldo Cruz, 94, 837-839.
47. Masonick, P., & Weirauch, C. (2020). Integrative species delimitation in Nearctic ambush bugs (Heteroptera: Reduviidae: Phymatinae): Insights from molecules, geometric morphometrics and ecological associations. Systematic Entomology, 45(1), 205-223.

654 48. Matias, A., De la Riva, J. X., Torrez, M., & Dujardin, J. P. (2001). *Rhodnius*
655 *robustus* in Bolivia identified by its wings. Memorias do Instituto Oswaldo Cruz,
656 96(7), 947-950.
657 49. Matos-Maraví, P., Wahlberg, N., Antonelli, A., & Penz, C. M. (2019). Species
658 limits in butterflies (Lepidoptera: Nymphalidae): reconciling classical taxonomy
659 with the multispecies coalescent. Systematic Entomology, 44(4), 745-756.
660 50. Mitteroecker, P., & Gunz, P. (2009). Advances in geometric morphometrics.
661 Evolutionary Biology, 36(2), 235-247.
662 51. Moo-Llanes, D. A. (2021). Inferring Distributional Shifts of Asian Giant Hornet
663 *Vespa mandarinia* Smith in Climate Change Scenarios. Neotropical Entomology,
664 50(4), 673-676.
665 52. Morrone, J. J. (2005). Hacia una síntesis biogeográfica de México. Revista
666 mexicana de biodiversidad, 76(2), 207-252.
667 53. Muscarella, R., Galante, P. J., Soley-Guardia, M., Boria, R. A., Kass, J. M., Uriarte,
668 M., & Anderson, R. P. (2014). ENM eval: An R package for conducting spatially
669 independent evaluations and estimating optimal model complexity for Maxent
670 ecological niche models. Methods in ecology and evolution, 5(11), 1198-1205.
671 54. Nattero, J., Piccinali, R. V., Macedo Lopes, C., Hernández, M. L., Abrahan, L.,
672 Lobbia, P. A., ... & Carbajal de la Fuente, A. L. (2017). Morphometric variability
673 among the species of the *Sordida* subcomplex (Hemiptera: Reduviidae:
674 Triatominae): evidence for differentiation across the distribution range of *Triatoma*
675 *sordida*. Parasites & vectors, 10(1), 1-14.
676 55. Oliveira, J., Marcet, P. L., Takiya, D. M., Mendonca, V. J., Belintani, T., Bargues,
677 M. D., ... & Almeida, C. E. (2017). Combined phylogenetic and morphometric
678 information to delimit and unify the *Triatoma brasiliensis* species complex and the
679 *Brasiliensis* subcomplex. Acta tropica, 170, 140-148.
680 56. Oropeza, A. M., Perri Fernández, C. A., Liria, J., & Soto Vivas, A. (2017). Head
681 geometric morphometrics of two Chagas disease vectors from Venezuela.
682 57. Padial, J. M., Miralles, A., De la Riva, I., & Vences, M. (2010). The integrative
683 future of taxonomy. Frontiers in zoology, 7(1), 1-14.

58. Patterson, J. S. (2007). Comparative Morphometric and Molecular Genetic Analyses of Triatominae (Hemiptera: Reduviidae) (Doctoral dissertation, London School of Hygiene and Tropical Medicine (University of London)).
59. Patterson, J. S., Schofield, C. J., Dujardin, J. P., & Miles, M. A. (2001). Population morphometric analysis of the tropicopolitan bug *Triatoma rubrofasciata* and relationships with Old World species of *Triatoma*: evidence of New World ancestry. Medical and veterinary entomology, 15(4), 443-451.
60. Pavan, A. C., & Marroig, G. (2016). Integrating multiple evidences in taxonomy: species diversity and phylogeny of mustached bats (Mormoopidae: *Pteronotus*). Molecular Phylogenetics and Evolution, 103, 184-198.
61. Pech-May, A., Mazariegos-Hidalgo, C. J., Izeta-Alberdi, A., López-Cancino, S. A., Tun-Ku, E., De la Cruz-Felix, K., ... & Ramsey, J. M. (2019). Genetic variation and phylogeography of the *Triatoma dimidiata* complex evidence a potential center of origin and recent divergence of haplogroups having differential *Trypanosoma cruzi* and DTU infections. PLoS neglected tropical diseases, 13(1), e0007044.
62. Peterson, A. T., & Nyari, A. S. (2008). Ecological niche conservatism and Pleistocene refugia in the thrush-like mourner, *Schiffornis* sp., in the neotropics. Evolution: International Journal of Organic Evolution, 62(1), 173-183.
63. Peterson, A. T., Soberón, J., & Sánchez-Cordero, V. (1999). Conservatism of ecological niches in evolutionary time. Science, 285(5431), 1265-1267.
64. Pfenninger, M., & Schwenk, K. (2007). Cryptic animal species are homogeneously distributed among taxa and biogeographical regions. BMC evolutionary biology, 7(1), 1-6.
65. Phillips, S. J., Anderson, R. P., & Schapire, R. E. (2006). Maximum entropy modeling of species geographic distributions. Ecological modelling, 190(3-4), 231-259.
66. Phillips, S. J., Anderson, R. P., Dudík, M., Schapire, R. E., & Blair, M. E. (2017). Opening the black box: An open-source release of Maxent. Ecography, 40(7), 887-893.

67. Qiao, H., Peterson, A. T., Campbell, L. P., Soberón, J., Ji, L., & Escobar, L. E. (2016). NicheA: creating virtual species and ecological niches in multivariate environmental scenarios. Ecography, 39(8), 805-813.
68. Radosavljevic, A., & Anderson, R. P. (2014). Making better Maxent models of species distributions: complexity, overfitting, and evaluation. Journal of biogeography, 41(4), 629-643.
69. Ramsey, J. M., Peterson, A. T., Carmona-Castro, O., Moo-Llanes, D. A., Nakazawa, Y., Butrick, M., ... & Ibarra-Cerdeña, C. N. (2015). Atlas of Mexican Triatominae (Reduviidae: Hemiptera) and vector transmission of Chagas disease. Memórias do Instituto Oswaldo Cruz, 110, 339-352.
70. Ripley, B., Venables, B., Bates, D. M., Hornik, K., Gebhardt, A., Firth, D., & Ripley, M. B. (2013). Package 'mass'. Cran r, 538, 113-120.
71. Rissler, L. J., & Apodaca, J. J. (2007). Adding more ecology into species delimitation: ecological niche models and phylogeography help define cryptic species in the black salamander (*Aneides flavipunctatus*). Systematic biology, 56(6), 924-942.
72. Rivera, P. C., González-Ittig, R. E., Robainas Barcia, A., Trimarchi, L. I., Levis, S., Calderón, G. E., & Gardenal, C. N. (2018). Molecular phylogenetics and environmental niche modeling reveal a cryptic species in the *Oligoryzomys flavescens* complex (Rodentia, Cricetidae). Journal of Mammalogy, 99(2), 363-376.
73. Rohlf, F. J. (2015). The tps series of software. Hystrix, 26(1).
74. Rohlf, F. J., & Slice, D. (1990). Extensions of the Procrustes method for the optimal superimposition of landmarks. Systematic biology, 39(1), 40-59.
75. Sangster, G. (2018). Integrative taxonomy of birds: the nature and delimitation of species. In Bird species (pp. 9-37). Springer, Cham.
76. Santillán-Guayasamín, S., Villacís, A. G., Grijalva, M. J., & Dujardin, J. P. (2017). The modern morphometric approach to identify eggs of Triatominae. Parasites & vectors, 10(1), 1-10.
77. Schlager, S. (2017). Morpho and Rvcg–Shape Analysis in R: R-Packages for geometric morphometrics, shape analysis and surface manipulations. In Statistical shape and deformation analysis (pp. 217-256). Academic Press.

744 78. Schluter, D. (2001). Ecology and the origin of species. Trends in ecology &
745 evolution, 16(7), 372-380.
746 79. Sites Jr, J. W., & Marshall, J. C. (2004). Operational criteria for delimiting species.
747 Annu. Rev. Ecol. Evol. Syst., 35, 199-227.
748 80. Stacey, D. A., & Fellowes, M. D. E. (2002). Temperature and the development rates
749 of thrips: evidence for a constraint on local adaptation?. European Journal of
750 Entomology, 99(3), 399-404.
751 81. Tatsuta, H., Takahashi, K. H., & Sakamaki, Y. (2018). Geometric morphometrics in
752 entomology: Basics and applications. Entomological Science, 21(2), 164-184.
753 82. Tarquino-Carbonell, A. D. P., Ojeda, R. A., & Ojeda, A. A. (2020). Influence of
754 climate change on the predicted distributions of the genus *Tympanoctomys*
755 (Rodentia, Hystricomorpha, Octodontidae), and their conservation implications.
756 Journal of Mammalogy, 101(5), 1364-1379.
757 83. Van Aelst, S., & Rousseeuw, P. (2009). Minimum volume ellipsoid. Wiley
758 Interdisciplinary Reviews: Computational Statistics, 1(1), 71-82.
759 84. Vargas, E., Espitia, C., Patiño, C., Pinto, N., Aguilera, G., Jaramillo, C., ... & Guhl,
760 F. (2006). Genetic structure of *Triatoma venosa* (Hemiptera: Reduviidae):
761 molecular and morphometric evidence. Memórias do Instituto Oswaldo Cruz,
762 101(1), 39-45.
763 85. Vendrami, D. P., Obara, M. T., Gurgel-Gonçalves, R., Ceretti-Junior, W., &
764 Marrelli, M. T. (2017). Wing geometry of *Triatoma* sordida (Hemiptera:
765 Reduviidae) populations from Brazil. Infection, Genetics and Evolution, 49, 17-20.
766 86. Villegas, J., Feliciangeli, M. D., & Dujardin, J. P. (2002). Wing shape divergence
767 between *Rhodnius prolixus* from Cojedes (Venezuela) and *Rhodnius robustus* from
768 Mérida (Venezuela). Infection, Genetics and Evolution, 2(2), 121-128.
769 87. Warren, D. L., Glor, R. E., & Turelli, M. (2008). Environmental niche equivalency
770 versus conservatism: quantitative approaches to niche evolution. Evolution:
771 International Journal of Organic Evolution, 62(11), 2868-2883.
772 88. Zelditch, M. L., Swiderski, D. L., & Sheets, H. D. (2012). Geometric
773 morphometrics for biologists: a primer. academic press.

89. Zhao, Q., Zhang, H., & Wei, J. (2019). Climatic niche comparison across a cryptic species complex. PeerJ, 7, e7042.

Supplementary data

Manuscript: Geometric morphometrics and ecological niche modelling for delimitation of *Triatoma pallidipennis* haplogroups

Daryl D. Cruz1*, Sandra Milena Ospina-Garces2, Elizabeth Arellano1, Carlos N. Ibarra-Cerdeña3, Elizabeth Nava-García4 and Raúl Alcalá1

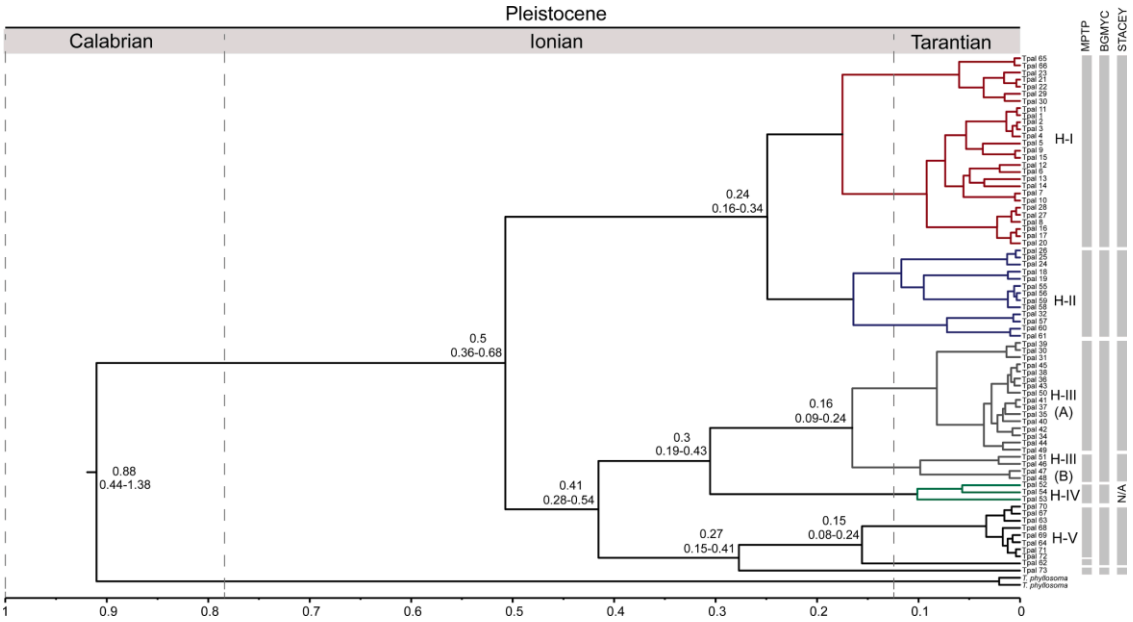

Figure S1. ND4 phylogeny estimated divergence times, and species delimitation in *Triatoma pallidipennis* (Hemiptera: Reduviidae: Triatominae) implementing the evolutionary model HKY+F+I for partitions 1+2 and HKY+F+G4 for partition 3. Divergence times (top) are shown above each branch. The bars on the right side of the figure correspond to the species delimitation obtained by the Multi-rate Poisson Tree Process (mPTP; leftmost), the Bayesian General Mixed Yule-Coalescent Model (bGMYC; middle), and the Species Tree And Classification Estimation, Yarely (STACEY; rightmost). Cruz and Arellano (2022).

Table S1. Number of samples per haplogroup of *Triatoma pallidipennis* used for morphometric analysis. Haplogroup I: specimens of Morelos, Haplogroup II: specimens of State of Mexico and Guerrero, Haplogroup III: specimens of State of Mexico, Haplogroup V: specimens of Colima and Jalisco.

	Head			**Pronotum**		
Haplogroup	♂	♀	Total	♂	♀	Total
I	8	12	20	8	13	21
II	8	19	27	9	19	28
III	22	13	35	23	16	39
V	12	13	25	13	12	25

Capítulo IV.

Identifying Chagas disease vectors using elliptic Fourier descriptors of body contour: a case for the cryptic dimidiata complex

Parasites & Vectors

RESEARCH Open Access

Identifying Chagas disease vectors using elliptic Fourier descriptors of body contour: a case for the cryptic *dimidiata* complex

Daryl D. Cruz[1*], Elizabeth Arellano[1], Dennis Denis Ávila[2] and Carlos N. Ibarra-Cerdeña[3]

Abstract

Background: *Triatoma dimidiata* (Reduviidae: Triatominae) is an important vector of Chagas disease in various countries in the Americas. Phylogenetic studies have defined three lineages in Mexico and part of Central America. While there is a marked genetic differentiation, methods for identifying them using morphometric analyses with landmarks have not yet been fully resolutive. Elliptical Fourier descriptors (EFDs), which mathematically describe the shape of any closed two-dimensional contours, could be a potentially useful alternative method. Our objective was to validate the use of EFDs for the identification of three lineages of this species complex.

Method: A total of 84 dorsal view images of individuals of the three lineages were used. Body contours were described with EFDs using between 5 and 30 harmonics. The number of obtained coefficients was reduced by a principal components analysis and the first axis scores were used as shape variables. A linear discriminant function analysis and an ordination plot of the discriminant analysis were performed using the shape variables. A confusion matrix of the ordination plot of the discriminant analysis was obtained to estimate the classification errors, the first five PC scores were statistically compared, and a neural network were then performed using the shape variables.

Results: The first principal component explained 50% of the variability, regardless the number of harmonics used. The results of discriminant analysis get improved by increasing the number of harmonics and components considered. With 25 harmonics and 30 components, the identification of haplogroups was achieved with an overall efficiency greater than 97%. The ordering diagram showed the correct discrimination of haplogroups, with only one error of discrimination corroborated by the confusion matrix. When comparing the first five PC scores, significant differences were found among at least two haplogroups. The 30 multilayer perceptron neural networks were also efficient in identification, reaching 91% efficiency with the validation data.

Conclusions: The use of EFD is a simple and useful method for the identification of the main lineages of *Triatoma dimidiata*, with high values of correct identification.

Keywords: Triatomine, Identification, Morphometric analysis, Contours, Fourier

Background

Cryptic species are one of the great challenges for systematic biologists since, in many cases, speciation is not accompanied by distinctive morphological characters and allopatric distributions that facilitate the identification of different entities at the species level [1, 2]. For that reason, the actual number of biological species is likely to be greater than the current nominal species count,

*Correspondence: daryldavidcf@gmail.com
[1] Centro de Investigación en Biodiversidad y Conservación (CIByC), UAEM, Cuernavaca, Morelos, México
Full list of author information is available at the end of the article

most of which are delineated by purely morphological characteristics.

Research focused on cryptic species has increased over the last two decades mainly by the availability of DNA sequences [2]. The use of the term has grown and refers to two or more distinct species that are erroneously classified (hidden) under a single taxonomic entity, but through other evidence, mainly genetic, it can be proved that they have followed different evolutionary paths [3]. Cryptic species are found in almost all groups of organisms, and in the case of insects, their presence is a very frequent phenomenon in several orders [4, 5]. In the field of epidemiology, the correct identification of species in insect groups with medical importance is a key component for the design of vector control and surveillance strategies [6]. This is mainly because different species may vary in terms of their competence as vectors and their epidemiological importance as well as in their susceptibility to insecticides or other control strategies [7].

One of the most epidemiologically important groups of insects on the American continent is the triatomines (Triatominae: Reduviidae), the vectors of Chagas disease (CD). In this group, the genus *Triatoma* is the most diverse genus [8]; approximately 70 species have been described and it is the genus with the largest geographical distribution within the subfamily [9, 10]. Multiple inter- and intraspecies taxonomic questions have arisen in this group, with species repeatedly included and excluded from different complexes throughout the history of the study of their systematics and taxonomy [11–14]. The combination of unresolved taxonomic relationships and the detection of cryptic species within this genus highlight the need to address the systematics of this group [15–18]. The phenomenon of cryptic speciation is common in the Triatominae [19–21] and results in species that are nearly identical morphologically, which often makes identification based only on traditional morphological characters difficult or impossible.

The identification of triatomine species has usually been carried out using traditional morphometry [11, 14, 22, 23]. However, the use of geometric morphometry has led to new techniques for evaluating morphological characters in a taxonomic context; it complements the use of other methods of discrimination [24] and has been used for the recognition of very close species with a long history of controversy among taxonomists [25] and apparently cryptic species, including some of the genus *Triatoma* [7, 26–32].

The *Triatoma dimidiata* complex represents one of the major vectors of Chagas disease in all the countries where it is distributed [18, 33, 34]. It is present in Mexico, all the countries of Central America, Colombia, Ecuador and Perú [18, 35]. Throughout its range, it can be found in jungle, peridomestic and domestic habitats, where non-domiciled populations act as sources of re-infestation and participate in the transmission of the parasite to humans [35–38].

Phylogenetic studies using sequences from *cytb*, *nad4*, and *16S* rRNA genes, have defined three lineages in Mexico and part of Central America (with 6–14% divergence among haplogroups) [15, 39], which were recently reaffirmed by Pech-May et al. [18]. Using geometric morphometry techniques with a landmark-based analysis, Gurgel-Gonçalves et al. [40] reached correct identification rates of 70.5%, 76.7% and 82.5% for haplogroups 1, 2 and 3 of *T. dimidiata* respectively. More recently, Khalighifar et al. [41] using TensorFlow [42], an open-source software platform, representing the most recent addition to the deep learning toolbox [43] (Google Brain Team; https://research.google.com/teams/brain/), were able to increase the correct classification of specimens of the three haplogroups (84.1% H1, 86.7% H2 and 87.5% H3) [41]. Although these methodologies are the cutting-edge approach to the automatized species identification within the Triatomine group, this rate of identification is still insufficient and methods that guarantee higher power of correct discrimination are still necessary.

As an alternative, in this study we propose the use of elliptical Fourier descriptors (EFDs), which can delineate any shape with a two-dimensional closed contour, as suggested by Kuhl and Giardina [44]. Contour analysis is based on the digitalization of the silhouette of an object, which is expressed as a sequence of coordinates (x, y) that can be manipulated mathematically and adjusted to an equation derived from Fourier functions. For the extraction and digitization of outline characters, the elliptic Fourier algorithm has the advantages of being able to reconstruct outlines, eliminate errors in orientation caused by interference, size images and trace the starting point of an original image [45–48]. This method has been widely applied to the analysis of various biological shapes [48, 49] and more recently, as a tool for pattern detection, correct insect identification and automatic identification systems [50–52]. For the Triatominae in particular, the elliptic Fourier algorithm has been used with the objective of identifying species from the analysis of different structures [27, 53].

Here, we apply EFDs in order to evaluate their ability to identify the three described *T. dimidiata* haplogroups for Mexico and part of Central America. The results of this evaluation contribute to the implementation of tools for accurate discrimination between triatomine species and potentially to the control and prevention of CD.

Methods

Sample information

In order to test the ability of EFDs to discriminate among the haplogroups of *T. dimidiata*, we used the images obtained by Gurgel-Gonçalves et al. [40], which are available in the Dryad Digital Repository (http://dx.doi.org/10.5061/dryad.br14k). The original series of photos for triatomines were taken from entomological collections across Mexico (Centro Regional de Investigación en Salud, Instituto Nacional de Salud Pública, México; Laboratorio Estatal de Salud Pública de Guanajuato; Universidad Autónoma Benito Juárez, Oaxaca; Universidad Autónoma de Nuevo León, Monterrey), and 44, 30 and 40 images of haplogroups 1, 2 and 3 were obtained, respectively, with which the automated identification process tested by Gurgel-Gonçalves et al. [40] was performed. For this study, only images that had the necessary characteristics to perform the contour analysis were selected, i.e. only images with an unmodified contour and wings that were not broken or overlapped. This filtering process resulted in a total sample of 37 (21♀, 16♂), 23 (17♀, 6♂) and 36 (17♀, 19♂) images for haplogroups 1, 2 and 3, respectively. The conditions under which the photographs were taken, and more information about the samples, are detailed in Gurgel-Gonçalves et al. [40].

Images manual pre-processing

The images were manually pre-processed in Adobe Photoshop CS5. This pre-processing involved the removal of the legs and antennas from each image leaving only the body contour. The brightness and contrast values were adjusted to their minimum and maximum values, respectively, to leave only a binary image (Fig. 1). All images were saved as bitmaps (BMP) in 24-bit RGB format.

Obtention of *Triatoma dimidiata* haplogroups body contour and measurement error

To extract and quantify body contours of the *T. dimidiata* haplogroups we used SHAPE 1.3 software [54], designed to evaluate the contour shape based on elliptical Fourier transform. The observed contour is decomposed in terms of sine and cosine curves of successive frequencies called harmonics, and each harmonic is described by four coefficients. The closed contours of simple shapes can be expressed in polar coordinates with the radius as a function of the angle from a fixed internal point, which constitutes a periodic function. In this way, all the information about the shape in the sequence of points will be reduced to a smaller number of parameters whose distribution can be studied in the morphological space with the coefficients as axes [48]. Elliptical Fourier descriptors are an extension of this method, applicable when the contours are so complex that there could be more than one radius value per angle [55]. The method is developed by taking increments in X and Y between points, to define the periodic function [44]. A more detailed mathematical description of contour extraction based on EFDs can be found in Iwata et al. [56].

SHAPE has four subprograms (ChainCoder, Chc2Nef, PrinComp and PrinPrint) which together facilitate the processing of digital images, acquisition of the chain code and Fourier coefficients, and principal components analysis. It also includes routines for the visualization of the shape from previously digitized data (ChcViewer and NefViewer).

The chain code is a coding system to describe the spatial information of the contours with numbers from 0 to 7 [57]; digits indicate the direction of the next step around an outline: 0, one step to the right; 2, one step up; 4, one to the left; 6, one down; and the other digits are intermediate addresses. In order to obtain this code for each image, the ChainCoder subprogram was implemented for images of the haplogroups. This subprogram reads the BMP images, converts them to grayscale, binarizes them from a threshold value selected in the image histogram, eliminates possible noise existing in the images using erosion-dilution filters and obtains the chain code by edge detection and the contour information is stored as chain code, which is saved in an ASCII file with an extension chc. In all cases, digitization starts from the same homologous point from one image to another. Here, all images were converted to grayscale using the red channel, binarized with a threshold value of 150 and the erosion and dilution filters were worked with values of 1 and 10 respectively.

Once the chain code file was generated, for each image using the Chc2Nef program the Fourier transform coefficients for 5, 10, 15, 20, 25 and 30 harmonics were calculated consecutively, to evaluate the minimum number of harmonics that allow to achieve the best discrimination between haplogroups. We used the first harmonic ellipse parameters, to normalize the elliptic Fourier (NEF) coefficients so that they are invariant to size, rotation, and the starting position of the outline trace. NEF were stored in an ASCII file of extension.nef, and the four coefficients (related to the width-on-length ratio of the outline) were used for subsequent multivariate analyses [58].

Given that many variables (NEF) are produced (four coefficients for each harmonic), a principal components analysis (PCA) was performed using the variance-covariance matrices to reduce the dimensionality and obtain new derived variables that can be analyzed statistically. This was done using the PrinComp module, as proposed by Rohlf & Archie [48], and the scores of the first five principal components (PCs) that contributed most to the total variance were used as new shape variables.

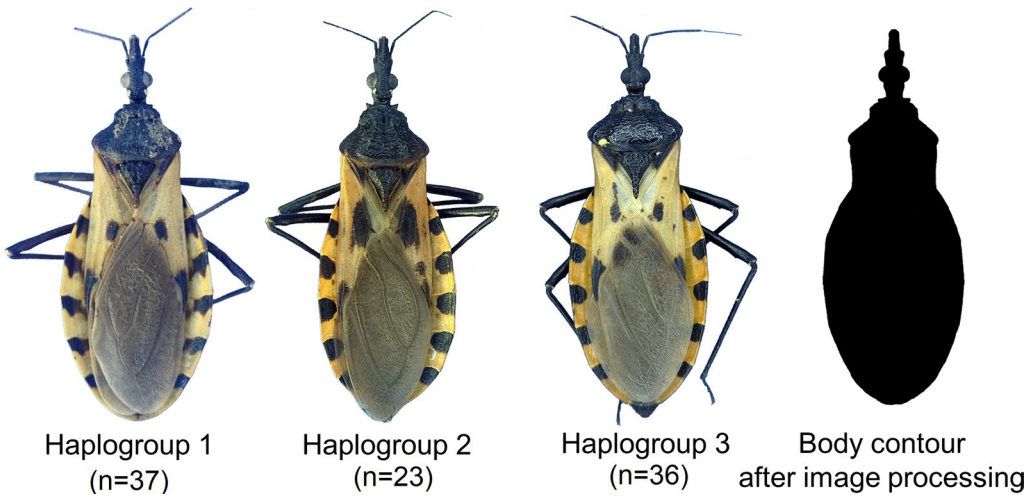

Fig. 1 Image examples of the three haplogroups of *Triatoma dimidiata* (Hemiptera: Reduviidae) and of a body contour after image processing for the analysis of the elliptical Fourier descriptors. Sample sizes per haplogroup are shown in parentheses under each image. Copyright: Creative Commons Attribution 1.0 Universal (CC0 1.0) Public Domain Dedication license (https://creativecommons.org/licenses/by/1.0). Images modified from Gurgel-Gonçalves R, Komp E, Campbell LP, Khalighifar A, Mellenbruch J, Mendonça VJ, et al. Automated identification of insect vectors of Chagas disease in Brazil and Mexico: the virtual vector lab. PeerJ. 2017;5:e3040 [40]

The variance contribution of all principal components is reported in Additional file 1: Table S1. The PCs contain all the information for each haplogroup body shape, as demonstrated by the fact that the contours can be graphically reconstructed from these, using an inverse Fourier transform in the PrinPrint module, according to the procedure of Furuta et al. [59]. Because in some cases, several main components can recover the contour with a high degree of precision, the first three that contributed most to the total variance were used to evaluate the interspecific and intraspecific differences in the contour. The rest of the reconstructions (the overlap between haplogroups and the individual reconstruction of each haplogroup) are shown in Additional file 2: Figure S1.

To estimate the measurement error of intraspecific variations, we produced 30 replications of 15 specimens for each haplogroups [60, 61]. Each contour of an individual was imaged and edited 30 times. An ANOSIM analysis was used to partition the total of the 1st PCs for each haplogroup into within and between-individual variations. The percentage measurement error was determined by the method indicated in Yezerinac et al. [60].

Contour shape discrimination and statistical analysis

To evaluate the ability of FEDs to discriminate among three haplogroups of *T. dimidiata*, a discriminant function analysis was performed to determine the minimum number of harmonics needed to produce the best classifications. Here we considered as the best classification the highest percentage of correct discrimination obtained for each haplogroup. For this, the PCs recovered from the PrinComp module were used. For the first five harmonics, the number of principal components was 16, while for 10, 15, 20, 25 and 30 harmonics, 30 principal components were recovered. An ordination plot of the discriminant analysis was then generated with the PC of the minimum number of harmonics that allowed the best haplogroup discrimination and the confusion matrix was obtained to estimate the classification errors.

We also compared statistically the first five principal components among the three haplogroups. This allowed us to detect if the information related to the shape of the contour contained in the PCs presented enough differences between haplogroups. Because all the data were not normally distributed, we performed a Kruskal-Wallis test to compare among the three haplogroups.

As an alternative method of discrimination and identification, a multilayer perceptron neural networks were trained. Artificial neural networks are mathematical models constructed by simulating the functioning of biological neural networks (the nervous system). They present a set of processing units called neurons, cells or nodes (formed by several mathematical equations), interconnected by connections that include a weight that modifies the values that pass through them between neurons [61]. Artificial neural networks (ANNs) have been advocated in many disciplines for addressing complex pattern-recognition problems. The advantages of ANNs over traditional, linear approaches include their ability to model non-linear associations with a variety of data

types (e.g. continuous, discrete) and to accommodate interactions among predictor variables without any a priori specification [62]. Neural networks are considered universal approximators of continuous functions, and as such, they exhibit flexibility for modeling non-linear relationships between variables. For example, ANNs exhibit substantially greater predictive power than traditional, linear approaches when modeling non-linear data (based on empirical and simulated data) [63].

The variables used to make the network were the scores of the principal components that contributed most to the total variance, obtained from the Fourier coefficients from 25 harmonics. For the basic topology, the automated search procedure of Statistica version 8.0 software was used, with an input layer of 30 neurons, corresponding to each shape variable, and the output layer with three neurons, one for each haplogroup to identify.

In the exploratory step, the most efficient network was evaluated by testing with hidden layers of between 10 and 40 neurons. Two error functions (sum of squares and cross-entropy) and four activation functions (identity, logistics, tangent and exponential) were used. The learning rate was 0.1, the inertia 0.66, and the stopping rule was set when the training error was below 0.001. Network learning was represented using the behavior of the maximum, average and minimum errors. Sixty percent of the data were randomly selected for network training and the remaining 40% was used for validation. Of the 30 networks, the one with the lowest classification error of the validation data was selected as best. The classification power for the species was analyzed using the confusion matrix and the calculation of the percentages of omission and commission errors.

Results

Measurement error of intraspecific variations and statistical difference in shape

On the first PC (the one that most contributed to the total variance), the percentage measurement error reached 2.3% of the intraspecific variance for the haplogroup 1, 3.3% for the haplogroup 2 and 3.6% for the haplogroup 3.

Contour reconstruction and variance explained by PCA

With the result of the first component, and when using the inversion of the Fourier transforms, the contour of the haplogroups of *T. dimidiata* was reconstructed and the variability among and within groups was graphically characterized (Fig. 2). The greatest variability among haplogroups was observed in the posterior lobe of the pronotum and the terminal region of the head and neck. This pattern of variation was also observed internally within haplogroups 1 and 2. The greatest variation within haplogroup 3 specimens was in the anterior lobe and distal tubers (Fig. 2).

Regardless of the number of harmonics used to describe the contour, the first component explained about half of the contour variability (between 44–55%) (Fig. 3). As the number of harmonics used increased, more components were required to explain 90% of the variation in shape, but in general, this value was reached with 8 principal components (Fig. 3).

Discriminant analysis and neural network

When performing the discriminant analysis to assess the number of harmonics that offers the best discriminations among haplogroups, it was observed that correct discriminations generally increased with the number of harmonics used. This pattern stopped at 30 harmonics when correct discrimination began to fail (Table 1). Haplogroup 1 was successfully differentiated 10 harmonics with 100% correct discrimination. Haplogroup 2 reached a 100% correct discrimination when the contour was described with 20 and 25 harmonics. Haplogroup 3 only reached 88.24% and 94.12% correct discrimination with the maximum number of harmonics tested. Overall, the best results were obtained when describing the contours of haplogroups using 25 harmonics.

The ordering diagram of the discriminating axes for the shape of the specimens, for the description of the contour with 25 harmonics and using 30 PCs is shown in Fig. 4. The separation of the minimum convex polygons demonstrated the possibility of discriminating the haplogroups using the PC as shape variables. Haplogroup 1 is separated perfectly from the rest, showing the greatest differentiation from haplogroups 2 and 3 along canonical axis 1. Haplogroups 2 and 3 presented greater variation along canonical axis 2. One individual from haplogroup 3 was located within the polygon of haplogroup 2, which was corroborated as an error of discrimination of the analysis in the confusion matrix (Table 2).

When comparing the first five PC scores among the three haplogroups, significant differences were found among, at least, two haplogroups for all principal components except for PC2 and PC3 (Fig. 5). The greatest differences were always found between haplogroups 1 and 3.

All trained networks achieved 100% correct classification with training data, but the most efficient with validation data was a perceptron of 13 neurons in the hidden layer, which reached 91% correct classification. This network used a BFGS18 training algorithm and an SOS error function. The activation function of the hidden layer was 'Logistics' and for the output layer, 'Tangent'. This network confused only one individual of haplogroup 1 (out of a total of 20) which was classified as haplogroup 2 (dropping to 94% of correct classification),

and two individuals of haplogroup 2 (of 16) were classified as haplogroup 3 (for 85% of correct classification). The eight individuals belonging to haplogroup 2 used to validate the network were correctly classified (100%). Components 1, 5, 15 and 2 had the highest weight in the network.

Discussion

In entomological studies, much attention has been given to the use of different parts of the body to identify, name and classify insects [64]. To date, wings have been the most commonly used structures to assess species discrimination through geometric morphometry methods, mainly using anatomical reference points [7, 26]. Here, to the best of our knowledge, we use for the first time the whole-body contour of an insect to discriminate among haplogroups. The use of EFDs has been little explored, though on several occasions it has demonstrated its ability to discriminate among even closely related species [65, 66]. Even more, some studies with triatomines [27, 53] and other insects of medical importance [27, 67–69]

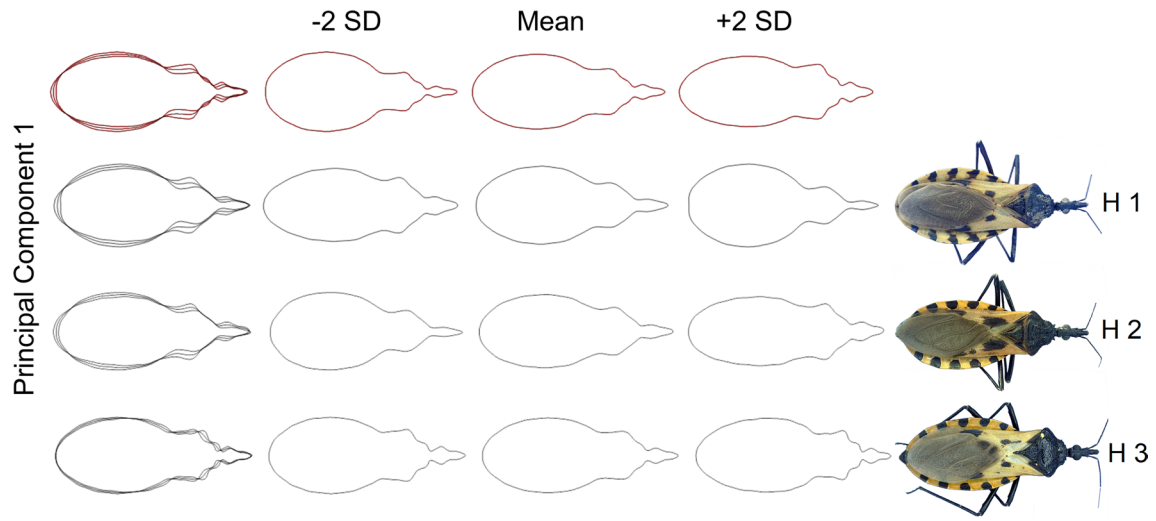

Fig. 2 Digital reconstruction and variability of the contours in three haplogroups of *Triatoma dimidiata* (Hemiptera: Reduviidae). The contours were obtained from the first principal components obtained with the elliptical Fourier descriptors. Red contours represent the consensus of the three haplogroups. *Abbreviations*: H1, haplogroup 1; H2, haplogroup 3; H3, haplogroup 3

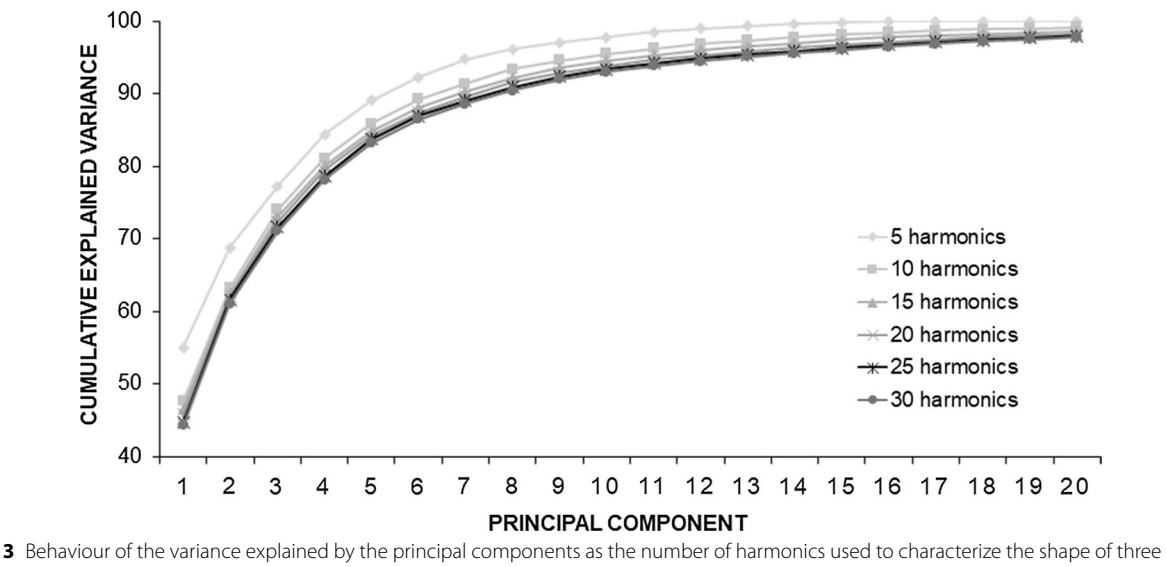

Fig. 3 Behaviour of the variance explained by the principal components as the number of harmonics used to characterize the shape of three haplogroups of *Triatoma dimidiata* (Hemiptera: Reduviidae) is increased

Table 1 Percentage of correct discrimination for three haplogroups of *Triatoma dimidiata* (Hemiptera: Reduviidae) for discriminant analysis using 5, 10, 15, 20, 25 and 30 harmonics

No. of harmonics	Correct classification (%)			Total
	Haplogroup 1	Haplogroup 2	Haplogroup 3	
5	97.14	60	88.24	85.39
10	100	85	94.12	94.38
15	100	90	94.12	95.51
20	100	100	91.18	96.63
25	**100**	**100**	**94.12**	**97.75**
30	100	95	94.12	96.63

Note: The best correct discrimination values for a certain number of harmonics are highlighted in bold

have demonstrated the usefulness of these methods for species recognition in this genus.

When using the inversion of the Fourier transforms, it was possible to visualize that the greatest differences in contour shape between the haplogroups were found in the pronotum and the head. Both structures have been used in morphometric studies, both traditional and geometric, because important variations in their shape have been detected [7, 14, 40]. In the case of the head, Bustamante et al. [14] consider that an important factor in the variability observed in this region is due to the geographical isolation of the populations of *T. dimidiata*, which has led to divergent evolution. The haplogroups used in this study mainly have allopatric populations, which could explain the morphometric differences found, although there are areas of sympatry [18]. In turn, differences in the head may have an evolutionary cause related to feeding strategies and growth patterns of this area of the body. Some authors have suggested that the shape of the head may reflect evolutionary mechanisms related to the ability to ingest blood. If the allopatry of the haplogroups populations of *T. dimidiata* is taken into account and that these must have diverged approximately 0.97 to 0.85 mya, according to results obtained from sequences of the *nad*4 gene [16], dissimilar feeding strategies may have been established among the haplogroups, which

Table 2 Confusion matrix of the discrimination process of the three haplogroups of *Triatoma dimidiata* (Hemiptera: Reduviidae) for the ordination plot of the discriminant analysis for 25 harmonics

Haplogroup	H1	H2	H3	Total
H1	37	0	0	37
H2	0	23	0	23
H3	0	1	35	36

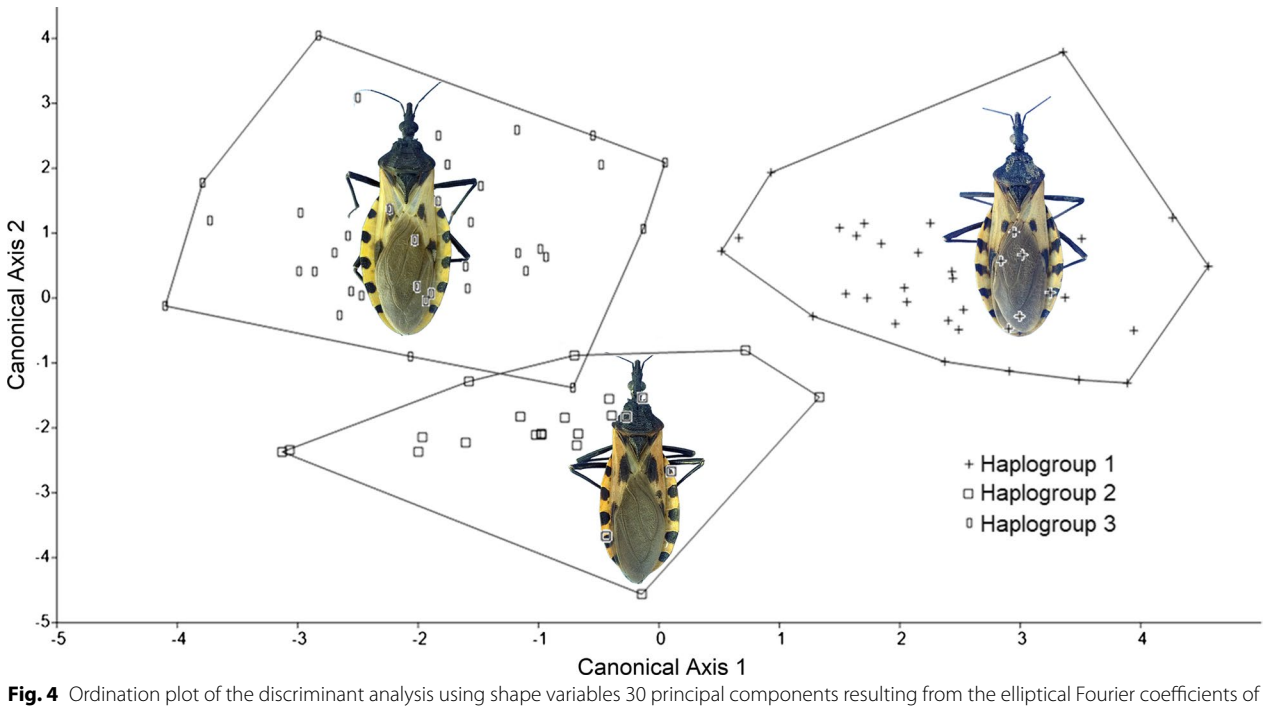

Fig. 4 Ordination plot of the discriminant analysis using shape variables 30 principal components resulting from the elliptical Fourier coefficients of 25 harmonics of three haplogroups of *Triatoma dimidiata* (Hemiptera: Reduviidae)

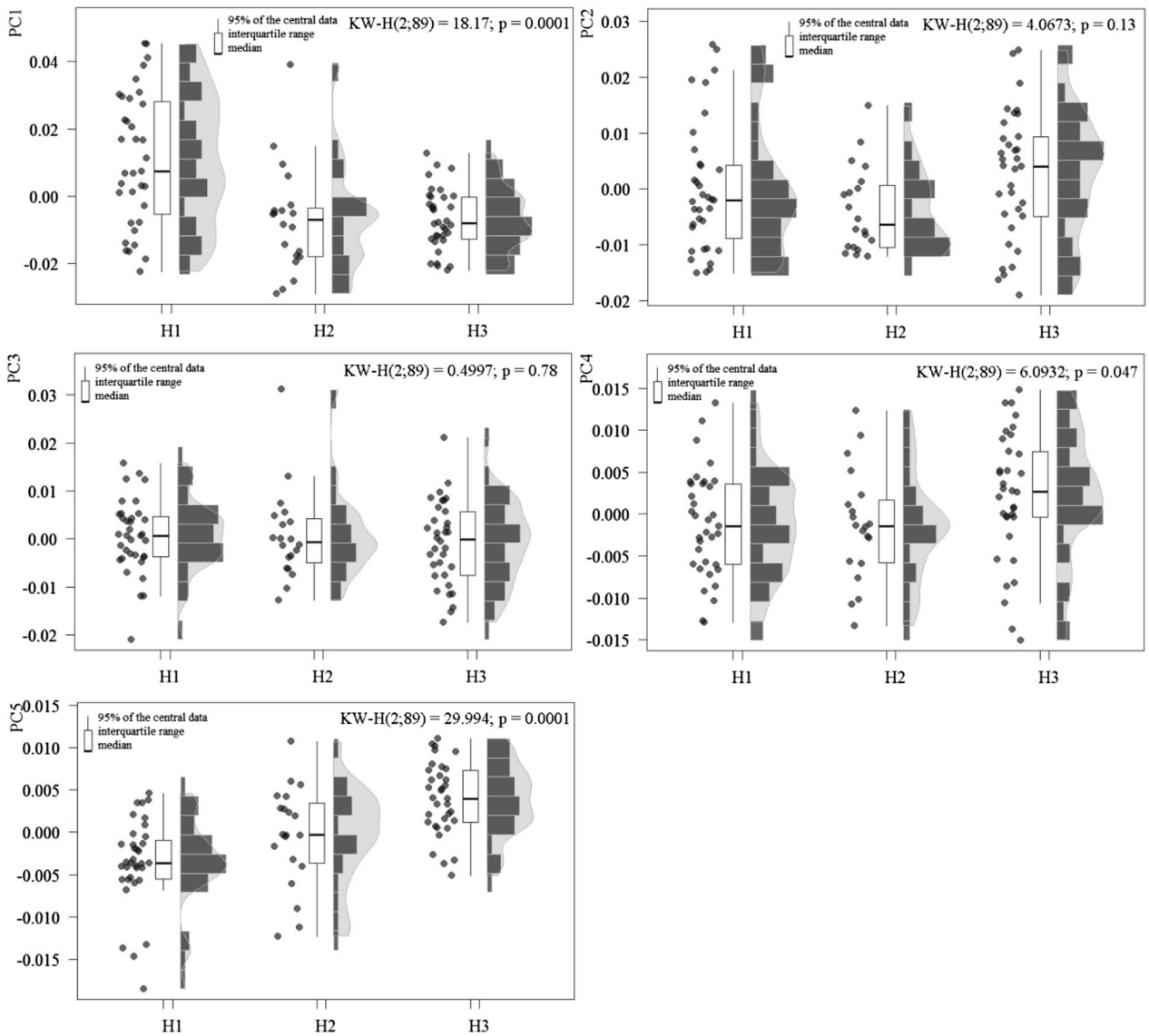

Fig. 5 Score differences in the first five principal components among three haplogroups of *Triatoma dimidiata* (Hemiptera: Reduviidae). *Abbreviations*: H1, haplogroup 1; H2, haplogroup 2; H3, haplogroup 3

then generated morphological differences. However, because the information related to the localities where individuals where obtained is not available in the original paper [40], more precise conclusions cannot be reached.

In the case of the pronotum, significant variability in the shape of the contour between the haplogroups was also observed. This structure has been used in the traditional morphological description of triatomine species [9] and has been used in attempts to discriminate species [50]. To our knowledge, only one study has used geometric morphometry techniques on this structure in triatomines [32], in the future a comparative study of the pronotum could evaluate its utility in the discrimination among triatomines.

When comparing the results obtained by Gurgel-Gonçalves et al. [40], who reached correct discrimination values between 70.5% and 82.5% of the three haplogroups and the results obtained by Khalighifar et al. [41] (with correct discrimination values of 84.1% H1, 86.7% H2 and 87.5% H3) our results reached 100% correct discrimination values for haplogroup 1 and 2 and 94.12% for haplogroup 3, with total discrimination results of 97.75%,

through discriminant function analysis. This is probably because, in comparison to the methods used in the studies mentioned above, EFDs can recover a greater variability of the shape through the contour analysis. Perhaps the integration of both, the methods of the previous studies [40, 41] (which have demonstrated their ability with good values of correct discrimination in the recognition of these haplogroups) and EFDs, can help to establish an identification system of the haplogroups of *T. dimidiata* with higher values of correct identification.

This method of describing shapes and reconstructing images is advantageous when the analysis based on anatomical reference points fails to fully discriminate the objects of study. McLellan and Endler [70] suggested that the use of EFDs provides a precise reconstruction of the contour of the complex object and can explain the overall complexity of the shape with greater resolution than the methods of anatomical reference points and semilandmarks. This has been demonstrated in other insect groups, where the use of EFDs has allowed the correct discrimination between species [71]. Francoy et al. [24] used both methods (anatomical reference points and elliptical Fourier descriptors) for the identification of euglossine bees. These authors found better results in the differentiation of species using EFD. However, they suggest the combined use of data matrices obtained by anatomical reference points and EFDs.

Species concepts and delimitation have always been highly controversial and complicated, especially when the focal organisms are considered cryptic or hypercryptic [64]. In the *Triatoma* genus, the presence of cryptic species has been widely addressed. Several authors have assembled the *Triatoma* species into different groups and complexes based on their external characters and the genitalia of both sexes [72–74]. Currently, the most accepted group was proposed by Schofield and Galvão [74], with the subdivision of *Triatoma* species into groups, complexes and subcomplexes.

Triatominae species show high morphological variation, which suggests that ecological factors may be the main force driving speciation in the Triatominae [22]. Very closely related species can develop rapid morphological changes in adaptation to new environments. Conversely, similar morphs adapted to the same ecotope could be derived from different ancestors [22]. Thus, the existence of morphologically similar species could be reflecting their evolution from a common ancestor or convergent adaptation to the same ecological niche. This phenotypic flexibility leads to the misidentification of distinct genetic units by morphological convergence, resulting in taxonomic uncertainties in the description of new subspecies, species or even genera. Considering that the Triatominae species groupings into complexes and subcomplexes are mainly based on morphological similarities [75], the morphological plasticity complicates both species identification and the establishment of evolutionarily related groups. In this sense, traditional morphological analysis has failed to clarify the differences that other sources of evidence, such as genetic, chromosomal, karyotype analyses, etc., have contributed to the clarification of the cryptic species complexes.

Specifically, in *T. dimidiata*, wide distribution and variation in morphology (historically explained by wide clinal variation along its distribution range) [11], has resulted in a long history of reconsiderations of its taxonomic status, from a single species to a species complex of distinct taxonomic groups [76]. Studies focused on the analysis of morphological variation using classical morphometry techniques have led to the inclusion of *T. dimidiata* populations within other species complexes such as *phyllosoma* [14]. However, these considerations have been rejected due to genetic evidence that has demonstrated the presence of different haplogroups within the *dimidiata* complex; this demonstrates that it is impossible for classical morphological techniques to correctly discriminate among these haplogroups.

Conclusions

The use of elliptic Fourier descriptors allows the identification of three haplogroups of *Triatoma dimidiata* with higher precision than previous works, where higher values of correct discriminations were 82.5% [40] and 87.5% [41]. With 25 harmonics and 30 components, the identification of haplogroups was achieved with an overall efficiency greater than 97% by using discriminant analysis. The multilayer perceptron neural networks were also efficient in identification, reaching 91% efficiency with the validation data. The main advantage is its easy application from easily obtainable digital images with minimal and uncomplicated processing, which guarantees its replicability. Despite its relative mathematical complexity, it can be partially automated, which minimizes the researcher manipulation errors when processing the samples. Its ability to reconstruct the shape automatically, after statistical processing, is also attractive and does not require any drawing skills from the researcher, allowing the visual identification of the location of the differences detected. The assessment of the identification ability of this method in other triatomine species is a necessary aspect to advance procedures that allow the automation of the identification of these important vectors of Chagas disease.

Supplementary information

Supplementary information accompanies this paper at https://doi.org/10.1186/s13071-020-04202-2.

Additional file 1: Table S1. Variance contribution of all principal components obtained with the PrinComp module. https://doi.org/10.6084/m9.figshare.12014976.v1

Additional file 2: Figure S1. Digital reconstruction and variability of the contours in three haplogroups of *Triatoma dimidiata* (Hemiptera: Reduviidae), obtained from all principal components derived from the elliptical Fourier descriptors. https://doi.org/10.6084/m9.figshare.12014979.v1.

Abbreviations

CD: Chagas disease; EFD: Elliptic Fourier descriptors; H1: Haplogroup 1; H2: Haplogroup 2; H3: Haplogroup 3.

Acknowledgments

The authors want to thank Daily Martínez Borrego who provided comments on the manuscript. We also want to thank the anonymous reviewers and associate editors, whose review, comments, and suggestions were extremely valuable in improving this work.

Authors' contributions

DDC and EA conceived the study. DDC and DDA conducted all statistical analyses. DDCF, EA, DDA and CNIB wrote the manuscript. All authors contributed to the final draft of the manuscript. All authors read and approved the final manuscript.

Funding

DDC was supported by a CONACYT scholarship program 2018-000012-01NACF-11846.

Availability of data and materials

Data supporting the conclusions of this article are included in the article and its additional files. Raw data are available upon request to the first author. Also, all data derived from this investigation are deposited in the Figshare repository (https://doi.org/10.6084/m9.figshare.11344073.v1)

Ethics approval and consent to participate

Not applicable.

Consent for publication

Not applicable.

Competing interests

The authors declare that they have no competing interests.

Author details

[1] Centro de Investigación en Biodiversidad y Conservación (CIByC), UAEM, Cuernavaca, Morelos, México. [2] Departamento de Biología Animal y Humana, Facultad de Biología, Universidad de La Habana, Havana, Cuba. [3] Departamento de Ecología Humana, Centro de Investigación y de Estudios Avanzados del IPN (CINVESTAV), Unidad Mérida, Yucatán, México.

Received: 2 April 2020 Accepted: 20 June 2020
Published online: 01 July 2020

References

1. Rivera PC, González-Ittig R, Robainas A, Trimarchi LI, Levis S, Calderón G, Gardenal C. Molecular phylogenetics and environmental niche modeling reveal a cryptic species in the *Oligoryzomys flavescens* complex (Rodentia, Cricetidae). J Mamm. 2018;99:363–76.
2. Bickford D, Lohman DJ, Sodhi NS, Ng PK, Meier R, Winker K, et al. Cryptic species as a window on diversity and conservation. Trends Ecol Evol. 2007;22:148–55.
3. Struck TH, Feder JL, Bendiksby M, Birkeland S, Cerca J, Gusarov VI, et al. Finding evolutionary processes hidden in cryptic species. Trends Ecol Evol. 2018;33:153–63.
4. Jackson JK, Resh VH. Morphologically cryptic species confound ecological studies of the caddisfishy genus *Gumaga* (Trichoptera: Sericostomatidae) in northern California. Aquat Insect. 1998;20:69–84.
5. Schonrogge K, Barr B, Wardlaw JC, Napper E, Gardner MG, Breen J, et al. When rare species become endangered: cryptic speciation in myrmecophilous hoverfishes. Biol J Linn Soc. 2002;75:291–300.
6. Abad-Franch F, Monteiro FA. Molecular research and the control of Chagas disease vectors. Anais Acad Bras Ciências. 2005;77:437–54.
7. Gurgel-Gonçalves R, Ferreira JBC, Rosa AF, Bar ME, Galvao C. Geometric morphometrics and ecological niche modelling for delimitation of near-sibling triatomine species. Med Vet Entomol. 2011;25:84–93.
8. Martínez FH, Villalobos GC, Cevallos AM, De la Torre P, Laclette JP, Alejandre-Aguilar R, Espinoza B. Taxonomic study of the *Phyllosoma* complex and other triatomines (Insecta: Hemiptera: Reduviidae) species of epidemiological importance in the transmission of Chagas disease using ITS-2 and mtCytB sequences. Mol Phylogenet Evol. 2006;41:279–87.
9. Panzera F, Hornos S, Pereira J, Cestau R, Canale D, Diotaiutu L, Dujardin JP, Pérez R. Genetic variability and geographic differentiation among three species of triatomine bugs (Hemiptera: Reduviidae). Am J Trop Med Hyg. 1997;57:732–9.
10. Ramsey JM, Peterson AT, Carmona-Castro O, Moo-Llanes DA, Nakazawa Y, Butrick M, et al. Atlas of Mexican Triatominae (Reduviidae: Hemiptera) and vector transmission of Chagas disease. Mem Inst Oswaldo Cruz. 2015;110:339–52.
11. Lent H, Wygodzinsky P. Revision of Triatominae (Hemiptera: Reduviidae) and their significance as vector of Chagas' disease. Bull Am Museum Nat His. 1979;163:123–520.
12. Schofield CJ. Triatominae: biology and control. Bognor Regis: Eurommunica Publications; 1994. p. 80.
13. Flores A, Magallón-Gastélum E, Bosseno MF, Ordoñez R, Kasten FL, Espinoza B, et al. Isoenzyme variability of five principal triatomine vector species of Chagas disease in Mexico. Infect Genet Evol. 2001;1:21–8.
14. Bustamante DM, Monroy C, Menes M, Rodas A, Salazar-Schettino PM, Rojas G, et al. Metric variation among geographic populations of the Chagas vector *Triatoma dimidiata* (Hemiptera: Reduviidae: Triatominae) and related species. J Med Entomol. 2004;41:296–301.
15. Bargues MD, Klisiowicz DR, Gonzalez-Candelas F, Ramsey JM, Monroy C, Ponce C, Salazar-Schettino PM, et al. Phylogeography and genetic variation of *Triatoma dimidiata*, the main Chagas disease vector in Central America, and its position within the genus *Triatoma*. PLoS Negl Trop Dis. 2008;2:e233.
16. Ibarra-Cerdeña CN, Zaldívar-Riverón A, Peterson AT, Sánchez-Cordero V, Ramsey JM. Phylogeny and niche conservatism in North and Central American triatomine bugs (Hemiptera: Reduviidae: Triatominae), vectors of Chagas' disease. PLoS Negl Trop Dis. 2014;8:e3266.
17. Justi SA, Russo CA, Mallet JR, Obara MT, Galvao C. Molecular phylogeny of Triatomini (Hemiptera: Reduviidae: Triatominae). Parasit Vectors. 2014;7:149.
18. Pech-May A, Mazariegos-Hidalgo CJ, Izeta-Alberdi A, López-Cancino SA, Tun-Ku E, De la Cruz-Félix K, et al. Genetic variation and phylogeography of the *Triatoma dimidiata* complex evidence a potential center of origin and recent divergence of haplogroups having differential *Trypanosoma cruzi* and DTU infections. PLoS Negl Trop Dis. 2019;13:e0007044.
19. Monteiro FA, Barrett TV, Fitzpatrick S, Cordon-Rosales C, Feliciangeli D, Beard CB. Molecular phylogeography of the Amazonian Chagas disease vectors *Rhodnius prolixus* and *R. robustus*. Mol Ecol. 2003;12:997–1006.
20. Gardim S, Almeida CE, Takiya DM, Oliveira J, Araújo RF, Cicarelli RM, da Rosa JA. Multiple mitochondrial genes of some sylvatic Brazilian *Triatoma*: non-monophyly of the *T. brasiliensis* subcomplex and the need for a generic revision in the Triatomini. Infect Genet Evol. 2014;23:74–9.
21. Jurberg J, Cunha V, Cailleaux S, Raigorodschi R, Lima MS, Rocha DDS, Moreira F. *Triatoma pintodiasi* sp nov do subcomplexo *T rubrovaria* (Hemiptera, Reduviidae, Triatominae). Rev Pan-Amaz Saude. 2013;4:43–56.
22. Dujardin JP, Panzera P, Schofield CJ. Triatominae as a model of morphological plasticity under ecological pressure. Mem Inst Oswaldo Cruz. 1999;94(Suppl. 1):223–8.
23. Carcavallo RU, Martínez A. Comunicaciones científicas: entomoepidemiología de la República Argentina. La Plata: Junta de Investigaciones

Científicas de las Fuerzas Armadas Argentinas. 1968. http://www.worldcat.org/oclc/7247216.
24. Francoy TM, Silva RAO, Nunes-Silva P, Menezes C, Imperatriz-Fonseca VL. Gender identification of five genera of stingless bees (Apidae, Meliponini) based on wing morphology. Genet Mol Res. 2009;8:207–14.
25. Bargues MD, Schofield C, Dujardin JP. The phylogeny and classification of the triatominae. In: Telleria J, Tibayrenc M, editors. American trypanosomiasis: Chagas disease, one hundred years of research. Amsterdam: Elsevier; 2010.
26. Nouvellet P, Ramirez-Sierra MJ, Dumonteil E, Gourbiere S. Effects of genetic factor and infection status on wing morphology of *Triatoma dimidiata* species complex in the Yucatan peninsula, Mexico. Infect Genet Evol. 2011;11:1243–9.
27. Dujardin JP, Kaba D, Solano P, Dupraz M, McCoy KD, Jaramillo-O N. Outline-based morphometrics, an overlooked method in arthropod studies? Infect Genet Evol. 2014;28:704–14.
28. Gurgel-Gonçalves R, Abad-Franch F, Ferreira JB, Santana DB, Cuba CAC. Is *Rhodnius prolixus* (Triatominae) invading houses in central Brazil? Acta Trop. 2008;107:90–8.
29. Vendrami DP, Obara MT, Gurgel-Gonçalves R, Ceretti-Junior W, Marrelli MT. Wing geometry of *Triatoma sordida* (Hemiptera: Reduviidae) populations from Brazil. Infect Genet Evol. 2017;49:17–20.
30. Dujardin JP, Beard CB, Ryckman R. The relevance of wing geometry in entomological surveillance of Triatominae, vectors of Chagas disease. Infect Genet Evol. 2007;7:161–7.
31. Oliveira J, Marcet PL, Takiya DM, Mendonça VJ, Belintani T, Bargues MD, et al. Combined phylogenetic and morphometric information to delimit and unify the *Triatoma brasiliensis* species complex and the Brasiliensis subcomplex. Acta Trop. 2017;170:140–8.
32. Nattero J, Piccinali RV, Lopes CM, Hernández ML, Abrahan L, Lobbia PA, Rodríguez CS, de la Fuente ALC. Morphometric variability among the species of the Sordida subcomplex (Hemiptera: Reduviidae: Triatominae): evidence for differentiation across the distribution range of *Triatoma sordida*. Parasit Vectors. 2017;10:412.
33. Dujardin JP, Schofield J, Panzera F, Matias A, De La Riva J. Los vectores de la enfermedad de Chagas. Bruxelles: Académie Royale des Sciences d'Outre-Mer. 2002;25:189. (Mémoire in-8°.Nouvelle Série; 3).ISBN 90-75652-27-5.
34. Galvão C, Carcavallo R, Da Silva Rocha D, Jurberg J. A check-list of the current valid species of the subfamily Triatominae Jeannel, 1919 (Hemiptera, Reduviidae) and their geographical distribution with nomenclatural and taxonomic note. Zootaxa. 2003;202:1–36.
35. Zeledón, R. El *Triatoma dimidiata* (Latreille, 1811): y su relación con la enfermedad de chagas (No. 595.754 Z49t). San José, CR: EUNED; 1981.
36. Acevedo F, Godoy E, Schofield CJ. Comparison of intervention strategies for control of *Triatoma dimidiata* in Nicaragua. Mem Inst Oswaldo Cruz. 2000;95:867–71.
37. Monroy MC, Bustamante DM, Rodas AG, Enriquez ME, Rosales RG. Habitats, dispersion and invasion of sylvatic *Triatoma dimidiata* (Hemiptera: Reduviidae: Triatominae) in Peten, Guatemala. J Med Entomol. 2003;40:800–6.
38. Nakagawa J, Juárez J, Nakatsuji K, et al. Geographical characterization of the triatomine infestations in north-central Guatemala. Ann Trop Med Parasitol. 2005;99:307–15.
39. Harris K. Taxonomy and phylogeny of North American Triatominae: public health implications. Atlanta: Moorehouse School of Medicine; 2003.
40. Gurgel-Gonçalves R, Komp E, Campbell LP, Khalighifar A, Mellenbruch J, Mendonça VJ, et al. Automated identification of insect vectors of Chagas disease in Brazil and Mexico: the virtual vector lab. PeerJ. 2017;5:e3040.
41. Khalighifar A, Komp E, Ramsey JM, Gurgel-Gonçalves R, Peterson AT. Deep learning algorithms improve automated identification of Chagas disease vectors. J Med Entomol. 2019;56:1404–10.
42. Abadi M, Barham P, Chen J, Chen Z, Davis A, Dean J, et al. Tensorflow: a system for large-scale machine learning. In: 12th Symposium on Operating Systems Design and Implementation (ODSI 16), 2–4 November 2016, Savannah, USA; 2016. p. 265–83.
43. Rampasek L, Goldenberg A. Tensorflow: biology's gateway to deep learning? Cell Syst. 2016;2:12–4.
44. Kuhl FP, Giardina CR. Elliptic Fourier features of a closed contour. Comput Gr Image Process. 1982;18:236–58.
45. Iwata H, Nesumi H, Ninomiya S, Takano Y, Ukai Y. Diallel analysis of leaf shape variations of citrus varieties based on elliptic Fourier descriptors. Breed Sci. 2002;52:89–94.
46. Iwata H, Niikura S, Matsuura S, Takano Y, Ukai Y. Evaluation of variation of root shape of Japanese radish (*Raphanus sativus* L.) based on image analysis using elliptic Fourier descriptors. Euphytica. 1998;102:143–9.
47. Kincaid DT, Schneider RB. Quantification of leaf shape with a microcomputer and Fourier transformation. Can J Bot. 1983;61:2333–42.
48. Rohlf FJ, Archie JW. A comparison of Fourier methods for the description of wing shape in mosquitoes (Diptera: Culicidae). Syst Zool. 1984;33:302–17.
49. Sheets HD, Covino KM, Panasiewicz JM, Morris SR. Comparison of geometric morphometric outline methods in the discrimination of age-related differences in feather shape. Front Zool. 2006;3:15.
50. Singh K, Gupta I, Gupta S. Classification of bamboo species by Fourier and Legendre moment. Int J Eng Sci Technol. 2013;50:61–70.
51. Zhan QB, Wang XL. Elliptic Fourier analysis of the wing outline shape of five species of antlion (Neuroptera: Myrmeleontidae: Myrmeleontini). Zool Stud. 2012;51:399–405.
52. Yang HP, Ma CS, Wen H, Zhan QB, Wang XL. A tool for developing an automatic insect identification system based on wing outlines. Sci Rep. 2015;5:12786.
53. Santillán-Guayasamín S, Villacís AG, Grijalva MJ, Dujardin JP. The modern morphometric approach to identify eggs of Triatominae. Parasit Vectors. 2017;10:55.
54. Iwata H, Ukai Y. SHAPE: A computer program package for quantitative evaluation of biological shapes based on elliptic Fourier descriptors. J Hered. 2002;93:384–5.
55. Ferson S, Rohlf FJ, Koehn RK. Measuring shape variation of two-dimensional outlines. Syst Zool. 1985;34:59–68.
56. Iwata H, Ebana K, Uga Y, Hayashi T. Genomic prediction of biological shape: elliptic Fourier analysis and kernel partial least squares (PLS) regression applied to grain shape prediction in rice (*Oryza sativa* L.). PLoS ONE. 2015;10:e0120610.
57. Freeman H. Computer processing of line-drawing images. Comp Surv. 1974;6:57–97.
58. Santillán-Guayasamín S, Villacís AG, Grijalva MJ, Dujardin JP. Triatominae: does the shape change of non-viable eggs compromise species recognition. Parasit Vectors. 2018;11:543.
59. Furuta N, Ninomiya S, Takahashi N, Ohmori H, Yasuo U. Quantitative evaluation of soybean (*Glycine max* L. Merr.) leaflet shape by principal component scores based on elliptic Fourier descriptor. Jpn J Bot. 1995;45:315–20.
60. Yezerinac SM, Loogheed SC, Handford P. Measurement error and morphometric studies: statistical power and observer experience. Syst Biol. 1992;41:471–82.
61. Samarasinghe S. Neural networks for applied sciences and engineering: from fundamentals to complex pattern recognition. Boca Raton: Auerbach Publications; 2016.
62. Bishop CM. Neural networks for pattern recognition. Oxford: Oxford University Press; 1995.
63. Olden JD, Jackson DA. Illuminating the "black box": a randomization approach for understanding variable contributions in artificial neural networks. Ecol Model. 2002;154:135–50.
64. Tatsuta H, Takahashi KH, Sakamaki Y. Geometric morphometrics in entomology: basics and applications. Entomol Sci. 2018;21:164–84.
65. Arribas P, Andújar C, Sánchez-Fernández D, Abellán P, Millán A. Integrative taxonomy and conservation of cryptic beetles in the Mediterranean region (Hydrophilidae). Zool Scr. 2013;42:182–200.
66. Polášek M, Godunko RJ, Rutschmann S, Svitok M, Novikmec M, Zahrádková S. Integrative taxonomy of genus *Electrogena* (Ephemeroptera: Heptageniidae): the role of innovative morphological analyses for species delimitation. Arthropod Syst Phylo. 2018;76:449–62.
67. Changbunjong T, Sumruayphol S, Weluwanarak T, Ruangsittichai J, Dujardin JP. Landmark and outline-based geometric morphometrics analysis of three *Stomoxys* flies (Diptera: Muscidae). Folia Parasitol. 2016;63:37.
68. Chaiphongpachara T, Tubsamut P. Geometric morphometry of pupae to identify four medically important flies (Order: Diptera) in Thailand. Biodiversitas. 2019;20:1504–9.

69. Dos Santos CMD, Jurberg J, Galvão C, Martínez M. Morfometria comparada de *Triatoma infestans*, *T.rubrovaria* e *T. platensis* (Hemiptera, Reduviidae, Triatominae) do Uruguai, Iheringia. Sér Zool. 2009;99:56–60.
70. McLellan T, Endler JA. The relative success of some methods for measuring and describing the shape of complex objects. Syst Biol. 1998;47:264–81.
71. Chávez B, Cruz DD. Valor taxonómico de la forma del ala en seis especies de esfíngidos (Lepidoptera: Sphingidae). Revista Cubana de Ciencias Biológicas. 2015;4:98–103.
72. Usinger RL, Wygodzinsky P, Ryckman RE. The biosystematics of Triatominae. Annu Rev Entomol. 1966;11:309–30.
73. Carcavallo RU, Jurberg J, Lent H, Noireau F, Galvão C. Phylogeny of the Triatominae (Hemiptera Reduviidae). Proposals for taxonomic arrangements. Entomol Vectores. 2000;7:1–99.
74. Schofield CJ, Galvão C. Classification, evolution and species groups within the Triatominae. Acta Trop. 2009;110:88–100.
75. Pita S, Lorite P, Nattero J, Galvão C, Alevi KC, Teves SC, et al. New arrangements on several species subcomplexes of *Triatoma* genus based on the chromosomal position of ribosomal genes (Hemiptera-Triatominae). Infect Genet Evol. 2016;43:225–31.
76. Dorn PL, Monroy C, Curtis A. *Triatoma dimidiata* (Latreille, 1811): a review of its diversity across its geographic range and the relationship among populations. Infect Genet Evol. 2007;7:343–52.

Publisher's Note

Capítulo V.

Quantitative imagery analysis of spot patterns for the three-haplogroup classification of *Triatoma dimidiata* (Latreille, 1811) (Hemiptera: Reduviidae), an important vector of Chagas disease

Parasites & Vectors

RESEARCH Open Access

Quantitative imagery analysis of spot patterns for the three-haplogroup classification of *Triatoma dimidiata* (Latreille, 1811) (Hemiptera: Reduviidae), an important vector of Chagas disease

Daryl D. Cruz[1*], Dennis Denis[2], Elizabeth Arellano[1] and Carlos N. Ibarra-Cerdeña[3]

Abstract

Background: Spots and coloring patterns evaluated quantitatively can be used to discriminate and identify possible cryptic species. Species included in the *Triatoma dimidiata* (Reduviidae: Triatominae) complex are major disease vectors of Chagas disease. Phylogenetic studies have defined three haplogroups for Mexico and part of Central America. We report here our evaluation of the possibility of correctly discriminating these three *T. dimidiata* haplogroups using the pattern of the dorsal spots.

Methods: Digital images of the dorsal region of individuals from the three haplogroups were used. Image processing was used to extract primary and secondary variables characterizing the dorsal spot pattern. Statistical analysis of the variables included descriptive statistics, non-parametric Kruskal–Wallis tests, discriminant function analysis (DFA) and a neural classification network.

Results: A distinctive spot pattern was found for each haplogroup. The most differentiated pattern was presented by haplogroup 2, which was characterized by its notably larger central spots. Haplogroups 1 and 3 were more similar to each other, but there were consistent differences in the shape and orientation of the spots. Significant differences were found among haplogroups in almost all of the variables analyzed, with the largest differences seen for relative spot area, mean relative area of central spots, central spots Feret diameter and lateral spots Feret diameter and aspect ratio. Both the DFA and the neural network had correct discrimination values of > 90%.

Conclusions: Based on the results of this analysis, we conclude that the spot pattern can be reliably used to discriminate among the three haplogroups of *T. dimidiata* in Mexico, and possibly among triatomine species.

Keywords: Cryptic species, Coloring pattern, Species complex, Taxonomy, Neural classification network

Background

Genetic and morphological divergences associated with speciation processes may not appear at the same time or progress at the same rate [1]. The emergence of new species usually results from the isolation of populations due to geographic, ecological or behavioral barriers that can act individually or synergistically [2]. This can lead to

*Correspondence: daryldavidcf@gmail.com
[1] Centro de Investigación en Biodiversidad y Conservación (CIByC), Universidad Autónoma del Estado de Morelos (UAEM), Cuernavaca, Morelos, México
Full list of author information is available at the end of the article

populations that have substantial genetic differentiation that has not been expressed phenotypically (at least not obviously), giving rise to cryptic species [3]. Identifying cryptic species complexes is one of the most important challenges facing taxonomy in recent years [4].

The correct delimitation of cryptic species has important implications for research in many fields of biology, such as studies on biodiversity, conservation and behavioral ecology [4], and is frequently achieved using different types of data, such as molecular, ecological, behavioral and geometric morphometric data [5]. This combination of methods, known as integrative taxonomy [5, 6], is the surest and most precise way of determining species limits [7, 8].

Cryptic species in the genus *Triatoma* (main vectors of Chagas disease) have primarily been recognized using molecular tools [9–12], although both ecological and morphometric analyses have also been used [13]. Within the genus *Triatoma*, the *dimidiata* complex has received considerable attention, in part because it is one of the most widely distributed triatomine species complexes. It is the only triatomine bug that naturally occurs throughout the northern neotropical realm of North, Central and South America [14]. Analysis of genetic data has led to at least five new species being proposed as members of the *dimidiata* complex [15]. In addition, the species in this complex have different morphological patterns [16, 17]. In the field of epidemiological entomology, the delimitation of species of medical importance is vital for the establishment of efficient control strategies [13, 18]. Geometric morphometric techniques using landmarks [19–22] or body contour descriptors [23–26] have been used for this purpose, mainly because of the superiority of this approach over traditional morphometric methods [27] and because it is a much cheaper than, for example, molecular ones.

In Mexico, three haplogroups have been reported within the *T. dimidiata* complex. Haplogroup 1 (H1) is distributed east of the Isthmus of Tehuantepec and has been recently found in northern Guatemala. Haplogroup 2 (H2) is only found in Mexico and is distributed in two states along the Gulf of Mexico (Tabasco, Veracruz), five states in Central Mexico (Guanajuato, San Luis Potosí, Hidalgo, Puebla, Morelos), in small foci along the Pacific coast (Nayarit, Jalisco, Colima, Michoacán, Guerrero, Oaxaca) and, recently, in the Yucatán peninsula (Campeche, Yucatán) [9, 11]. Haplogroup 3 (h3) has only been recorded in Chiapas, Mexico [11].

Spot patterns are widely used to describe species in traditional taxonomy [28]. However, because spot pattern is highly variable due to its ecological functions, it is usually described in subjective, qualitative terms. Alternatively, using digital tools to quantify spot patterns can minimize bias, increase precision and allow automated identification processes [29]. However, since few studies use quantitative measurements of pattern properties for taxonomic purposes, evidence on the usefulness of color patterns to separate (or discriminate) species is still lacking [30].

The general body color of triatomines is black or spruce, with pattern elements ranging from light yellow to light brown, orange or red shades [31]. The lighter pattern elements can be present on any area of the body or appendages, and the color, intensity and distribution of these elements are of considerable importance for systematic purposes. The pattern of the connexivum region is particularly notable [32]. However, despite the taxonomic importance of these pattern elements, there have been very few quantitative studies of color and pattern variation in *Triatoma*. The first studies to quantify color patterns in a species of *Triatoma* were by carried out by Nattero et al. [33], who analyzed the melanic and non-melanic forms of domestic and peridomestic populations of *Triatoma infestans*, and by Carmona-Galindo et al. [34] who, in addition to other aspects, explored pattern variation as a function of elevation in triatomines from El Salvador, including populations of *T. dimidiata*. To date, the utility of the spot pattern to discriminate among haplogroups within the *dimidiata* complex or any other triatomine complex has not been explored.

Although there are no obvious external morphological differences based on our observations of *dimidiata* complex specimens, we hypothesize that the evaluation of more detailed quantitative differences in the spot pattern among haplogroups could be used to distinguish them morphologically. This method could potentially improve the separation criteria for known species and cryptic species in this group without the need for genetic data. This is possible because several species of triatomines have distinctive spot patterns, and these may be of relevant taxonomic value. In the study reported here, we evaluated the reliability of discriminating among the three *T. dimidiata* haplogroups reported for Mexico and part of Central América using the dorsal spot pattern. If successful, this technique could be extended to other species in this (and other) group and lay the foundations for an automated identification system to facilitate correct species recognition within the genus *Triatoma*. These systems could be employed by taxonomists, vector ecologists, health personnel, among others, interested in the rapid identification of these triatomines.

Methods

Sample information

Images of individuals from each of the haplogroups of *Triatoma dimidiata* were obtained from Gurgel-Gonçalves

et al. [20]. These images are part of a collection of images of 51 triatomine species from Mexico and Brazil available for public use in the Dryad repository (http://dx.doi.org/10.5061/dryad.br14k). The original series of images that represent the species distributed in Mexico was taken from the following entomological collections in Mexico: Regional Center for Health Research, National Institute of Public Health of Mexico, Guanajuato State Public Health Laboratory, Benito Juárez Autonomous University of Oaxaca and the Autonomous University of Nuevo León, Monterrey, and details of how these images were taken are described in the referenced publications. We obtained 44, 30, and 40 images of individuals belonging to haplogroups 1, 2, and, 3 respectively; the haplogroup assignment of these individuals was corroborated genetically, and this corroboration constitutes a major factor for using these images in a quantitative analysis like our work [see 11]. In addition, the specimens in the photographs in [20] belong to the locations mentioned by Pech-May et al. [11], so the ecological variability of their distribution is included. From the 114 images, we selected only high-quality images that clearly captured the spot pattern, eliminating those cases where the spots were fused or covered by hyperchromatic wings (Additional file 1: Figure S1), resulting in a final sample of 101 images (39 for H1, 23 for H2, and 39 for H3).

Image processing

The images were processed to facilitate the extraction of standardized measurements of the spot pattern (Fig. 1). The abdomens were clipped manually, removing the legs and cutting off the head at the thorax level. The images were then aligned and re-scaled, using the insertion angles of the abdomen and thorax and the back of the body as references for alignment and scaling all individuals to the width of the first individual that was taken as a reference (image H10355). These transformations may slightly alter the shape and absolute values of the spot measurements, but they are essential for standardizing the spatial patterns of the spots and making them comparable, eliminating differences due to body shape or size, whose identifying value has been tested in previous studies [20, 26]. For this reason, the quantitative estimates of areas in this study are always expressed relative to the total area of the abdomen and linear measurements as relative to the square root of the total abdomen area.

Processing for spot pattern extraction included removing color information (desaturation) and reducing levels to the central 50% of the image histogram. In some cases, noise produced by surface reflectance of the specimens or shadows that artificially connected adjacent spots during the binarization of the images were manually eliminated.

In the ImageJ program [35], a macro (Additional file 2) was programmed to automate image processing and measurements. This included 8-bit image conversion, binarization with a minimum automatic threshold, background removal, mask conversion and gap filling. The outlier points, both black and white (using radius 6 and threshold 50) were then removed and the resulting particles (spots) were measured.

Heat maps were obtained by superimposing the images of the spot patterns of all individuals per haplogroup, using the PAT-GEOM v1.0.0 package, developed by Chan et al. [36]. This package allows the analysis of different measures of the coloration pattern quantitatively, and it was designed to work with macros on ImageJ. These maps allowed us to visually explore and qualitatively describe the general patterns that characterized each haplogroup.

Quantitative characterization of the spot pattern

The spots were automatically numbered consecutively for identification. The central spots were designated spots 1 and 2, respectively, and spots on the edge of the abdomen were numbered consecutively using odd numbers on the

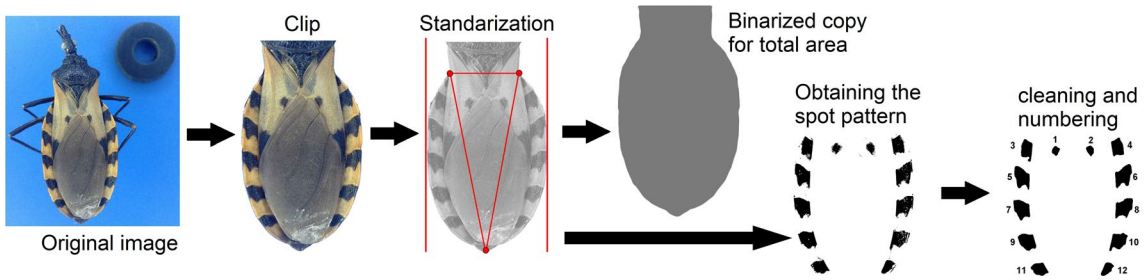

Fig. 1. Steps in the image processing of three haplogroups of *Triatoma dimidiata* (Hemiptera: Reduviidae) for the analysis of spot patterns. Standardization includes isometric rescaling, translation and rotation following common reference guidelines. Spot removal and cleaning were done with a macro code in ImageJ. Copyright: CreativeCommons Attribution 1.0 Universal (CC0 1.0) Public Domain Dedication license163 (https://creativecommons.org/licenses/by/1.0). Images were modified from Gurgel-Gonçalves et al. [20], with permission

left and even numbers on the right. To quantitatively describe the pattern of spots, a series of primary variables were taken at the spot level, as well as derived variables that included both the spot and individual levels.

The variables measured are shown in Fig 2. The total body area (Ta) was used for standardization purposes only. The relative area (Ra) is the area of each spot relativized as a percentage of the Ta (%). The sum of the Euclidean distances was calculated by taking the centroid coordinate of each spot and calculating, at the individual level, the distance between the central spots and lateral spots, but only after making a Procrustes record of the complete configurations. The maximum and minimum Feret diameters (MaxFd and MinFd, respectively), as well as the Feret angle, were calculated for each spot. These variables refer to the maximum and minimum distances between any pair of contour points of a shape, and although they are identified as diameter, they are not strictly analogous to a diameter since they do not pass through the center of the figure or divide it into symmetrical sections. The Fa refers to the angle of the vector of the MaxFd and indicates the general directionality of the spot (its inclination). The aspect ratio (Ar) of each spot (ratio of the minor to the major diameter) was used as an indicator of its shape.

For each individual, the averages of the variables per spot, the sum of the total Ra of the spots, and the ratio of the mean Ra of the central spots to that of the lateral spots were calculated as derived variables. For the calculation of the average inclination angle, both for the central spots and lateral spots, the angles of the spots from the left to the right quadrant (0–90°) were recorded.

Data analysis

Non-parametric descriptive statistics (median, quartiles and range) were used because the distribution of the data was not normal, and traditional descriptors gave a false impression of precision and marked differences. Statistical comparisons among haplogroups were performed using Kruskal–Wallis tests in Statistica v8 software (StatSoft, Tulsa, OK, USA). A linear discriminant function analysis (forward stepwise) (LDFA) was also performed to estimate the ability to discriminate haplogroups based on the variables used. Since this method has a series of restrictive premises and can only linearly differentiate the groups, a multilayer perceptron type neural classification network was used as an alternative method. Neural networks are supervised machine learning procedures and do not have statistical premises on the nature of the data, making them more powerful and capable of exploring nonlinear relationships in complex sets of variables. The option ANS (Automated Network Search) in Statistica v8 software was used to find the topology that most efficiently identified the haplogroups by using all variables. The network was trained with 60% of the individuals by haplogroup and validated with the remaining 40%. Assignment to each group was random, except for individuals wrongly classified by the LDFA, who were forced into the validation sample for a more robust check of network performance. The weight assigned by the neural network to each variable was estimated to identify those of greatest importance in the discrimination process.

Results

The heat maps generated by superimposing all of the individuals within each haplogroup revealed those spot patterns that characterize each haplogroup and provided evidence of a well-differentiated pattern between the haplogroups (Fig. 3). The most differentiated pattern was presented by haplogroup 2, being primarily apparent in the notably larger central spots. Haplogroups 1 and 3 were more similar to each other, but there were

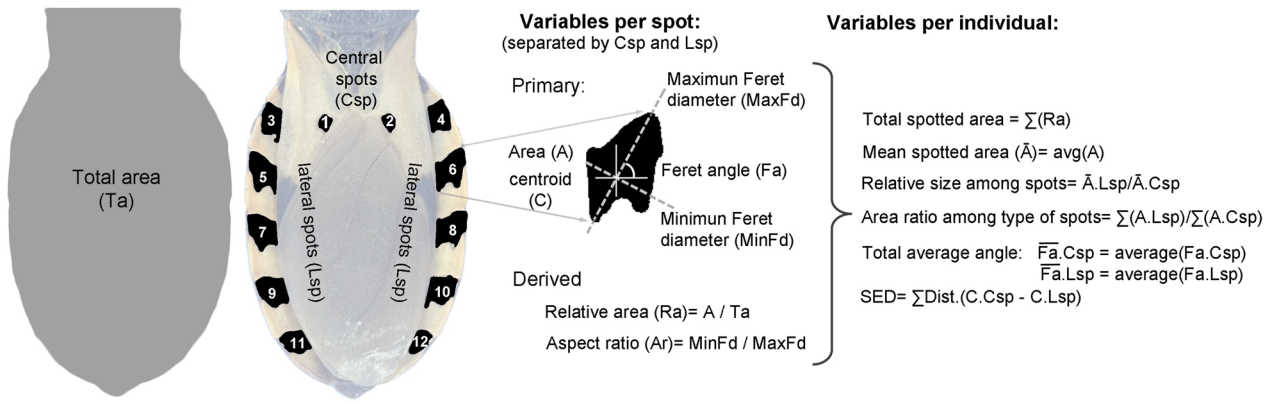

Fig. 2. Variables used for the quantitative description of the spot pattern in three haplogroups of *T. dimidiata* (Hemiptera: Reduviidae).

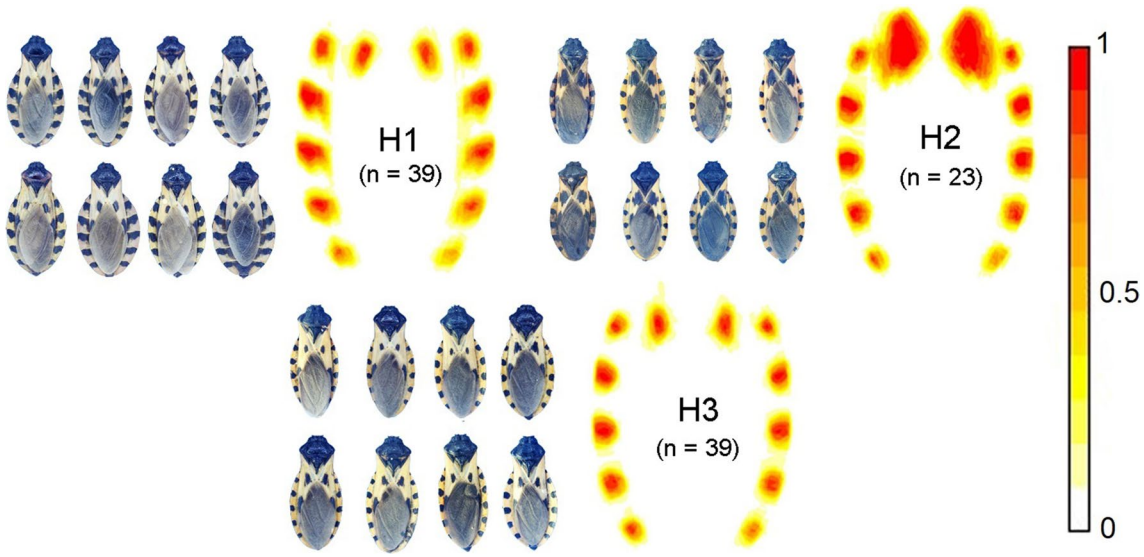

Fig. 3. Heat maps obtained by superimposing the spot patterns of all the individuals from the samples of three haplogroups (*H1*, *H2*, *H3*) of *T. dimidiata* (Hemiptera: Reduviidae), and a sample of the images used to visualize the differences between the haplogroups. Heat maps are composed of overlapping individuals by haplogroup. The color scale represents the areas of overlap between spots, with high values representing the most shared pattern among individuals, and low values representing extreme patterns.

consistent differences in the shape and orientation of the spots between these two haplogroups.

The ratio of spotted area to Ta differed among haplogroups. The highest Ra was presented by haplogroup 2, with 15.6 %, while the Ra for haplogroup 3 was only 8.7 % (Fig. 4a). When comparing the ratio of the area of the central spots to that of the lateral spots, haplogroups 1 and 3 had higher relative lateral spots. In haplogroup 2, the lateral spots and central spots contributed almost equally to the total spot area, while the percentage that the central spot area contributed to total spot area was slightly higher. Statistical comparison of the mean Ra of the central spots and lateral spots revealed that only the central spots differed significantly among haplogroups (Fig. 4b, c).

The average spot size, characterized by Feret diameters, was significantly different among haplogroups, both for the central spots and the lateral spots (Fig. 5). In the case of the central spots, haplogroup 2 was the most strongly differentiated (Fig. 5a), while for the lateral spots, haplogroup 1 presented the most notable differences (Fig. 5b).

The orientation of the abdominal spots, expressed by the Fa, were markedly different between haplogroup 1 and the other groups. The largest differences were observed in the orientations of the first three pairs of lateral spots (3/4, 5/6 and 7/8), which tended to be more forward oriented. For the remaining spots, although differences in orientation were observed, these were less noticeable, both in the Fa value and in its variation among individuals (Fig. 6).

When comparing the mean orientations of the lateral spots of the abdomen (Fa), significant differences were found between the three haplogroups. Haplogroup 1 was the most distinct and had less variation in Fa than the remaining haplogroups (Fig. 7).

The shapes of the central and lateral spots (Ar) differed among haplogroups, both for the lateral and central spots (Fig. 8). The shape of the central spots in haplogroup 2 showed the greatest differences among the haplogroups, while the most differentiated lateral spots were from haplogroup 3.

The LDFA correctly assigned 93.8% of the individuals into the correct haplogroups based on spot pattern (Fig. 9). One individual from H2 (H2 0504) was erroneously assigned to H3, and one H3 individual (H3 0847) was misassigned to H2. Haplogroups 1 and 3 had more overlap in the ranking space, with three H1 individuals (H1 0367, H1 0372, H1 0374) assigned to H3 and two H3 individuals (H3 0388 and H3 0395) assigned to H1.

The most efficient neural classification network had a topology with 20 neurons in the hidden layer. This achieved an overall performance of 94.7% with a BFGS-12 training algorithm and an entropy error function. Of the individuals in the training data, 100% were correctly identified; considering only the validation data, 87.2% of the individuals were correctly identified. The hidden layer had sine activation functions and the output layer

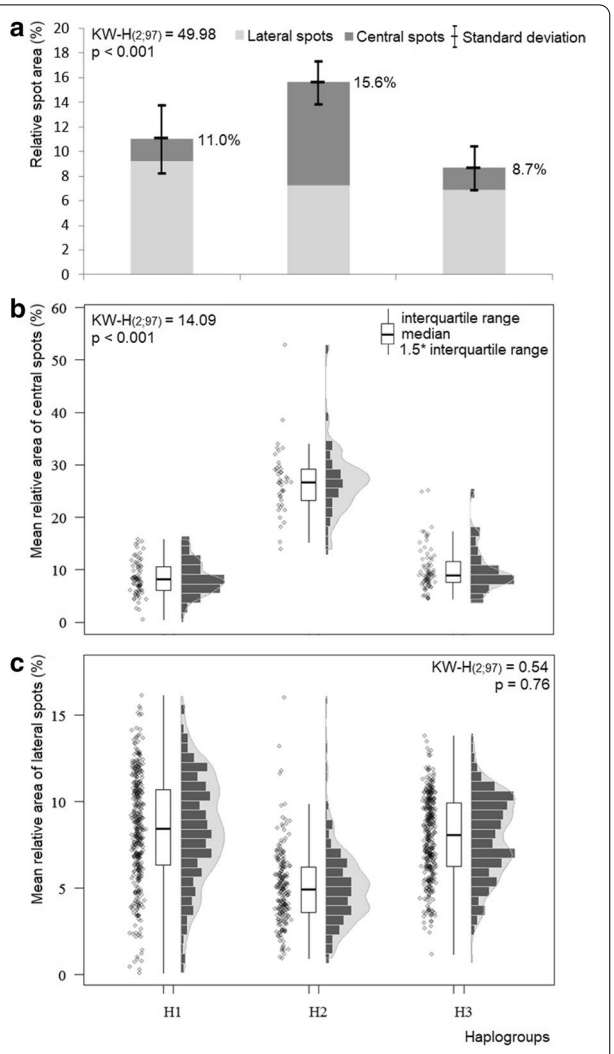

Fig. 4. Differences in relative spot area of the abdomen (**a**) and the mean relative areas of the central (**b**) and lateral (**c**) spots in the three haplogroups of *Triatoma dimidiata* (Hemiptera: Reduviidae). *KW-H* Kruskal–Wallis H test

logistic functions, with sum of squares as an error function. This network achieved 100% correct classification of H2 specimens and misclassified three H1 individuals (H1 0367, H1 0372 and H1 0374; from a total of 16 in the validation sample) as H3, and two H3 individuals (H3 0847 and H3 0862) as H2. The remaining three individuals that had been incorrectly classified by LDFA were correctly assigned to their haplogroups by the neural network (H2 0504; H3 0388 and H3 0395).

Classification methods made similar use of variables. The LDFA used only five variables in the final model: size of the central spots, shape, angle and diameter of the lateral spots and total relative spot area. The neural network assigned greater importance to these same variables and additionally included the relative area of the lateral spots.

When analyzing the weights assigned to each variable used in the neural network procedure (Fig. 10), the most important factor in the classification process was the Feret diameter of the lateral spots and the aspect ratio of the lateral spots, respectively. The variable that contributed the least to the classification was the ratio of the central spot area to lateral spot area.

Discussion

The cryptic *dimidiata* species complex has been largely supported using molecular tools, which has led to the identification of three phylogenetically well-differentiated haplogroups in Mexico and part of Central America [9, 11, 12], and two taxa have been formally described as new species [37, 38]. We report here the first time that the spot pattern presented by this complex has been used to discriminate among haplogroups (possible cryptic species) by extracting and analyzing quantifiable variables from digital images.

Our results demonstrate the ability to use these measures to correctly recognize the haplogroups analyzed. Of the variables used for discrimination, only one (mean relative area of the lateral spots) did not differ significantly among haplogroups, indicating that overall, pattern variables were useful for delimitation. This was verified both by the discriminant analysis ordination plot and the results obtained by the most efficient neural network.

The study of coloration in triatomines and its application in taxonomy has mainly been used in traditional qualitative approaches [32]. This has led to the assumption of a lack of clear morphological diagnostic characters to facilitate recognition and formal descriptions at the species level [15]. However, using heat maps, three well-differentiated spot patterns were evident, corresponding to the three haplogroups. This results once again highlights the importance of using quantitative tools to study complex patterns such as coloration, where subtle aspects, such as the orientation of groups of spots or other patterns, may not be apparent or easily distinguishable to a human observer.

The variation found among the haplogroups in spot pattern may be a response of various different processes. In other groups of insects, such as butterflies, coloration patterns have been shown to vary depending on environmental conditions, such as temperature [39, 40], that are associated with processes of genetic assimilation of phenotypic changes [41]. Although there are populations in which the three *T. dimidiata* haplogroups analyzed in this study are found sympatrically [see 11], their distributions are mostly allopatric; therefore, the pattern of variation among these

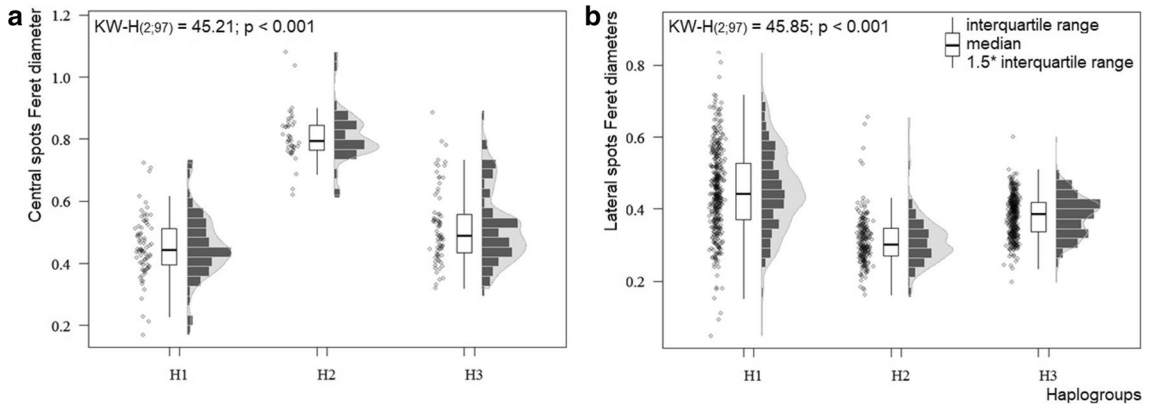

Fig. 5. Differences in the average size (Feret diameters), of the central (**a**) and lateral (**b**) spots on the abdomen of three haplogroups of *T. dimidiata* (Hemiptera: Reduviidae)

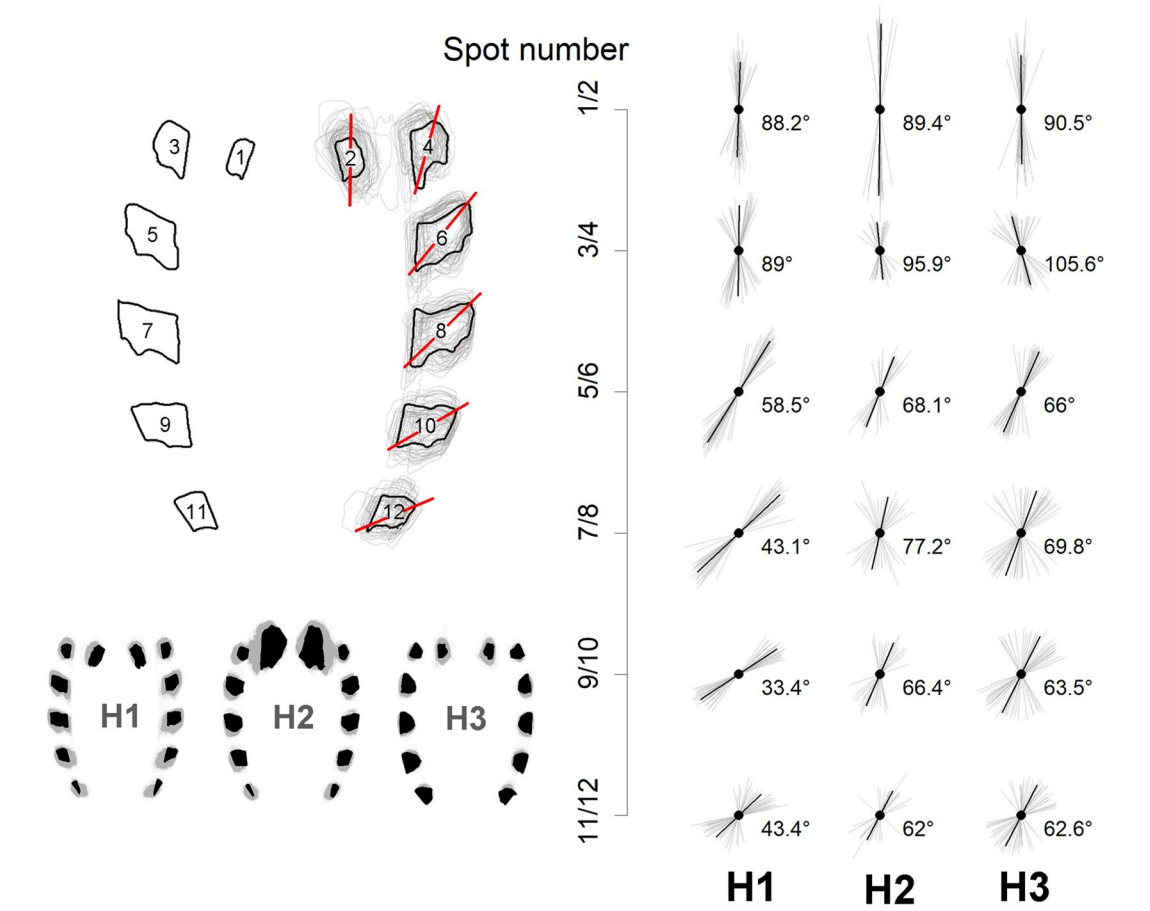

Fig. 6. Orientation patterns of the spots (Feret diameter angle). Red and black lines represent the orientation of Feret diameter angle.

haplogroups may reflect adaptation to environments with different characteristics in response to environmental stress. Genetic assimilation in the evolution of phenotypic plasticity has recently been demonstrated not only for butterflies but also for various other groups of organisms [42–45]. However, corroborating this

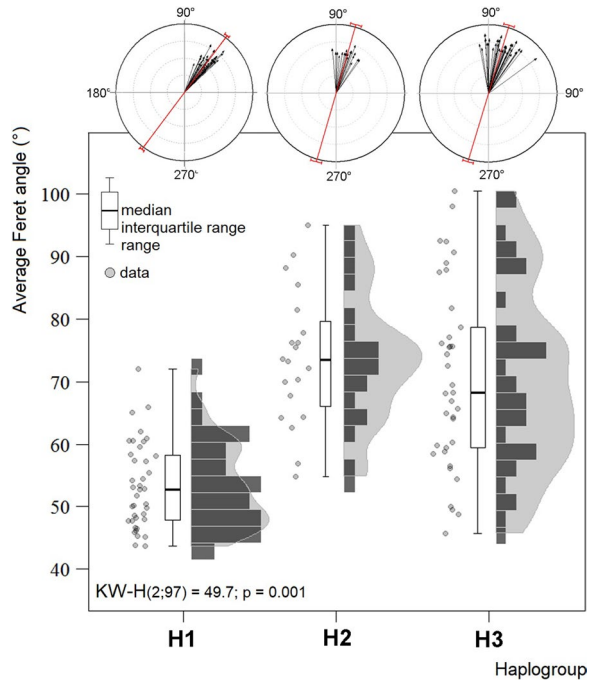

Fig. 7. Comparison of the mean orientations of the lateral spots of the abdomen (Feret angle) between three haplogroups of *T. dimidiata* (Hemiptera: Reduviidae)

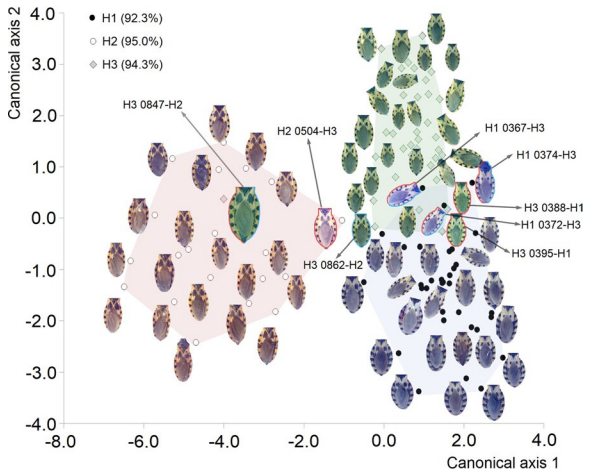

Fig. 9. Ordination plot of the discriminant analysis of the individuals of *T. dimidiata* (Hemiptera: Reduviidae) according to the analysis of discriminant function, based on the properties of their spots. The correct classification percentages of the discriminant analysis are shown, and the poorly classified individuals are outlined (red: according to the linear discriminant function analysis, blue: according to the neural network), and their numbers and the haplogroup with which they were confused are given. Full colors represent the minimum convex polygon per haplogroup: blue (H1), pink (H2) and green (H3)

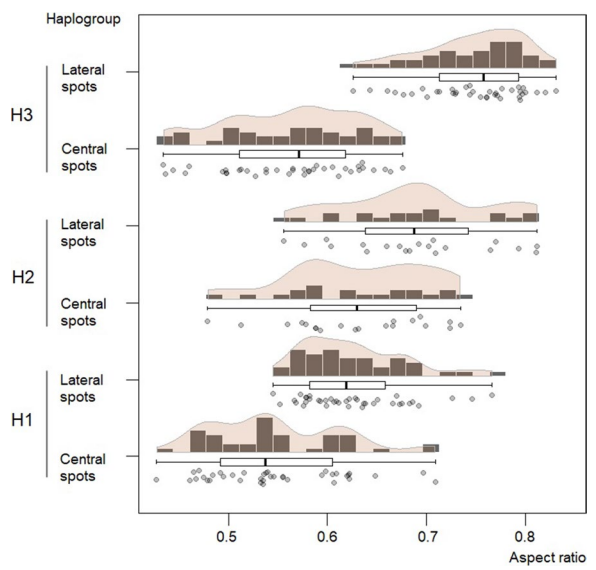

Fig. 8. Comparison of the shape (aspect ratio) of the central and lateral spots of the abdomen in the three haplogroups of *T. dimidiata* (Hemiptera: Reduviidae). The aspect ratio differed among haplogroups, both for the central ($KW\text{-}H_{(2;96)} = 15.45$; $p < 0.001$) and lateral spots ($KW\text{-}H_{(2;97)} = 46.25$; $p = 0.001$).

phenomenon in *T. dimidiata* will require specifically designed studies.

Another important aspect that this research demonstrates is the value of the combination of digital image analysis and machine learning for taxonomy purposes [46]. The potential of this combination of approaches in species delimitation has been broadly demonstrated [47]. However, even though its utility is clear and, in many cases, superior to the traditional taxonomy, it is still relatively rarely used.

Classical taxonomy is a science that is essentially in danger of extinction, especially due to the lack of expert taxonomists and specialists in species identification, a science which requires many years of training and experience [48]. In the era of big data, image pattern recognition is a new technology that provides many potential advantages for taxonomists, including speeding up and automating the classification process, reducing error and assimilating quantitative information that would be impossible for a human observer [49].

Specifically, with triatomines, there have been recent efforts to employ these methods to establish in automated identification systems. These include the studies of Gurgel-Goncalves et al. [20] and Khalighifar et al. [50], in which geometric morphometry techniques and deep learning algorithms, respectively, were used, representing the first steps toward applying these methods

Predictor variables	F to enter	p-level	No. Of Var	Lambda	F-value
Aspect ratio of central spot	0.405	0.668	-	-	-
Ratio of lateral spots area / central spots area	1.491	0.231	8.000	0.057	34.012
Mean relative area of central spots (%)	1.045	0.356	7.000	0.059	38.446
Mean relative area of lateral spots (%)	2.785	0.067	6.000	0.060	44.661
Spotted area (%)*	8.057	0.001	5.000	0.064	52.016
Feret diameter of lateral spots*	5.314	0.007	4.000	0.076	58.662
Feret angle of lateral spots*	17.513	0.000	3.000	0.085	73.111
Aspect ratio of lateral spot*	41.437	0.000	2.000	0.118	87.184
Feret diameter of central spots*	158.730	0.000	1.000	0.225	158.730

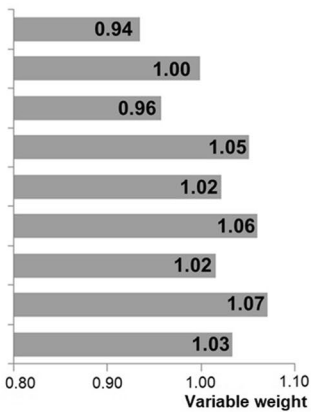

Fig. 10. Relative importance of each variable in the classification procedures used to assign individuals to three haplogroups of *T. dimidiata* (Hemiptera: Reduviidae) based on spot pattern. The statistical results of the linear discriminant function analysis are included, in which only the variables identified with a red asterisk and the weights assigned to the variables by the neural classification network obtained were included in the model. Wilks Lambda: 0.057; approximate $F_{(16, 170)} = 34.01$; $p < 0.001$

in automated identification systems. Another example is the study of Cruz et al. [26] who were able to discriminate *T. dimidiata* haplogroups with high correct discrimination values by characterizing the entire body contour using Fourier elliptical descriptors; the same method has been successfully used to generate automated identification systems in other groups of insects [51]. The integration of this method with the analysis of the spot pattern is potentially a novel and powerful tool to generate a computer-based approach for species identification in cryptic groups. Although classification processes still need improvement, these novel studies bring new challenges and novel perspectives in the field of epidemiological entomology, and the integration of methods should be a central aspect in the future of automated identification in this group, given its epidemiological importance, as well as in other groups of insects. In the context of haplogroup identification, these methods could generate a whole range of tools that allow their correct identification without the need for genetic testing that is, in most cases, costly and not even possible to perform.

Although the research presented here was focused on evaluating the possibility of correctly discriminating three haplogroups of *T. dimidiata* using the dorsal spot pattern, the value of coloration patterns in species biology cannot be forgotten. Color in insects has important biological functions, including mate choice, intra-sexual competition, dominance relationships and other social interactions [52]. Therefore, the study of color is relevant in many contexts beyond taxonomy, and research should be increased to explore the role that coloration patterns play in nature. In relation to other groups of insects, such as Coleoptera, Lepidoptera and Hymenoptera, in the Hemiptera, and especially the Triatominae subfamily, there are very few studies associated with coloring patterns [52].

Conclusions

The importance of the correct recognition of insect species of epidemiological importance is vital for the establishment of good control measures [13, 18]. The results obtained in this investigation allow us to conclude that the spot pattern in triatomines constitutes a significant source of information that can be used directly in the taxonomic analysis of this group of insects. If we consider that the haplogroups used here may constitute phylogenetically close cryptic species [9, 11, 53], similar pattern analysis in a larger number of less closely related species will likely find larger, more easily distinguishable differences in the spotting pattern than those found here. A fruitful avenue for future research would be to compare spot patterns among multiple species in order to discriminate among them. If such comparisons are similarly successful as this study, pattern recognition could allow, in the not too distant future, the development of a reliable automated identification system to use as a tool for the recognition of vectors of Chagas disease, one of the most important tropic parasitic disease on the American continents.

Supplementary Information

The online version contains supplementary material available at https://doi.org/10.1186/s13071-021-04598-5.

Additional file 1: Figure S1. Unused individuals in the spot pattern analyses (1.25mb) (https://doi.org/10.6084/m9.figshare.12910007.v1).

Additional file 2: Image J macro code programmed to automate image processing and measurements (466b) (https://doi.org/10.6084/m9.figshare.12910010).

Abbreviations

A: Area; Ar: Aspect ratio; C: Centroid; Csp: Central spots; Fa: Ferret angle; H1, H2, H2: Haplogroups 1, 2, 3; LDFA: Linear discriminant function analysis; Lsp: Lateral spots; MaxFd: Maximun Feret diameter; MinFd: Minimun ferret diameter; SED: Sum of the Euclidean distances; Ra: Relative area; Ta: Total area.

Acknowledgements

We would like to extend our thanks to Félix N. Estrada, Alejandro López Michelena and Daily Martínez who offered useful comments to improve the manuscript.

Authors' contributions

DDC, DD conceived the study. DDC, DD conducted all statistical analyses. DDC, EA, DD and CNIB wrote the manuscript. All authors contributed to the final draft of the manuscript. All authors read and approved the final manuscript.

Funding

Financial support for this study was provided by a CONACYT scholarship program 2018-000012-01NACF-11846 to the first author. We acknowledge financial support by the Secretaría de Educación Pública-Cinvestav (Project: FIDSC2018/160) to CNIC.

Availability of data and materials

Data supporting the conclusions of this article are included in the article. Also, all data derived from this investigation are deposited in the Figshare repository (https://doi.org/10.6084/m9.figshare.12909968.v1).

Ethics approval and consent to participate

Not applicable.

Consent for publication

Not applicable.

Competing interests

The authors declare that they have no competing interests.

Author details

[1] Centro de Investigación en Biodiversidad y Conservación (CIByC), Universidad Autónoma del Estado de Morelos (UAEM), Cuernavaca, Morelos, México. [2] Departamento de Biología Animal y Humana, Facultad de Biología, Universidad de La Habana, Havana, Cuba. [3] Departamento de Ecología Humana, Centro de Investigación y de Estudios Avanzados del IPN (CINVESTAV), Unidad Mérida, Yucatán, México.

Received: 16 September 2020 Accepted: 13 January 2021
Published online: 29 January 2021

References

1. de Jesús-Bonilla VS, García-París M, Ibarra-Cerdeña CN, Zaldívar-Riverón A. Geographic patterns of phenotypic diversity in incipient species of North American blister beetles (Coleoptera: Meloidae) are not determined by species niches, but driven by demography along the speciation process. Invertebr Syst. 2018;32:672–88.
2. Yoder AD, Yang Z. Estimation of primate speciation dates using local molecular clocks. Mol Biol Evol. 2000;17:1081–90.
3. Struck TH, Feder JL, Bendiksby M, Birkeland S, Cerca J, Gusarov VI, et al. Finding evolutionary processes hidden in cryptic species. Trends Ecol Evol. 2018;33:153–63.
4. Bickford D, Lohman DJ, Sodhi NS, Ng PK, Meier R, Winker K, et al. Cryptic species as a window on diversity and conservation. Trends Ecol Evol. 2007;22:148–55. https://doi.org/10.1016/j.tree.2006.11.004.
5. Dayrat B. Towards integrative taxonomy. Biol J Linn Soc. 2005;85:407–15. https://doi.org/10.1111/j.1095-8312.2005.00503.x.
6. Jörger KM, Schrödl M. How to describe a cryptic species? Practical challenges of molecular taxonomy. Front Zool. 2013;10:59.
7. Brower AV. Problems with DNA barcodes for species delimitation: 'ten species' of *Astraptes fulgerator* reassessed (Lepidoptera: Hesperiidae). Syst Biodivers. 2006;4:127–32. https://doi.org/10.1017/S147720000500191X.
8. Smith MA, Rodriguez JJ, Whitfield JB, Deans AR, Janzen DH, Hallwachs W, et al. Extreme diversity of tropical parasitoid wasps exposed by iterative integration of natural history, DNA barcoding, morphology, and collections. Proc Natl Acad Sci USA. 2008;105:12359–64. https://doi.org/10.1073/pnas.0805319105.
9. Bargues MD, Klisiowicz DR, Gonzalez-Candelas F, Ramsey JM, Monroy C, Ponce C, et al. Phylogeography and genetic variation of *Triatoma dimidiata*, the main Chagas disease vector in Central America, and its position within the genus Triatoma. PLoS Negl Trop Dis. 2008;2:e233.
10. Justi SA, Russo CA, Mallet JR, Obara MT, Galvao C. Molecular phylogeny of Triatomini (Hemiptera: Reduviidae: Triatominae). Parasites Vectors. 2014;7:149.
11. Pech-May A, Mazariegos-Hidalgo CJ, Izeta-Alberdi A, López-Cancino SA, Tun-Ku E, De la Cruz K, et al. Genetic variation and phylogeography of the *Triatoma dimidiata* complex evidence a potential center of origin and recent divergence of haplogroups having differential *Trypanosoma cruzi* and DTU infections. PLoS Negl Trop Dis. 2019;13:e0007044.
12. Aguilera-Uribe M, Meza-Lázaro RN, Kieran TJ, Ibarra-Cerdeña CN, Zaldívar-Riverón A. Phylogeny of the North-Central American clade of blood-sucking reduviid bugs of the tribe Triatomini (Hemiptera: Triatominae) based on the mitochondrial genome. Infect Genet Evol. 2020;202084:104373.
13. Gurgel-Gonçalves R, Ferreira JBC, Rosa AF, Bar ME, Galvao C. Geometric morphometrics and ecological niche modelling for delimitation of nearsibling triatomine species. Med Vet Entomol. 2011;25:84–93.
14. Monteiro FA, Peretolchina T, Lazoski C, Harris K, Dotson EM, Abad-Franch F, et al. Phylogeographic pattern and extensive mitochondrial DNA divergence disclose a species complex within the Chagas disease vector *Triatoma dimidiata*. PloS One. 2013;8:e70974.
15. Bargues MD, Schofield C, Dujardin JP. The phylogeny and classification of the triatominae. In: Telleria J, Tibayrenc M, editors. American trypanosomiasis: Chagas disease, one hundred years of research. Amsterdam: Elsevier; 2017. p. 117–47.
16. Bustamante DM, Monroy C, Menes M, Rodas A, Salazar-Schettino PM, Rojas G, et al. Metric variation among geographic populations of the Chagas vector *Triatoma dimidiata* (Hemiptera: Reduviidae: Triatominae) and related species. J Med Entomol. 2004;41:296–301.
17. Panzera F, Ferrandis I, Ramsey J, Ordonez R, Salazar-Schettino PM, Cabrera M, et al. Chromosomal variation and genome size support existence of cryptic species of *Triatoma dimidiata* with different epidemiological importance as Chagas disease vectors. Trop Med Int Health. 2006;11:1092–103.
18. Abad-Franch F, Monteiro FA. Molecular research and the control of Chagas disease vectors. An Acad Bras Cienc. 2005;77:437–54.
19. Dujardin JP, Beard CB, Ryckman R. The relevance of wing geometry in entomological surveillance of Triatominae, vectors of Chagas disease. Infect Genet Evol. 2007;7:161–7.
20. Gurgel-Gonçalves R, Komp E, Campbell LP, Khalighifar A, Mellenbruch J, Mendonça VJ, et al. Automated identification of insect vectors of Chagas disease in Brazil and Mexico: the virtual vector lab. PeerJ. 2017;5:e3040.
21. Oliveira J, Marcet PL, Takiya DM, Mendonça VJ, Belintani T, Bargues MD, et al. Combined phylogenetic and morphometric information to delimit and unify the *Triatoma brasiliensis* species complex and the *Brasiliensis* subcomplex. Acta Trop. 2017;170:140–8.
22. Nattero J, Piccinali RV, Lopes CM, Hernández ML, Abrahan L, Lobbia PA, et al. Morphometric variability among the species of the Sordida subcomplex (Hemiptera: Reduviidae: Triatominae): evidence for differentiation across the distribution range of *Triatoma sordida*. Parasites Vectors. 2017;10:412.

23. Dujardin JP, Kaba D, Solano P, Dupraz M, McCoy KD, Jaramillo-O N. Outline-based morphometrics, an overlooked method in arthropod studies? Infect Genet Evol. 2014;28:704–14.
24. Santillán-Guayasamín S, Villacís AG, Grijalva MJ, Dujardin JP. The modern morphometric approach to identify eggs of Triatominae. Parasites Vectors. 2017;10:55.
25. Santillán-Guayasamín S, Villacís AG, Grijalva MJ, Dujardin JP. Triatominae: does the shape change of non-viable eggs compromise species recognition. Parasites Vectors. 2018;11:543.
26. Cruz DD, Arellano E, Ávila DD, Ibarra-Cerdeña CN. Identifying Chagas disease vectors using elliptic Fourier descriptors of body contour: a case for the cryptic *dimidiata* complex. Parasites Vectors. 2020;13:1–12.
27. Tatsuta H, Takahashi KH, Sakamaki Y. Geometric morphometrics in entomology: basics and applications. Entomol Sci. 2018;21:164–84.
28. Padula V, Bahia J, Stöger I, Camacho-García Y, Malaquias MAE, Cervera JL, et al. A test of color-based taxonomy in nudibranchs: molecular phylogeny and species delimitation of the *Felimida clenchi* (Mollusca: Chromodorididae) species complex. Mol Phyl Evol. 2016;103:215–29.
29. Yu X, Wang J, Kays R, Jansen PA, Wang T, Huang T. Automated identification of animal species in camera trap images. J Image Video Proc 2013;52(2013). https://doi.org/10.1186/1687-5281-2013-52.
30. Chan IZ, Chang JJM, Huang D, Todd PA. Colour pattern measurements successfully differentiate two cryptic Onchidiidae Rafinesque, 1815 species. Mar Biodivers. 2019;49:1743–50. https://doi.org/10.1007/s12526-019-00940-4.
31. Kieran TJ, Gordon ERL, Zaldívar-Riverón A, Ibarra-Cerdeña CN, Glenn TC, Weirauch C. Ultraconserved elements reconstruct the evolution of the Chagas disease-vectoring kissing bugs (Hemiptera: Reduviidae: Triatominae). Syst Entomol. 2020 (accepted).
32. Lent H, Wygodzinsky P. Revision of Triatominae (Hemiptera: Reduviidae) and their significance as vector of Chagas' disease. Bull Am Mus Nat Hist. 1979;163:123–520.
33. Nattero J, de la Fuente ALC, Piccinali RV, Cardozo M, Rodríguez CS, Crocco LB. Characterization of melanic and non-melanic forms in domestic and peridomestic populations of *Triatoma infestans* (Hemiptera: Reduviidae). Parasites Vectors. 2020;13:47.
34. Carmona-Galindo VD, Recinos MFM, Hidalgo SAG, Paredes GR, Vaquerano EEP, et al. Morphological variability and ecological characterization of the Chagas disease vector *Triatoma dimidiata* (Hemiptera: Reduviidae) in El Salvador. Acta Trop. 2020;205:105392. https://doi.org/10.1016/j.actatropica.2020.105392.
35. Schneider CA, Rasband WS, Eliceiri KW. NIH image to ImageJ: 25 years of image analysis. Nat Methods. 2012;9:671–5. https://doi.org/10.1038/nmeth.2089.
36. Chan IZW, Stevens M, Todd PA. PAT-GEOM: a software package for the analysis of animal patterns. Methods Ecol Evol. 2018. https://doi.org/10.1111/2041-210X.13131.
37. Dorn PL, Justi SA, Dale C, Stevens L, Galvão C, Lima-Cordónet, et al. Description of *Triatoma mopan* sp. n. from a cave in Belize (Hemiptera, Reduviidae, Triatominae). ZooKeys. 2018;775:69-95.
38. Justi SA, Cahan S, Stevens L, Monroy C, Lima-Cordón R, Dorn PL. Vectors of diversity: genome wide diversity across the geographic range of the Chagas disease vector *Triatoma dimidiata* sensu lato (Hemiptera: Reduviidae). Mol Phyl Evol. 2018;120:144–50.
39. Otaki JM, Yamamoto H. Color-pattern modifications and speciation in lycaenid butterflies. Trans Lepidopterol Soc Jpn. 2003;54:197–205.
40. Otaki JM, Yamamoto H. Species-specific color-pattern modifications on butterfly wings. Dev Growth Differ. 2004;46:1–14.
41. Otaki JM, Hiyama A, Iwata M, Kudo S. Phenotypic plasticity in the range-margin population of the lycaenid butterfly *Zizeeria maha*. BMC Evol Biol. 2010;10:252. https://doi.org/10.1186/1471-2148-10-252.
42. Aubret F, Shine R. Genetic assimilation and the post colonization erosion of phenotypic plasticity in island tiger snakes. Curr Biol. 2009;19:1932–6.
43. Buckley J, Bridle JR, Pomiankowski A. Novel variation associated with species range expansion. BMC Evol Biol. 2010;10:382. https://doi.org/10.1186/1471-2148-10-382.
44. Scoville AG, Pfrender ME. Phenotypic plasticity facilitates recurrent rapid adaptation to introduced predators. Proc Natl Acad Sci USA. 2010;107:4260–3.
45. Muschick M, Barluenga M, Salzburger W, Meyer A. Adaptive phenotypic plasticity in the Midas cichlid fish pharyngeal jaw and its relevance in adaptive radiation. BMC Evol Biol. 2011;11:116. https://doi.org/10.1186/1471-2148-11-116.
46. Lukhtanov VA. Species delimitation and analysis of cryptic species diversity in the XXI century. Entomol Rev. 2019;99:463–72. https://doi.org/10.1134/S0013873819040055.
47. Wäldchen J, Mäder P. Machine learning for image based species identification. Methods Ecol Evol. 2018;9:2216–25. https://doi.org/10.1111/2041-210X.13075.
48. Martineau M, Conte D, Raveaux R, Arnault I, Munier D, Venturini G. A survey on image-based insect classification. Pattern Recognit. 2017;65:273–84.
49. Zerdoumi S, Sabri AQM, Kamsin A, Hashem IAT, Gani A, Hakak S, et al. Image pattern recognition in big data: taxonomy and open challenges: survey. Multimed Tools Appl. 2018;77:10091–121. https://doi.org/10.1007/s11042-017-5045-7.
50. Khalighifar A, Komp E, Ramsey JM, Gurgel-Gonçalves R, Peterson AT. Deep learning algorithms improve automated identification of Chagas disease vectors. J Med Entomol. 2019;56:1404–10.
51. Yang HP, Ma CS, Wen H, Zhan QB, Wang XL. A tool for developing an automatic insect identification system based on wing outlines. Sci Rep. 2015;5:12786.
52. Mora R, Hanson PE. Widespread occurrence of Black-Orange-Black color pattern in Hymenoptera. J Insect Sci. 2019;19:13. https://doi.org/10.1093/jisesa/iez021.
53. Gómez-Palacio A, Arboleda S, Dumonteil E, Peterson AT. Ecological niche and geographic distribution of the Chagas disease vector, *Triatoma dimidiata* (Reduviidae: Triatominae): Evidence for niche differentiation among cryptic species. Infect Genet Evol. 2015;36:15–22.

Publisher's Note

DISCUSIÓN GENERAL

El concepto de especie es uno de los varios conceptos clave en biología (Keller y Lloyd, 1992; Pigliucci y Kaplan, 2006; Sober, 2006). Si bien el descubrimiento, la descripción y el nombramiento de especies son responsabilidad de los taxónomos y sistemáticos, la correcta definición de las especies es de vital importancia para muchas otras disciplinas de la sociedad, incluida la conservación (inclusión de especies en las listas de la UICN), la salud pública (p. ej., enfermedades infecciosas transmitidas por vector), la definición de marcos legales (Geist, 1992) entre otras.

A su vez, las especies son cruciales para varios conceptos en otras ramas de la biología y la sociedad en general, como se refleja en términos como "especies clave" (ecología), "especies emblemáticas" (conservación), "especiación" (biología evolutiva) y "especismo" (ética). En biología, el concepto de especie se comparte en varias jerarquías. La amplia relevancia del concepto de especie no significa que el término signifique lo mismo para diferentes biólogos o que los taxones de especies sean uniformes entre los grupos (Sangster, 2018).

La definición y delimitación de especies en Triatominae ha evolucionado considerablemente, teniendo en cuenta que los estudios taxonómicos del grupo comenzaron en el siglo 18, con la descripción de *Triatoma rubrofasciata* (De Geer, 1773) (originalmente como *Cimex rubro-fasciatus*) (Alevi *et al*., 2021). La mayoría de las clasificaciones formales de triatominos se han basado en el empleo de la taxonomía clásica (similar a la mayoría de los grupos descritos), mediante el uso de la morfología descriptiva, morfología comparativa y/o morfometría (Alevi *et al*., 2021). Si bien, varios enfoques de taxonomía clásica son de gran relevancia para continuar la formalización de nuevas entidades taxonómicas dentro del

grupo, también son la causa de más de 190 actos de sinonimia en la subfamilia Triatominae (Galvao *et al*., 2003). La presencia de un gran número de complejos de especies cripticas, solo detectados mayormente por análisis filogenéticos, aseveran aun más las deficiencias de la taxonomía clásica para el correcto reconocimiento de las especies de triatominos (Bargues *et al*., 2008; Gomez-Palacio *et al*., 2015; Ibarra-Cerdena *et al*., 2014; Justi *et al*., 2014; Pech-May *et al*., 2019; Cruz y Arellano, 2022).

Es por estas razones, que la integración de datos en lo que, actualmente se conoce como taxonomía integrativa, es probablemente la manera más eficiente de describir nuevas especies. El uso de métodos combinados para delimitar una especie de triatomino ocurrió por primera vez en 1998 por Frías *et al*. (1998). Sin embargo, solo en la última década se ha aplicado más la taxonomía integradora en el estudio de estos vectores (Alevi *et al*., 2021), permitiendo el correcto reconocimiento y la descripción formal de nuevas especies dentro del grupo (p. ej.: Dorn *et al*., 2018; Lima-Cordon *et al*., 2019).

Los resultados obtenidos en esta tesis apoyan el uso de la taxonomía integradora como la manera más eficiente de detectar y delimitar nuevas especies de triatominos, principalmente cuando estamos ante complejos de especies crípticas. En primer lugar, nuestro trabajo resalta la importancia de partir de reconstrucciones filogenéticas robustas, con alta representatividad geográfica, que nos permitan recuperar la historia evolutiva de las poblaciones analizadas. En el caso de *Triatoma pallidipennis*, si bien existían estudios donde se alertaba sobre su estatus de complejo de especies crípticas (Harris, 2003; Mayares, 2014), la falta de un amplio muestreo geográfico imposibilitó llegar a conclusiones firmes. En este sentido, en esta tesis se realizó la reconstrucción filogenética más completa de esta especie hasta el momento (ver Cruz y Arellano, 2022), permitiendo aclarar finalmente la interrogante

taxonómica relacionada a lo que consideramos formalmente como el complejo *Pallidipennis*. Un aspecto importante derivado de nuestra investigación es la utilidad de métodos de delimitación de especies para aclarar los límites de especies en el género *Triatoma*. Esto no es común en estudios similares al nuestro (ver Bargues *et al*., 2008; Pech-May *et al*., 2019), y su uso debería ser una práctica común en el futuro. Por otra parte, la presencia de este nuevo complejo de especies crípticas genera nuevas interrogantes respecto a su posición evolutiva dentro del género, y más aún dentro del complejo *Phyllosoma*. Las reconstrucciones filogenéticas clásicas y recientes que han incluido a *Triatoma pallidipennis* han carecido de representación de especímenes de diferentes localidades, siendo Morelos la más utilizada. (ver Bargues *et al*., 2000; Ibarra-Cerdena *et al*., 2014; Justi *et al*., 2014; Rengifo-Correa *et al*., 2020). Por lo tanto, futuras reconstrucciones filogenéticas deberán considerar la presencia de estos nuevos linajes crípticos y esclarecer su relación con el resto de las especies distribuidas en México.

Complementar hipótesis filogenéticas con métodos como la morfometría geométrica (tanto por puntos anatómicos de referencia y métodos de contorno como los descriptores elípticos de Fourier) constituyen una excelente vía de validar la existencia de nuevas especies y establecer límites entre las formalmente descritas (Camul y Polly 2005; Pavan y Marroig; 2016, Cruz *et al*., 2020). En nuestro trabajo, el empleo de variables de forma asociadas a la cabeza y el pronoto de cuatro haplogrupos de *Triatoma pallidipennis* mostró tener valor taxonómico para discriminar entre estos, al menos parcialmente. Si bien no se observó una discriminación completa entre estos, las diferencias encontradas en la forma de la cabeza y el pronoto pueden ser consideradas como un indicio de que los haplogrupos analizados están siguiendo caminos evolutivos diferentes, donde el aislamiento genético/geográfico puede

estar jugando un papel importante en la fijación de características morfológicas que permitan, eventualmente, su correcto reconocimiento. Esto demuestra, una vez más, la importancia de incluir este tipo de métodos de análisis de la forma en estudios taxonómicos con triatominos (Matias *et al*., 2001; Jaramillo *et al*., 2002; Lehmann *et al*., 2005; Vargas *et al*., 2006; Feliciangeli *et al*., 2007; Nattero *et al*., 2017).

Por otra parte, el empleo de otras herramientas enfocadas al análisis morfométrico como los Descriptores Elípticos de Fourier mostró ser de alto valor para la discriminación de haplogrupos de triatominos (Cruz *et al*., 2020). Hasta donde sabemos, nuestro trabajo constituye el primero en emplear el contorno del cuerpo entero de un triatomino para discriminar entre haplogrupos. El uso de los Descriptores Elípticos de Fourier ha sido poco explorado, aunque en varias ocasiones ha demostrado su capacidad para discriminar entre especies estrechamente relacionadas (Arribas *et al*., 2013; Polášek *et al*., 2018) e incluso con triatominos (Dujardin *et al*., 2014; Santillán-Guayasamín *et al*., 2017).

Si bien la morfometría geométrica, bajo sus diferentes enfoques, constituye una práctica bastante común en la delimitación de especies en triatominos (Alevi *et al*., 2021), nuestro trabajo mostró que existen otras líneas de evidencia que pueden ser empleadas para diferenciar especies, incluso hacia el interior de complejos de especies crípticas. En este sentido, nuestros resultados obtenidos a partir del análisis del patrón de manchas en triatominos constituye una fuente importante de información que se puede utilizar directamente en el análisis taxonómico de este grupo de insectos Si consideramos que los haplogrupos utilizados aquí (los tres haplogrupos de *Triatoma dimidiata* propuestos por Bargues *et al*., 2008; Pech-May *et al*., 2019) constituyen especies crípticas filogenéticamente cercanas, análisis similares en un mayor número de buenas especies probablemente

encontrarán diferencias marcadas fácilmente distinguibles en el patrón de manchas, ayudando esto a la discriminación específica. Una vía fructífera para futuras investigaciones sería comparar patrones de manchas entre varias especies para discriminar entre ellas. Si tales comparaciones tienen el mismo éxito que este estudio, el reconocimiento de estos patrones podría permitir, el desarrollo de sistemas automatizados confiables de identificación, los cuales pueden ser utilizados como herramienta para el reconocimiento de este grupo de vectores. Con los triatominos, ha habido recientes esfuerzos para establecer en sistemas de identificación automatizados. Estos incluyen los estudios de Gurgel-Goncalves *et al*. (2017) y Khalighifar *et al*. (2019), en el que se utilizan técnicas de morfometría geométrica y algoritmos de aprendizaje profundo, respectivamente. Estos trabajos representan los primeros pasos hacia la aplicación de estos métodos en sistemas de identificación automatizados en triatominos.

El enfoque de taxonomía integradora también incluye otras líneas de evidencia, como el uso de datos ecológicos (Dayrat, 2005). En particular, las características del nicho ambiental pueden ser útiles para delimitar especies crípticas o grupos relacionados filogenéticamente (Martínez-Borrego *et al*., 2022). El empleo combinado de información filogenética y ecológica (específicamente modelos de nicho ecológico) (Chan *et al*., 2011) en esta tesis demostró ser una herramienta muy útil para evaluar la existencia o no de flujo genético entre los haplogrupos detectados (Cruz y Arellano, 2022). Esto es especialmente importante, ya que analizar los patrones genéticos sin tener en cuenta la complejidad espacial puede subestimar el efecto de la historia ambiental en la dispersión de los organismos a través del tiempo (Kozak *et al*., 2008) y, por ende, en sus posibles procesos de especiación.

A su vez, la evaluación del espacio ambiental de los haplogrupos analizados a partir de la reconstrucción de los hipervolúmenes y las proyecciones obtenidas por los modelos de nicho demostraron que sus distribuciones están limitadas por un conjunto de condiciones ambientales. Si bien se observó cierta superposición en las condiciones ambientales relacionadas con la distribución de los haplogrupos analizados, los hipervolúmenes mostraron también que habían marcadas diferencias ambientales, algo que pudo ser corroborado con la comparación estadística de los puntajes de los componentes principales como variables ambientales secundarias. Esto podría ser un indicio de que la segregación ecológica efectivamente ha jugado un papel importante en la diferenciación de los haplogrupos analizados, algo que se ha demostrado en otros triatominos como *T. dimidiata* (Gómez-Palacio *et al*., 2015).

Consideraciones finales

Los resultados mostrados en esta tesis nos permiten concluir que *Triatoma pallidipennis* es un complejo de especies crípticas, evidenciándose esto debido a la gran divergencia genética que existen entre los haplogrupos detectados por los métodos de delimitación de especies, las diferencias morfométricas encontradas a partir del análisis de la forma de la cabeza y el pronoto y la divergencia ambiental encontrada entre estos (enfoque de taxonomía integradora). A su vez, el empleo de métodos alternativos a los anteriormente mencionados, como los Descriptores Elípticos de Fourier y el análisis del patrón de manchas del conexivo de triatominos permiten la correcta discriminación de linajes genéticos cercanos, tal y como se demostró para los haplogrupos de *Triatoma dimidiata*. Todos estos elementos demuestran la efectividad de emplear una taxonomía integradora como enfoque moderno y novedoso en la nueva taxonomía del siglo XXI.

LITERATURA CITADA

1. Alevi, K. C. C., de Oliveira, J., da Silva Rocha, D., & Galvão, C. (2021). Trends in Taxonomy of Chagas Disease Vectors (Hemiptera, Reduviidae, Triatominae): From Linnaean to Integrative Taxonomy. Pathogens, 10(12), 1627.
2. Bargues, M. D., Marcilla, A., Ramsey, J. M., Dujardin, J. P., Schofield, C. J., & Mas-Coma, S. (2000). Nuclear rDNA-based molecular clock of the evolution of Triatominae (Hemiptera: Reduviidae), vectors of Chagas disease. Memórias do Instituto Oswaldo Cruz, 95(4), 567-573.
3. Bargues, M.D., Klisiowicz, D.R., Gonzalez-Candelas, F., Ramsey, J.M., Monroy, C., *et al*., 2008. Phylogeography and genetic variation of *Triatoma dimidiata*, the main Chagas disease vector in central America, and its position within the genus *Triatoma*. PLoS Negl. Trop. Dis. 2 (5), e233. https://doi.org/10.1371/journal.pntd.0000233.
4. Caumul, R., & Polly, P. D. (2005). Phylogenetic and environmental components of morphological variation: skull, mandible, and molar shape in marmots (Marmota, Rodentia). Evolution, 59(11), 2460-2472.
5. Chan, L. M., Brown, J. L., & Yoder, A. D. (2011). Integrating statistical genetic and geospatial methods brings new power to phylogeography. Molecular phylogenetics and evolution, 59(2), 523-537.
6. Cruz, D. D., & Arellano, E. (2022). Molecular data confirm *Triatoma pallidipennis* Stål, 1872 (Hemiptera: Reduviidae: Triatominae), as a novel cryptic species complex. Acta Tropica, 106382.
7. Cruz, D. D., Arellano, E., Denis Ávila, D., & Ibarra-Cerdeña, C. N. (2020). Identifying Chagas disease vectors using elliptic Fourier descriptors of body contour: a case for the cryptic *dimidiata* complex. Parasites & vectors, 13(1), 1-12.
8. Dayrat, B. (2005). Towards integrative taxonomy. Biological journal of the Linnean society, 85(3), 407-417.
9. Dorn, P. L., Justi, S. A., Dale, C., Stevens, L., Galvão, C., Lima-Cordón, R., & Monroy, C. (2018). Description of *Triatoma* mopan sp. n. from a cave in Belize (Hemiptera, Reduviidae, Triatominae). ZooKeys, (775), 69.
10. Dujardin, J. P., Kaba, D., Solano, P., Dupraz, M., McCoy, K. D., & Jaramillo-o, N. (2014). Outline-based morphometrics, an overlooked method in arthropod studies?. Infection, Genetics and Evolution, 28, 704-714.
11. Feliciangeli, M. D., Sanchez-Martin, M., Marrero, R., Davies, C., & Dujardin, J. P. (2007). Morphometric evidence for a possible role of Rhodnius prolixus from palm trees in house re-infestation in the State of Barinas (Venezuela). Acta tropica, 101(2), 169-177.
12. Frias, D. A., Henry, A. A., & Gonzalez, C. R. (1998). Mepraia gajardoi: a new species of Triatominae (Hemiptera: Reduviidae) from Chile and its comparison with Mepraia spinolai. Rev Chil Hist Nat, 71, 177-188.

13. Galvão, C., Carcavallo, R., Rocha, D. D. S., & Jurberg, J. (2003). A checklist of the current valid species of the subfamily Triatominae Jeannel, 1919 (Hemiptera, Reduviidae) and their geographical distribution, with nomenclatural and taxonomic notes. Zootaxa, 202(1), 1-36.
14. Geist, V. (1992). Endangered species and the law. Museums in the Material World. Nature, 357:274–276
15. Gómez-Palacio, A., Arboleda, S., Dumonteil, E., & Peterson, A. *T.* (2015). Ecological niche and geographic distribution of the Chagas disease vector, *Triatoma dimidiata* (Reduviidae: Triatominae): Evidence for niche differentiation among cryptic species. Infection, genetics and evolution, 36, 15-22.
16. Gurgel-Gonçalves, R., Komp, E., Campbell, L. P., Khalighifar, A., Mellenbruch, J., Mendonça, V. J., ... & Ramsey, J. M. (2017). Automated identification of insect vectors of Chagas disease in Brazil and Mexico: the Virtual Vector Lab. PeerJ, 5, e3040.
17. Harris, K. (2003). Taxonomy and Phylogeny of North American Triatominae: Public Health Implications. Moorehouse School of Medicine, Atlanta, GA. Doctoral Thesis.
18. Ibarra-Cerdeña, C. N., Zaldívar-Riverón, A., Peterson, A. *T.*, Sánchez-Cordero, V., & Ramsey, J. M. (2014). Phylogeny and niche conservatism in North and Central American triatomine bugs (Hemiptera: Reduviidae: Triatominae), vectors of Chagas' disease. PLoS neglected tropical diseases, 8(10), e3266.
19. Jaramillo O, N., Castillo, D., & Wolff E, M. (2002). Geometric morphometric differences between Panstrongylus geniculatus from field and laboratory. Memórias do Instituto Oswaldo Cruz, 97, 667-673.
20. Justi, S. A., Russo, C. A., Mallet, J. R. D. S., Obara, M. *T.*, & Galvão, C. (2014). Molecular phylogeny of Triatomini (Hemiptera: Reduviidae: Triatominae). Parasites & vectors, 7(1), 1-12.
21. Keller, E. F., & Lloyd, E. A. (Eds.). (1994). Keywords in evolutionary biology. Harvard University Press.
22. Khalighifar, A., Komp, E., Ramsey, J. M., Gurgel-Gonçalves, R., & Peterson, A. *T.* (2019). Deep learning algorithms improve automated identification of Chagas disease vectors. Journal of medical entomology, 56(5), 1404-1410.
23. Kozak, K. H., Graham, C. H., & Wiens, J. J. (2008). Integrating GIS-based environmental data into evolutionary biology. Trends in ecology & evolution, 23(3), 141-148.
24. Lehmann, P., Ordoñez, R., Ojeda-Baranda, R., Lira, J., Hidalgo-Sosa, L., Monroy, C., & Ramsey, J. M. (2005). Morphometric analysis of *Triatoma dimidiata* populations (Reduviidae: Triatominae) from Mexico and northern Guatemala. Memórias do Instituto Oswaldo Cruz, 100(5), 477-486.
25. Lima-Cordón, R. A., Monroy, M. C., Stevens, L., Rodas, A., Rodas, G. A., Dorn, P. L., & Justi, S. A. (2019). Description of *Triatoma*huehuetenanguensis sp. n., a potential Chagas disease vector (Hemiptera, Reduviidae, Triatominae). ZooKeys, (820), 51.

26. Martínez-Borrego, D., Arellano, E., Cruz, D. D., González-Cózatl, F. X., Nava-García, E., & Rogers, D. S. (2021). Morphological and ecological data confirm Reithrodontomys cherrii as a distinct species from Reithrodontomys mexicanus. THERYA, 13(1), 115.
27. Matias, A., De la Riva, J. X., Torrez, M., & Dujardin, J. P. (2001). Rhodnius robustus in Bolivia identified by its wings. Memorias do Instituto Oswaldo Cruz, 96(7), 947-950.
28. Mayares, D.I. (2014). Phylogeography of *Triatoma pallidipennis* (Hemíptera: Reduviidae) in the State of Morelos. UAEM, Mexico. Master's thesis.
29. Nattero, J., Piccinali, R. V., Macedo Lopes, C., Hernández, M. L., Abrahan, L., Lobbia, P. A., ... & Carbajal de la Fuente, A. L. (2017). Morphometric variability among the species of the Sordida subcomplex (Hemiptera: Reduviidae: Triatominae): evidence for differentiation across the distribution range of *Triatoma* sordida. Parasites & vectors, 10(1), 1-14.
30. Pavan, A. C., & Marroig, G. (2016). Integrating multiple evidences in taxonomy: species diversity and phylogeny of mustached bats (Mormoopidae: Pteronotus). Molecular Phylogenetics and Evolution, 103, 184-198.
31. Pech-May, A., Mazariegos-Hidalgo, C. J., Izeta-Alberdi, A., López-Cancino, S. A., Tun-Ku, E., De la Cruz-Felix, K., ... & Ramsey, J. M. (2019). Genetic variation and phylogeography of the *Triatoma dimidiata* complex evidence a potential center of origin and recent divergence of haplogroups having differential Trypanosoma cruzi and DTU infections. PLoS neglected tropical diseases, 13(1), e0007044.
32. Massimo, P., & Jonathan, K. (2006). Making Sense of Evolution: The Conceptual Foundations of Evolutionary Biology. University Chicago Press, Chicago.
33. Rengifo-Correa, L., Abad-Franch, F., Martínez-Hernández, F., Salazar-Schettino, P. M., Téllez-Rendón, J. L., Villalobos, G., & Morrone, J. J. (2021). A biogeographic–ecological approach to disentangle reticulate evolution in the *Triatoma* phyllosoma species group (Heteroptera: Triatominae), vectors of Chagas disease. Journal of Zoological Systematics and Evolutionary Research, 59(1), 94-110.
34. Sangster, G. (2018). Integrative taxonomy of birds: the nature and delimitation of species. In Bird species (pp. 9-37). Springer, Cham.Santillán-Guayasamín S, Villacís AG, Grijalva MJ, Dujardin JP. The modern morphometric approach to identify eggs of Triatominae. Parasit Vectors. 2017;10:55.
35. Sober, E. (Ed.). (1994). Conceptual issues in evolutionary biology. Mit Press. Cambridge
36. Vargas, E., Espitia, C., Patiño, C., Pinto, N., Aguilera, G., Jaramillo, C., ... & Guhl, F. (2006). Genetic structure of *Triatoma* venosa (Hemiptera: Reduviidae): molecular and morphometric evidence. Memórias do Instituto Oswaldo Cruz, 101(1), 39-45.

Cuernavaca, Morelos, a 14 de febrero del 2022.

COMITÉ DE REVISIÓN DE TESIS

Dra. Elizabeth Arellano Arenas (directora de tesis, CIByC UAEM)
Dr. Raúl Alcalá Martínez (CIByC UAEM)
Dra. Elizabeth Nava García (CIByC UAEM)
Dra. Sandra Milena Ospina Garcés (CITRO UV)
Dr. Carlos Napoleón Ibarra Cerdeña (CINVESTAV IPN
Dra. Ana Erica Gutiérrez Cabrera (INSP)
Dra. María Ventura Rosas Echevarría (EESJ UAEM)

Tesis: Detección y delimitación de especies crípticas en vectores de la enfermedad de Chagas (Hemiptera: Reduviidae: Triatominae) bajo múltiples líneas de evidencia

Alumno que lo presenta a revisión: DARYL DAVID CRUZ FLORES

Programa: DOCTORADO EN CIENCIAS NATURALES

VOTO

El documento ha sido revisado y reúne los requisitos para editarse como TESIS por lo que es

APROBADO

ATENTAMENTE

_____

DRA. ELIZABETH ARELLANO ARENAS

Se expide el presente documento firmado electrónicamente de conformidad con el ACUERDO GENERAL PARA LA CONTINUIDAD DEL FUNCIONAMIENTO DE LA UNIVERSIDAD AUTÓNOMA DEL ESTADO DE MORELOS DURANTE LA EMERGENCIA SANITARIA PROVOCADA POR EL VIRUS SARS-COV2 (COVID-19) emitido el 27 de abril del 2020.

El presente documento cuenta con la firma electrónica UAEM del funcionario universitario competente, amparada por un certificado vigente a la fecha de su elaboración y es válido de conformidad con los LINEAMIENTOS EN MATERIA DE FIRMA ELECTRÓNICA PARA LA UNIVERSIDAD AUTÓNOMA DE ESTADO DE MORELOS emitidos el 13 de noviembre del 2019 mediante circular No. 32.

Sello electrónico

ELIZABETH ARELLANO ARENAS | Fecha:2022-05-18 17:42:42 | Firmante

MtkEkNrHj9b/DIuo69KvVcBlWXwDVQ1tlbAcZEIZ758Y2BCTuQfs9vFCMBYdO0qzKNebF0ILRya40yy6sVq41KJzYlW4Lsvww4EV94SLGeS0lcgEmZaO7kLSITSf77pOFmcUxcm
OkoaiDhnAvjRAjjqHe92mLBF+sjp4nbt49PvFlRIY88LqW3hw9OgKH2eswtxqI9czrVaUlCvX6+IGbWrVMD2zQxVEs9XefTPLXrRs6o8N7CS6DjmyTq/0UYGAyXXNnI0WNgQJzZsY
1OQdM0EXnVFZKTDP49CnrNZ9kdguLwXNub1PYKRfgJcvUZPJfyGS3sfvPS2zV5GtqmLrtg==

Puede verificar la autenticidad del documento en la siguiente dirección electrónica o escaneando el código QR ingresando la siguiente clave:

wUXKxvrRk

https://efirma.uaem.mx/noRepudio/10jikwu4o6RPHXBPN9eUvsatdGCMwPtq

Cuernavaca, Morelos, a 14 de febrero del 2022.

COMITÉ DE REVISIÓN DE TESIS

Dra. Elizabeth Arellano Arenas (directora de tesis, CIByC UAEM)
Dr. Raúl Alcalá Martínez (CIByC UAEM)
Dra. Elizabeth Nava García (CIByC UAEM)
Dra. Sandra Milena Ospina Garcés (CITRO UV)
Dr. Carlos Napoleón Ibarra Cerdeña (CINVESTAV IPN
Dra. Ana Erica Gutiérrez Cabrera (INSP)
Dra. María Ventura Rosas Echevarría (EESJ UAEM)

Tesis: Detección y delimitación de especies crípticas en vectores de la enfermedad de Chagas (Hemiptera: Reduviidae: Triatominae) bajo múltiples líneas de evidencia

Alumno que lo presenta a revisión: DARYL DAVID CRUZ FLORES

Programa: DOCTORADO EN CIENCIAS NATURALES

VOTO

El documento ha sido revisado y reúne los requisitos para editarse como TESIS por lo que es

APROBADO

ATENTAMENTE

_____

DR. RAÚL ALCALÁ MARTÍNEZ

Se expide el presente documento firmado electrónicamente de conformidad con el ACUERDO GENERAL PARA LA CONTINUIDAD DEL FUNCIONAMIENTO DE LA UNIVERSIDAD AUTÓNOMA DEL ESTADO DE MORELOS DURANTE LA EMERGENCIA SANITARIA PROVOCADA POR EL VIRUS SARS-COV2 (COVID-19) emitido el 27 de abril del 2020.

El presente documento cuenta con la firma electrónica UAEM del funcionario universitario competente, amparada por un certificado vigente a la fecha de su elaboración y es válido de conformidad con los LINEAMIENTOS EN MATERIA DE FIRMA ELECTRÓNICA PARA LA UNIVERSIDAD AUTÓNOMA DE ESTADO DE MORELOS emitidos el 13 de noviembre del 2019 mediante circular No. 32.

Sello electrónico

RAUL ERNESTO ALCALA MARTINEZ | Fecha:2022-05-18 16:19:36 | Firmante

pzB22+c3+N4egpBOmMVlqFqdXUzzp+eY+TdKAPbL4hAfm/Cm1eDL22Z7PqcJ+TLQnLItk8M1AybWtv1OIQxd2k+DEa2GWtESzy1H+Fzp8oMKCUxKZSXFz1f9NR5IB6REzJcPEDfMghDY/2/kNoSXtbhUQRJSewmwCO6jAilgYpVKZ95CBiuV4AwDsc3cY2p5DgSwa7x7/FkORrBkF5/vWMhpgRi1jZusN8kYGJ/NFin+x0a14siR/kbAsg/8HTH6siv1EMZcUmAw7juv463OUQPGQ96all77wY+uV8PKMr+k7E3ZGqAMhbFfPZLKc0aNrRPS2HsW+qxTxf7reuWJOg==

Puede verificar la autenticidad del documento en la siguiente dirección electrónica o escaneando el código QR ingresando la siguiente clave:

g6eVKlzWS

https://efirma.uaem.mx/noRepudio/5TxQyq66e8oGdzViQMKt6QVSoB6LuUm8

Cuernavaca, Morelos, a 14 de febrero del 2022.

COMITÉ DE REVISIÓN DE TESIS

Dra. Elizabeth Arellano Arenas (directora de tesis, CIByC UAEM)
Dr. Raúl Alcalá Martínez (CIByC UAEM)
Dra. Elizabeth Nava García (CIByC UAEM)
Dra. Sandra Milena Ospina Garcés (CITRO UV)
Dr. Carlos Napoleón Ibarra Cerdeña (CINVESTAV IPN
Dra. Ana Erica Gutiérrez Cabrera (INSP)
Dra. María Ventura Rosas Echevarría (EESJ UAEM)

Tesis: Detección y delimitación de especies crípticas en vectores de la enfermedad de Chagas (Hemiptera: Reduviidae: Triatominae) bajo múltiples líneas de evidencia

Alumno que lo presenta a revisión: DARYL DAVID CRUZ FLORES

Programa: DOCTORADO EN CIENCIAS NATURALES

VOTO

El documento ha sido revisado y reúne los requisitos para editarse como TESIS por lo que es

APROBADO

ATENTAMENTE

_____

DRA. ELIZABETH NAVA GARCÍA

Se expide el presente documento firmado electrónicamente de conformidad con el ACUERDO GENERAL PARA LA CONTINUIDAD DEL FUNCIONAMIENTO DE LA UNIVERSIDAD AUTÓNOMA DEL ESTADO DE MORELOS DURANTE LA EMERGENCIA SANITARIA PROVOCADA POR EL VIRUS SARS-COV2 (COVID-19) emitido el 27 de abril del 2020.

El presente documento cuenta con la firma electrónica UAEM del funcionario universitario competente, amparada por un certificado vigente a la fecha de su elaboración y es válido de conformidad con los LINEAMIENTOS EN MATERIA DE FIRMA ELECTRÓNICA PARA LA UNIVERSIDAD AUTÓNOMA DE ESTADO DE MORELOS emitidos el 13 de noviembre del 2019 mediante circular No. 32.

Sello electrónico

ELIZABETH NAVA GARCIA | Fecha:2022-05-18 14:16:41 | Firmante

XQ3BtXIOBp3CrFCJEcaFrJVuT4MVtpSK7TGexlWp8qQJpExsj4u2bORj8nzZ8DbZ6OsqoXnkkkrNPUnDSrZZ1vJbLzufXh3nOorM6niclz9fWY3PxFbmNFBgfx6Av+c54JSK8iuuL61DsNDUdpEBRaNgnzkjY6vtyHfKqCuvsMmV1dbs9jjdP3foJJEP4p/eNktMhQFyKywuYL5saRJ/uSN7vfKsZwAGeHv6nvXMlYTrzXuq0XCs9CsVbvcgE0mBmsNyySnYOFt6nUK0kJ+cjouQlN1FhlwsR8QKjmJjeLKTYwTi27wTgKCcbXFHy1/RbAtI7NuOFUFjw9orY7qgtQ==

Puede verificar la autenticidad del documento en la siguiente dirección electrónica o escaneando el código QR ingresando la siguiente clave:

cnNX6VaDu

https://efirma.uaem.mx/noRepudio/aoYneU3p21JvYHbr1LBWhMVIcBk94K2d

Cuernavaca, Morelos, a 14 de febrero del 2022.

COMITÉ DE REVISIÓN DE TESIS

Dra. Elizabeth Arellano Arenas (directora de tesis, CIByC UAEM)
Dr. Raúl Alcalá Martínez (CIByC UAEM)
Dra. Elizabeth Nava García (CIByC UAEM)
Dra. Sandra Milena Ospina Garcés (CITRO UV)
Dr. Carlos Napoleón Ibarra Cerdeña (CINVESTAV IPN
Dra. Ana Erica Gutiérrez Cabrera (INSP)
Dra. María Ventura Rosas Echevarría (EESJ UAEM)

Tesis: Detección y delimitación de especies crípticas en vectores de la enfermedad de Chagas (Hemiptera: Reduviidae: Triatominae) bajo múltiples líneas de evidencia

Alumno que lo presenta a revisión: DARYL DAVID CRUZ FLORES

Programa: DOCTORADO EN CIENCIAS NATURALES

VOTO

El documento ha sido revisado y reúne los requisitos para editarse como TESIS por lo que es

APROBADO

ATENTAMENTE

_____

DRA. SANDRA MILENA OSPINA GARCÉS

Se expide el presente documento firmado electrónicamente de conformidad con el ACUERDO GENERAL PARA LA CONTINUIDAD DEL FUNCIONAMIENTO DE LA UNIVERSIDAD AUTÓNOMA DEL ESTADO DE MORELOS DURANTE LA EMERGENCIA SANITARIA PROVOCADA POR EL VIRUS SARS-COV2 (COVID-19) emitido el 27 de abril del 2020.

El presente documento cuenta con la firma electrónica UAEM del funcionario universitario competente, amparada por un certificado vigente a la fecha de su elaboración y es válido de conformidad con los LINEAMIENTOS EN MATERIA DE FIRMA ELECTRÓNICA PARA LA UNIVERSIDAD AUTÓNOMA DE ESTADO DE MORELOS emitidos el 13 de noviembre del 2019 mediante circular No. 32.

Sello electrónico

SANDRA MILENA OSPINA GARCÉS | Fecha:2022-05-19 06:45:44 | Firmante

I6dWOREWwq5dl5xZCWpS0kyXJ2GWDFxVeAptTUiwI52Cjh5oOjAerEdwy0O2R7J3kZ1WRsXKm9WDVob9ND9eRhQ7VFf+4Y5FCawfTDvo69fEA1Gnr4wx02uiU9YhqDP3wTNFfP4vafnzf9ufo+X3PRdhIoax/hyaff1egq6Cw1Y97xT7DD1/OxvMTVDopZwVXwzK2Z/Tp1OUN7lHd6SsnyBuWOtMzq3+4EqGzIsrx6uNnYEnb0l8DgZYW9nCVzDON2nMxS9c+LjDAva7viuSxBPN+8lfAIlFX+G/XM9t1YooWXdAhaO1eOE7YW/21vmKX+mMdNxz5aj0vE3kam9hHQ==

Puede verificar la autenticidad del documento en la siguiente dirección electrónica o escaneando el código QR ingresando la siguiente clave:

cqKwuDzjJ

https://efirma.uaem.mx/noRepudio/Hap69BM29ZJEEkLXdrWoShyRIjEDFSws

Cuernavaca, Morelos, a 14 de febrero del 2022.

COMITÉ DE REVISIÓN DE TESIS

Dra. Elizabeth Arellano Arenas (directora de tesis, CIByC UAEM)
Dr. Raúl Alcalá Martínez (CIByC UAEM)
Dra. Elizabeth Nava García (CIByC UAEM)
Dra. Sandra Milena Ospina Garcés (CITRO UV)
Dr. Carlos Napoleón Ibarra Cerdeña (CINVESTAV IPN
Dra. Ana Erica Gutiérrez Cabrera (INSP)
Dra. María Ventura Rosas Echevarría (EESJ UAEM)

Tesis: Detección y delimitación de especies crípticas en vectores de la enfermedad de Chagas (Hemiptera: Reduviidae: Triatominae) bajo múltiples líneas de evidencia

Alumno que lo presenta a revisión: DARYL DAVID CRUZ FLORES

Programa: DOCTORADO EN CIENCIAS NATURALES

VOTO

El documento ha sido revisado y reúne los requisitos para editarse como TESIS por lo que es

APROBADO

ATENTAMENTE

_____

DR. CARLOS NAPOLEÓN IBARRA CERDEÑA

Se expide el presente documento firmado electrónicamente de conformidad con el ACUERDO GENERAL PARA LA CONTINUIDAD DEL FUNCIONAMIENTO DE LA UNIVERSIDAD AUTÓNOMA DEL ESTADO DE MORELOS DURANTE LA EMERGENCIA SANITARIA PROVOCADA POR EL VIRUS SARS-COV2 (COVID-19) emitido el 27 de abril del 2020.

El presente documento cuenta con la firma electrónica UAEM del funcionario universitario competente, amparada por un certificado vigente a la fecha de su elaboración y es válido de conformidad con los LINEAMIENTOS EN MATERIA DE FIRMA ELECTRÓNICA PARA LA UNIVERSIDAD AUTÓNOMA DE ESTADO DE MORELOS emitidos el 13 de noviembre del 2019 mediante circular No. 32.

Sello electrónico

CARLOS NAPOLEÓN IBARRA CERDEÑA | Fecha:2022-05-19 09:34:07 | Firmante

Sjj7nHc8C/omrfxmEj7L0mLRW5vDcSdnfFnGiDPIRNPZHDynk4/ZZEkp9BB3AP9sZ/UbXZ/4mlyyZ8Nfs/gjkV5TGlt9FaYL2nr1dmevAPgx8qi9ioGKiOICZ86SyOa4lbdXPHGKq7dW
SrxdojHlYeGU/GNY6XXLuG7RQY24UgezaafDqdRO/ZYzl0t3YussN/T6sBVZ0Puo9+k/ZhZlPJTrCBG3GMjxy2HKDZaIg8lbI8I+/thNYdpbmTFoOpLdYxUs39BOgCX+hJGJ+IU4o5
38bgrGwjlP5yynYJC6xPzi32PMnLRf1RRGbiVm8bKcMzEDiovhCtz0rUwqTqErLA==

Puede verificar la autenticidad del documento en la siguiente dirección electrónica o escaneando el código QR ingresando la siguiente clave:

9m0iHOB58

https://efirma.uaem.mx/noRepudio/M9Wm2W9Rxn8F14HcbPhSHwT6IVFZH5Lb

Cuernavaca, Morelos, a 14 de febrero del 2022.

COMITÉ DE REVISIÓN DE TESIS

Dra. Elizabeth Arellano Arenas (directora de tesis, CIByC UAEM)
Dr. Raúl Alcalá Martínez (CIByC UAEM)
Dra. Elizabeth Nava García (CIByC UAEM)
Dra. Sandra Milena Ospina Garcés (CITRO UV)
Dr. Carlos Napoleón Ibarra Cerdeña (CINVESTAV IPN
Dra. Ana Erica Gutiérrez Cabrera (INSP)
Dra. María Ventura Rosas Echevarría (EESJ UAEM)

Tesis: Detección y delimitación de especies crípticas en vectores de la enfermedad de Chagas (Hemiptera: Reduviidae: Triatominae) bajo múltiples líneas de evidencia

Alumno que lo presenta a revisión: DARYL DAVID CRUZ FLORES

Programa: DOCTORADO EN CIENCIAS NATURALES

VOTO

El documento ha sido revisado y reúne los requisitos para editarse como TESIS por lo que es

APROBADO

ATENTAMENTE

_____

DRA. ANA ERICA GUTIÉRREZ CABRERA

Se expide el presente documento firmado electrónicamente de conformidad con el ACUERDO GENERAL PARA LA CONTINUIDAD DEL FUNCIONAMIENTO DE LA UNIVERSIDAD AUTÓNOMA DEL ESTADO DE MORELOS DURANTE LA EMERGENCIA SANITARIA PROVOCADA POR EL VIRUS SARS-COV2 (COVID-19) emitido el 27 de abril del 2020.

El presente documento cuenta con la firma electrónica UAEM del funcionario universitario competente, amparada por un certificado vigente a la fecha de su elaboración y es válido de conformidad con los LINEAMIENTOS EN MATERIA DE FIRMA ELECTRÓNICA PARA LA UNIVERSIDAD AUTÓNOMA DE ESTADO DE MORELOS emitidos el 13 de noviembre del 2019 mediante circular No. 32.

Sello electrónico

ANA ERIKA GUTIÉRREZ CABRERA | Fecha:2022-05-18 16:23:32 | Firmante

r0+1SBmYRwlJ9+IzFQ8fZZbsWz9PQvAL50cdgICWtHKoK/8ctKDWQpVtOZe1K8mVkE3W22Tu8iebuGyWIdxJ9sha/ygxBC7qy6VBw/h48OKg99l+Y3KMC0mk0SOltYGIeRSrpCA
eXLnn3Dr0PsByA9/yRhMWL9z6tw6Kn+1vfMZW46oWVPuspu5rmPr+PsXFQ1av01FRiaeF5ePOc44ieV2U76aZz1Lm1PDiZc+MoP76j29+Att5td7FM+fYgQ9QvJhYx52iLgKhmw2
3SK+S++EK1wlg49JK4r2SLPqSKKrQbmaERPDb7YKrP9+jtEuuja1h5HgVRmIfaVGz3qOkOQ==

Puede verificar la autenticidad del documento en la siguiente dirección electrónica o escaneando el código QR ingresando la siguiente clave:

fu7XBlaJC

https://efirma.uaem.mx/noRepudio/uvKqL8Asyy5kcoT8XrBtDGXh1zBdCeAk

Cuernavaca, Morelos, a 14 de febrero del 2022.

COMITÉ DE REVISIÓN DE TESIS

Dra. Elizabeth Arellano Arenas (directora de tesis, CIByC UAEM)
Dr. Raúl Alcalá Martínez (CIByC UAEM)
Dra. Elizabeth Nava García (CIByC UAEM)
Dra. Sandra Milena Ospina Garcés (CITRO UV)
Dr. Carlos Napoleón Ibarra Cerdeña (CINVESTAV IPN
Dra. Ana Erica Gutiérrez Cabrera (INSP)
Dra. María Ventura Rosas Echevarría (EESJ UAEM)

Tesis: Detección y delimitación de especies crípticas en vectores de la enfermedad de Chagas (Hemiptera: Reduviidae: Triatominae) bajo múltiples líneas de evidencia

Alumno que lo presenta a revisión: DARYL DAVID CRUZ FLORES

Programa: DOCTORADO EN CIENCIAS NATURALES

VOTO

El documento ha sido revisado y reúne los requisitos para editarse como TESIS por lo que es

APROBADO

ATENTAMENTE

_____

DRA. MARÍA VENTURA ROSAS ECHEVARRÍA

Se expide el presente documento firmado electrónicamente de conformidad con el ACUERDO GENERAL PARA LA CONTINUIDAD DEL FUNCIONAMIENTO DE LA UNIVERSIDAD AUTÓNOMA DEL ESTADO DE MORELOS DURANTE LA EMERGENCIA SANITARIA PROVOCADA POR EL VIRUS SARS-COV2 (COVID-19) emitido el 27 de abril del 2020.

El presente documento cuenta con la firma electrónica UAEM del funcionario universitario competente, amparada por un certificado vigente a la fecha de su elaboración y es válido de conformidad con los LINEAMIENTOS EN MATERIA DE FIRMA ELECTRÓNICA PARA LA UNIVERSIDAD AUTÓNOMA DE ESTADO DE MORELOS emitidos el 13 de noviembre del 2019 mediante circular No. 32.

Sello electrónico

MA VENTURA ROSAS ECHEVERRIA | Fecha:2022-05-18 15:19:41 | Firmante

g/eOaxxPBC2ZdBcILbae1I3nNpPQems2sjUxS8upsPCRt15YxtQ9KK5uIFpnh/vx8VAWBcMGC581K7R5QX2mn8SW2S94qWZgaLHLDW+Nw9JjSZ6/Dtpp1N0fzvJLY8JzTZRrMg4CDdS6J4W+NO34ZXGJlu12ZSn+3jrx+Z/02I/WSYkpeZOOGinu1rAFrG1YSH+sAT5Bu8Hn7yOOI440FPg2/nuwqM1kXZQXSAEbmI+8XM2I/2m+x6qQN4lYvxDNHQp2woihTCD2orpAbnfr//tBeaHQL4q++aSHZngua4MrtSZEqCUmMKSrvx/B3iSuhbstr97NhVLqwbJtpQdLIg==

Puede verificar la autenticidad del documento en la siguiente dirección electrónica o escaneando el código QR ingresando la siguiente clave:

jOFndKJfs

https://efirma.uaem.mx/noRepudio/uIhvkWVhzV12nesy4AomFoT4ZV5gTGl6